2010

Generalized curvilinear advection formalism for finite volume codes doing relativistic hydrodynamics

Jay Michael Call
Louisiana State University and Agricultural and Mechanical College, jcall1@tigers.lsu.edu

GENERALIZED CURVILINEAR ADVECTION FORMALISM FOR FINITE VOLUME CODES DOING RELATIVISTIC HYDRODYNAMICS

A Dissertation

Submitted to the Graduate Faculty of the
Louisiana State University and
Agricultural and Mechanical College
in partial fulfillment of the
requirements for the degree of
Doctor of Philosophy

in

The Department of Physics and Astronomy

by
Jay Michael Call
B.S., Brigham Young University, 2003
M.S., Louisiana State University, 2008
August 2010

Dedication

To my loving wife Amber, for all the times she cooked, cleaned, and took care of kids while I was researching, writing, and attending meetings. She is the sun on a rainy day.

Acknowledgements

My advisor, Dr. Joel E. Tohline has been indispensable in providing direction for this project and in helping me to always keep the big picture in mind. His vision has helped me to direct my talents in a productive way. Furthermore, he is a natural teacher and it has been a pleasure to work for him.

Several additional members of the faculty and staff (including Dr. Luis Lehner, Dr. Juhan Frank, Dr. Eric Schnetter, and Dr. Patrick Motl) at Louisiana State University have contributed in one way or other to this project. Dr. David Neilsen and Dr. Eric Hirschmann from Brigham Young University also have provided some helpful suggestions and direction. I am appreciative to fellow graduate students Wes Even, Charles Bradley, Dominic Marcello, and Zach Byerly for numerous contributions to my research in the form of helpful conversations and computer code debugging.

This work has been supported, in part, by grants AST-0708551, PHY-0653369, and PHY-0326311 from the U.S. National Science Foundation and, in part, by grant NNX07AG84G from NASA's ATP program. This research also has been made possible by grants of high-performance-computing time on the TeraGrid (MCA98N043), at LSU, and across LONI (Louisiana Optical Network Initiative).

This work could never have been possible without the loving support and encouragment of my wife Amber, my parents, and her parents. Thank you for pushing me forward.

Table of Contents

List of Tables

List of Figures

Abstract

While it is possible to numerically evolve the relativistic fluid equations using any chosen coordinate mesh, typically there are distinct computational advantages associated with different types of candidate grids. For example, astrophysical flows that are governed by rotation tend to give rise to advection variables that are naturally conserved when a cylindrical mesh is used. On the other hand, Cartesian-like coordinates afford a more straightforward implementation of adaptive mesh refinement (AMR) and avoid the appearance of coordinate singularities. Here it is shown that it should be possible to reap the benefits associated with multiple types of coordinate systems simultaneously in numerical simulations. This could be accomplished by implementing a hybrid numerical scheme: one that evolves a set of state variables adapted to one particular set of coordinates on a mesh defined by an alternative type of coordinate system. A formalism (a generalization of the much-used Valencia formulation) that will aid in the implementation of such a hybrid scheme is provided. It is further suggested that a preferred approach to modeling astrophysical flows that are dominated by rotation may involve the evolution of inertial-frame cylindrical momenta (i.e., radial momentum, angular momentum, and vertical momentum) and the Jacobi energy—all on a corotating Cartesian coordinate grid.

1. Introduction

With a network of sensitive detectors actively collecting data and future upgrades enabling even higher sensitivity in approximately five years, experimental detection of gravitational wave signals appears to be on the horizon. Once this milestone has been achieved, focus will shift from detection to analysis, a stage that will require reliable, detailed models of astrophysical systems. From the standpoint of numerical relativity, the simplest type of astrophysical event that should be observable by modern gravitational-wave observatories is a binary black hole (BBH) merger. Numerical simulations of these types of systems are currently well in hand (e.g. [60, 22, 62, 41, 78, 39, 16, 57, 61, 60, 56]) and intense efforts are underway to incorporate the obtained knowledge in data analysis (e.g.[17, 1, 8, 77]).

A number of groups are engaged in studies of other promising compact binaries able to produce strong gravitational waves (e.g. [2, 70, 31, 30, 9, 67, 64, 29, 47, 76]). These correspond to neutron star-neutron star (NS-NS) and neutron star-black hole (NS-BH) binaries. Most of the numerical algorithms used by these groups have been divided into two modules that run in tandem — one that handles the relativistic hydrodynamic equations and one that handles the Einstein equations. Some of these groups have even extended their models to include magneto-hydrodynamic (MHD) effects. For example, the panels of Figure 1.1 show equatorial snapshots of the rest mass density and velocity fields for a double neutron star merger simulation published by Anderson, Hirschmann, Lehner, Liebling, Motl, Neilsen, Palenzuela, and Tohline (see [5]). This particular model shows some intriguing physical characteristics. Namely, double cores rotating about the center of mass, a ringing bar-like structure in the core, and large pulsations that cause gravitational waves. The final result of the merger is a hypermassive[1], differentially rotating neutron star.

In order to guarantee the accurate results of such simulations, a number of tests are typically performed on codes. Such tests include showing that the simulations can maintain stable rotating stars in stationary equilibrium, that they can reproduce the Oppen-

[1]Hypermassive means that the star is more massive than pressure alone could support without centrifugal effects.

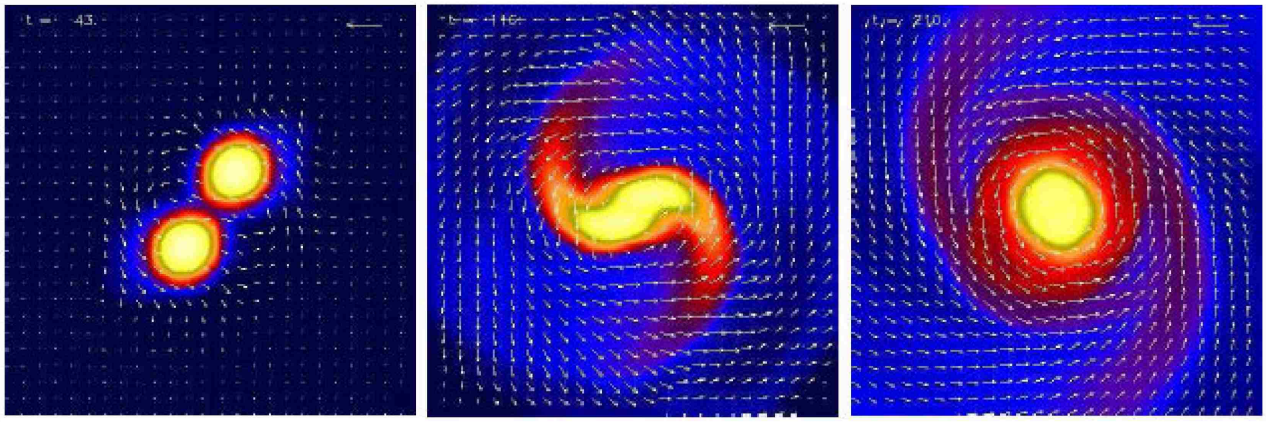

Figure 1.1: Density contours and velocity fields for double neutron star mergers published by Anderson, et al. Equatorial snapshots of the rest mass density and velocity fields for the simulation of a double neutron star merger. Double cores can be seen rotating about the center, and a ringing bar-like structure can be seen in the core. Figure from [5].

heimer/Snyder solution for gravitational collapse to a black hole, and that they can reproduce analytic solutions for shocks and nonlinear MHD wave propagation. Simulations are tested for magnetized Bondi accretion. Moreover, simulations of one or more physical events are compared using independent codes to verify that they are in agreement (see, e.g., [44]). A series of tests like these gives code developers added confidence that their simulations are reproducing actual physics.

While many of the rigorous tests imposed on general relativistic hydrodynamics (GR-HD) codes are clearly passed, occasionally a test produces unexpected results. One such test was performed recently (see again [44]). There is a mass limit for orbiting compact stars, beyond which quasistable circular orbits cannot be maintained. This mass limit depends on the separation of the orbiting stars. The limiting allowed orbit is typically referred to as the innermost stable circular orbit (ISCO). Once the stars cross inside the ISCO, a plunge-and-merger occurs. The recent code test initially placed binary neutron stars just outside the ISCO. The idea was that as mass was subsequently lost through gravitational radiation, the binary would cross below the stability cut-off and settle back down into a stable orbit. In the simulation, however, this did not occur. One naturally wonders why numerical tests

like this one occasionally produce unexpected results. Is it our understanding of the physics that is at fault, or is the code underperforming our expectations?

Stellar population synthesis models have predicted that NS-NS and NS-BH inspirals are among the most likely sources of gravitational radiation detectable by early generations of laser interferometer experiments such as LIGO and VIRGO. In this regard, it is important that the simulations be carried out with as high a degree of quantitative accuracy as possible because the first detections will likely require matched-filtering techniques to pull the inspiral signal out of the noise. A considerable amount of time already has been invested in the development of numerical simulation algorithms in an effort to ensure stability and accuracy. And codes have become increasingly economical and robust as, for example, superior flux reconstruction methods have been adopted. Here we explore avenues through which additional improvements in algorithm design may be gained to better enable the quantitative analysis of detected gravitational-wave signals.

Most groups employing grid-based schemes have started their modeling efforts with the Valencia formulation [10] of the relativistic Euler equations. There are many advantages to using this formulation. Its complete hyperbolic structure is known; it provides for the use of high-resolution shock-capturing (HRSC) techniques in the construction of fluid advection fluxes; and, given appropriate boundary conditions, it guarantees global conservation of key physical variables if their associated source terms are zero.

At the implementation level, most efforts have involved adopting an underlying regular Cartesian-like grid to discretize the Euler equations, as opposed to employing specialized coordinates (like spherical or cylindrical). The resulting schemes with the Cartesian-like meshes are flexible and applicable to general scenarios, though they typically fail to take advantage of possible underlying symmetries of the physical system. Cartesian grids make sense from a variety of perspectives. It is relatively straightforward to write out finite-difference/volume expressions for the partial differential equations (PDEs) in Cartesian coordinates; Cartesian coordinates lack singularities that arise in other familiar curvilinear coordinate systems (e.g., spherical and cylindrical); and the Courant limit generally is less restrictive on a Cartesian

grid. Furthermore, adaptive mesh refinement (AMR), is implemented most straightforwardly on such grids.

On the other hand, it has long been appreciated in the computational fluid dynamics (CFD) community that non-Cartesian grid designs offer alternate advantages. For a given number of grid cells (often limited by computational resources), a grid that conforms to the principal geometry of the problem can place highest resolution where it is needed for a particular problem; and grids structured on an orthogonal curvilinear coordinate system (e.g., cylindrical or spherical) are generally accompanied by components of the momentum vector that are more suitable than linear momentum as the principal conservative quantities — angular momentum being a key example in Newtonian flows. Some recent simulations carried out by the astrophysics group at Louisiana State University (LSU) that have focused on modeling near steady-state mass transfer in nonrelativistic (*i.e.,* Newtonian) close binary systems [26, 48] has benefitted significantly from adopting a cylindrical coordinate grid and evolving the associated radial and angular momentum components as the principal conservative variables. Despite the significant challenges of using a grid code to properly simulate two weakly interacting stars in a binary orbit (even in the Newtonian regime), this group has managed to conserve both angular momentum and mass to a very high degree of precision, and consequently has successfully followed binary evolutions through many 10s of orbits. To our knowledge, this is the only group that has successfully followed the evolution of equilibrium or near-equilibrium binaries through more than a few orbits using a grid code.[2]

If, in general, grid codes are struggling to faithfully represent weakly interacting binaries over long periods of time in the Newtonian regime, then one can imagine the difficulty in trying to model strongly interacting binaries in the relativistic regime (such as NS-NS mergers) with a high degree of quantitative accuracy. Groups hoping to meet with success in this relatively new undertaking should be interested to know specifically what has helped

[2]Groups using SPH techniques have been somewhat more successful at maintaining an equilibrium configuration for more than just a few orbits, but their simulations have more trouble resolving low-density regions without either using a very large number of particles or introducing distinct "types" of particles with masses that vary over several orders of magnitude.

the LSU astrophysics group achieve such a high degree of accuracy in simulations of near-equilibrium configurations. It appears that the primary contributing factor has been the great deal of attention that has been paid to the manner in which integration of the Euler equations is handled. In particular, we credit:

1. The strategic choice of a set of Euler equations for which the sources go to zero, thereby allowing identification of meaningful conserved quantities, and

2. The strategic choice of a rotating coordinate system in order to further minimize numerical diffusion by the advection term.

These two geometry choices may even be more important than a high-order treatment of shocks given that the code that the LSU group has been using over the past decade to successfully model Newtonian binaries has not implemented a high-order treatment of shocks, but it has implemented the Euler equations in a way that allows/causes each of the source terms to approach zero as the physical system approaches an equilibrium state.

One of the things that has made these two geometry choices possible is the group's adoption of angular momentum and radial momentum (through the choice of a cylindrical grid) – rather than the linear (Cartesian) components of momentum – as state variables. Generally, codes employing a Cartesian grid have had significantly more trouble than those employing cylindrical grids in maintaining the integrity of long-term evolutions because the corresponding Cartesian components of momentum are, of course, not conserved in nature – even for near equilibrium flows – while angular momentum is conserved. As the community can appreciate, choosing to evolve angular momentum results in a source that goes to zero due to the existence of an azimuthal Killing vector field, and it is accomplished by taking advantage of the underlying axisymmetry that is inherent to the problem. And Newtonian flows are not the only ones to reap benefits from non-Cartesian grids. Even in the relativity community, multiblock structures [59, 79, 83, 35, 65] have been introduced to retain the Cartesian-like character of the relevant modules by patching together blocks adapted to various symmetries.

Another thing that has made the two aforementioned geometry choices possible is the manner in which pressure terms are handled in the numerical construction of the Euler equations. By constructing Euler equations as though all the pressure terms appear on the right-hand side (R.H.S.) as part of the source, rather than on the left-hand side (L.H.S.) as part of the flux, it also has been possible to obtain a *radial* Euler equation with a source that vanishes in equilibrium. This has further helped to produce high-quality long-term evolutions of near-equilibrium systems.

Since one goal of the numerical relativity community is to model interacting binary neutron star systems with a high degree of precision in order to produce gravitational waveforms that can be used effectively in the analysis of LIGO data, it will likely be important for this community to demonstrate that their grid codes can maintain a (stable or nearly stable) equilibrium system for more than just a few orbits. Based on the difficulties that the Newtonian community has encountered while trying to use grid codes to accomplish this task, other communities (like the numerical relativity community) may also want to consider adopting a set of state variables that are conserved (or nearly conserved) and that lead to a form of the Euler equations that has no source (or a very small source).

Toward this end, I have spent a significant amount of time over the past few years exploring the richness of a generalized formalism (first suggested by Font and Papadopoulos [58]) that promises to allow the numerical relativity community to continue realizing the aforementioned benefits of using a Cartesian grid, while simultaneously adopting a set of generalized conservative state variables that will minimize – if not altogether eliminate – the sources and thereby make more precise conservation possible.

In order to effectively analyze a set of generalized Euler equations, it was first necessary to understand each of the terms appearing in the standard Euler equations — particularly within the context of finite volume codes. In particular, I needed to understand how to identify the conservative quantity that appears in the Euler equations, and I needed to understand why it is conserved. Furthermore, I needed to understand precisely in what sense and under what conditions it is conserved. I was able to accompish this and a summary of my findings is recorded in Chapter 2, particularly §2.3. Armed with this information,

it was possible for me to then interpret clearly the physical meaning of each of the terms appearing in the Euler equations, as is recorded in §2.4. Next, I needed to understand the well-used Valencia Formulation, which expresses the Euler equations in a form that places the conservative state variables, fluxes, and sources in the forefront by arranging them into the form of Eq. (2.28),

$$\frac{1}{\alpha\sqrt{\gamma}}\left(\partial_0\ \sqrt{\gamma}\ \mathcal{F}^0{}_{(\eta)} + \partial_j\ \alpha\sqrt{\gamma}\ \mathcal{F}^j{}_{(\eta)}\right) = \mathcal{S}_{(\eta)},$$

where α is the lapse, γ is the determinant of the induced metric, $\mathcal{F}^0{}_{(\eta)}$ is the collection of state variables, $\mathcal{F}^j{}_{(\eta)}$ is the corresponding collection of fluxes, and $\mathcal{S}_{(\eta)}$ is the collection of sources. In §2.5 I show how the original Euler equations can be molded into this form. Also, because the flux term plays such a critical role in advection, it was important for me to understand how the flux term appearing in the Euler equations relates back to a traditional flux (the product of an area, a velocity, and the state variable). This is outlined (through a series of progressively more complex examples) in §2.6. With this background in hand, my first step of original work involved identifying an unphysical, naked pressure term that arises on both sides of the Euler equations when, as a natural part of the stress-energy tensor, pressure appears inside the advection term. In any numerical integration of the Euler equations, an error can arise due to the lack of cancellation of this unphysical term. The conditions under which this error will be significant enough to have a consequential impact on the physics that is modeled by a given code are discussed in §§2.7 and 2.8. After this, I suggest an alternative approach to code designs that will avoid this difficulty.

Chapter 3 is devoted to generalizing the Euler equations so that state variables can be specified other than those identified by the coordinate system defining the computational grid. The formal procedure is straightforward and has already been outlined briefly by Papadopoulos and Font [58]. In §3.1, I consider the physical meaning of each step in this procedure, which can essentially be thought of as the construction of a weighted linear combination of the four original Euler equations. The particular weighting factors are specified through the choice of a *characteristic vector field* which can be chosen to produce certain benefits, like the removal of the source and, consequently, the identification of a state vari-

able that is conserved. After the generalized Euler equations have been constructed, in §3.2 they are arranged into a format that is similar to the familiar Valencia Formulation. Within the context of this fully-generalized Valencia formulation, I found that it is easy to become confused about the meaning of various pieces within different terms — particularly each of the factors appearing in the flux term. In an attempt to clarify any confusion, in §3.3 I have written out each of the terms appearing in the various dynamical equations (continuity, momentum, and energy) and have identified which pieces depend upon the choice of grid geometry (i.e., the coordinates) and which depend upon the choice of state variables.

Chapter 4 addresses the question, "Given a particular relativistic astrophysical problem, can an ideal characteristic vector field be identified?" Put another way, "How does one choose the ideal set of state variables to evolve?" This is a very open question. Given recent efforts that have been successful at following Newtonian binary systems through many 10s of orbits, I suggest that it would be desirable for relativistic simulations to identify a set of sourceless state variables since certain key quantities that are naturally conserved (e.g., angular momentum) tend to be better conserved numerically when the source is zero. In Chapter 4 I identify potential benefits and drawbacks of several different approaches to choosing the set of state variables. I also investigate the steps that can be taken in order to find the appropriate characteristic vector field in different physical contexts.

After all the formalism has been presented, Chapter 5 contains some example applications, as well as some additional insights that have arisen from our analysis of this generalized formalism. These insights already are providing guidance to efforts that are being made at LSU to design even more accurate codes for simulating Newtonian astrophysical systems. Most importantly, by strategically adopting certain hybrid numerical schemes whose construction is facilitated by our generalization of the Valencia formalism, it appears that the benefits of eliminating (or at least minimizing) the source can be obtained while still maintaining a familiar Cartesian grid and all of the numerical advantages associated with it.

2. Formalism Surrounding the Field Equations

2.1 Definitions

The five standard field equations of special relativity can be interpreted physically as conservation of mass, conservation of 3-momentum, and conservation of energy. They can be written as

$$\nabla_\mu J^\mu = 0 \tag{2.1}$$

$$\nabla_\mu T^{\mu\nu} = 0^\nu, \tag{2.2}$$

where

$$J^\mu \equiv \rho u^\mu \tag{2.3}$$

are the components of the proper rest mass current density, ρ is the proper rest mass density, $\mathbf{u}$ is the fluid 4-velocity, and

$$T^{\mu\nu} \equiv \rho h u^\mu u^\nu + P g^{\mu\nu} = \left(\rho + \frac{P}{c^2}\frac{\gamma}{\gamma - 1}\right) u^\mu u^\nu + P g^{\mu\nu} \tag{2.4}$$

is the energy-momentum tensor (sometimes also referred to as the stress-energy tensor), $h \equiv (1 + \epsilon/c^2 + P/\rho c^2)$ is the proper specific enthalpy of the fluid, ϵ is the proper specific internal energy of the fluid, c is the speed of light in a vacuum, γ is the adiabatic index, P is the pressure of the fluid, and the components of $g^{\mu\nu}$ are the components of the inverse metric — each of these quantities as measured in the coordinate frame. Eq. (2.1) is referred to as the continuity equation, while the components of Eq. (2.2) are known as the Euler equations. Collectively, (2.1) and (2.2) constitute the field equations of special relativity.

Numerical implementation of the field equations of special relativity is generally either carried out on some type of static background metric (such as that of Minkowski space-time) — in which case, the metric components needed for defining various tensor operations like index contraction are assumed at the onset of the problem and do not need to be computed

throughout the evolution — or on a dynamic background determined by numerically solving the collection of Einstein equations.

2.2 Degrees of Freedom

It can be helpful to consider the degrees of freedom that are inherent to the aforementioned field equations. When supplemented by the special relativistic constraint that the fluid's 4-velocity field be invariant,

$$u^\mu u_\mu = -c^2, \tag{2.5}$$

and by some equation of state, $P = P(\rho)$, which is frequently assumed to take a polytropic form,

$$P = k\rho^\gamma, \tag{2.6}$$

these field equations constitute a system of seven independent equations constraining seven unknowns: rest mass density ρ, pressure P, internal energy ϵ, and the four components of the 4-velocity u^μ. Whenever a static background metric is assumed, the components of the metric are known *a priori* and do not add to the list of unknowns.

When a dynamic metric is used, the ten components of the metric become additional unknowns. In order to solve for these additional unknowns, the above system of equations are further supplemented by the ten Einstein equations,

$$G_{\mu\nu} = \frac{8\pi G}{c^4} T_{\mu\nu}, \tag{2.7}$$

where $G_{\mu\nu}$ are the components of the symmetric Einstein tensor — a measure of the intrinsic curvature of a manifold, deriving its mathematical origin from a special combination of second-order partial derivatives of the components of the metric[1]. These equations, of course, can be viewed as a statement that the stress-energy tensor is the source of intrinsic curvature of a manifold, and consequently is the agent responsible for producing any per-

[1] $G_{\mu\nu} \equiv R_{\mu\nu} - \frac{1}{2} g_{\mu\nu} R$, where $R_{\mu\nu} \equiv R^\alpha{}_{\mu\alpha\nu}$ is the Ricci tensor, $R \equiv R^\mu{}_\mu$ is the Ricci scalar, and $g_{\mu\nu}$ are the components of the metric. Further, $R^\alpha{}_{\beta\mu\nu} \equiv \partial_\mu \Gamma^\alpha_{\beta\nu} - \partial_\nu \Gamma^\alpha_{\beta\mu} + \Gamma^\sigma_{\beta\nu}\Gamma^\alpha_{\sigma\mu} - \Gamma^\sigma_{\beta\mu}\Gamma^\alpha_{\sigma\nu}$. Finally, $\Gamma^\alpha_{\beta\gamma} \equiv \frac{1}{2} g^{\alpha\sigma}(\partial_\beta g_{\gamma\sigma} + \partial_\gamma g_{\sigma\beta} - \partial_\sigma g_{\beta\gamma})$ is known as a connection coefficient or a Christoffel symbol. See [46], [81], or [25] for more details.

ceived gravitational forces on a Lorentzian manifold.[2] All together, then, we have seventeen equations and seventeen unknowns.

No discussion of the degrees of freedom inherent in the field equations of general relativity would be complete without mentioning that there is also a four-fold gauge freedom in the components of the metric associated with the choice of coordinates, as described in the previous section. In fact, the gauge freedom is four-fold precisely because there are *four* independent coordinates. Because of this gauge freedom, there are really only six degrees of freedom in the components of the metric. This means that only thirteen of our seventeen unknowns are truly independent, and that seventeen independent equations would overspecify our set of unknowns.

Inescapably, it turns out that there is also a four-fold degeneracy among the ten Einstein equations, so that there are only six degrees of freedom among them. This four-fold degeneracy is also due to the gauge freedom that exists in the choice of coordinates, and can be expressed mathematically by a statement known as the Bianchi identities,

$$\nabla_\mu G^\mu{}_\nu \equiv 0. \tag{2.8}$$

All together, then, we have seventeen equations (with four degrees of degeneracy among them) and seventeen unknowns (with four degrees of gauge freedom among them), so all is well.

2.3 Conservative Form

The work of this dissertation will focus primarily on details surrounding the numerical implementation of the fluid conservation equations, (2.1) and (2.2). While Eqs. (2.1) and (2.2) represent fundamental physical conservation laws, only the first of these has the mathematical form of a conservation equation. This is because the derivatives that appear in Eqs. (2.1) and (2.2) are covariant derivatives, and are coordinate independent. Expressing them in terms of the chosen coordinates produces not only terms that involve partial derivatives, but also terms involving the coordinate-dependent connection coefficients. Writing this out

[2] From the standpoint of numerical simulations, boundary conditions also can act as a source.

for Eqs. (2.1) and (2.2), and multiplying both sides through by $\sqrt{-g}$, we have

$$\begin{aligned} \sqrt{-g}\ \partial_\mu J^\mu + \sqrt{-g}\ \Gamma^\mu_{\mu\nu} J^\nu &= 0 \\ \sqrt{-g}\ \partial_\mu T^{\mu\nu} + \sqrt{-g}\ \Gamma^\mu_{\alpha\mu} T^{\alpha\nu} + \sqrt{-g}\ \Gamma^\nu_{\alpha\mu} T^{\mu\alpha} &= 0^\nu. \end{aligned}$$

The product rule, then, allows us to move the $\sqrt{-g}$ inside the partial derivatives.

$$\begin{aligned} \partial_\mu \left(\sqrt{-g}\ J^\mu\right) - J^\mu \partial_\mu \sqrt{-g} + \sqrt{-g}\ \Gamma^\mu_{\mu\nu} J^\nu &= 0 \\ \partial_\mu \left(\sqrt{-g}\ T^{\mu\nu}\right) - T^{\mu\nu} \partial_\mu \sqrt{-g} + \sqrt{-g}\ \Gamma^\mu_{\alpha\mu} T^{\alpha\nu} + \sqrt{-g}\ \Gamma^\nu_{\alpha\mu} T^{\mu\alpha} &= 0^\nu. \end{aligned}$$

By noting that $\partial_\mu \sqrt{-g} = \Gamma^\nu_{\nu\mu} \sqrt{-g}$, the second and third terms on the left-hand side (L.H.S.) of each equation can be seen to cancel. While only the term involving a partial derivative remains in the continuity equation, an additional term involving the connection coefficients remains in the Euler equations. This term spoils conservation. After dividing the factor of $\sqrt{-g}$ back out, this term is usually moved to the right-hand side (R.H.S.) and is thought of as a source term.

$$\frac{1}{\sqrt{-g}}\ \partial_\mu \left(\sqrt{-g}\ J^\mu\right) = 0 \tag{2.9}$$

$$\frac{1}{\sqrt{-g}}\ \partial_\mu \left(\sqrt{-g}\ T^{\mu\nu}\right) = -T^{\mu\alpha} \Gamma^\nu_{\mu\alpha}. \tag{2.10}$$

Alternatively, one of the indices of the stress-energy tensor could be lowered. In that case, it can be shown, following the procedure just outlined, that Eq. (2.10) becomes[3]

$$\frac{1}{\sqrt{-g}}\ \partial_\mu \left(\sqrt{-g}\ T^\mu{}_\nu\right) = T^\mu{}_\alpha \Gamma^\alpha_{\mu\nu}. \tag{2.11}$$

The physical interpretation will be the same. Though (2.10)/(2.11) still represents a fundamental conservation law, the nonzero source makes it unclear just *what* is being conserved — certainly not the components of the stress-energy tensor, the apparent mathematical analogs of the (conserved) components of the current density $\mathbf{J}$.

Nevertheless, each of the field equations is now written in the form,

$$\partial_\mu \mathcal{Q}^\mu{}_{(\eta)} = \mathcal{S}_{(\eta)}, \tag{2.12}$$

[3]The different sign on the R.H.S. of (2.11) (vs. 2.10) results from the fact that the covariant derivative in (2.2) produces geometry terms, the sign of which depend on whether the quantity to be differentiated has covariant or contravariant indices. This should not be surprising since the Christoffel symbols are not tensors—and do not transform like tensors.

where $\mathcal{S}_{(\eta)}$ is called the *source* (for reasons that will be shown shortly), $\mathcal{Q}_{(\eta)}$ is a vector density[4] of weight +1, and η just counts equations[5]. This form of the field equations emphasizes the concept of conservation because in this form it is straightforward to show what is being conserved, and under what conditions. In particular, we will see that if two certain conditions are satisfied by (2.12), then a special quantity (closely related to $\mathcal{Q}^{\mu}{}_{(\eta)}$) will turn out to be conserved. As a result, this quantity is known as the *conservative variable*.

We begin by imagining the simplest possible four-dimensional region—a hypercube in Minkowski spacetime[6]; we will call this region Ω. (See Figs. 2.1 and 2.2.) An instantaneous hypersurface of Ω is typically referred to as the *control volume* within the fluid dynamics communities, and we will adopt this convention as well. If Eq. (2.12) is satisfied throughout Ω by any physical quantity $\mathcal{Q}_{(\eta)}$ (such as the current density $\sqrt{-g}\,\mathbf{J}$ in the case of Eq. 2.9), and if the corresponding $S_{(\eta)}$ appearing on the R.H.S. of (2.12) should happen to be zero, then the 4-divergence of $\mathcal{Q}_{(\eta)}$ must be zero throughout the region.

$$\int_{\Omega} \partial_{\mu} \mathcal{Q}^{\mu}{}_{(\eta)} \, \mathrm{d}\Omega = 0. \tag{2.13}$$

Furthermore, the divergence theorem,

$$\int_{\Omega} \partial_{\mu} \mathcal{Q}^{\mu}{}_{(\eta)} \, \mathrm{d}\Omega = \int_{\partial\Omega} \mathcal{Q}^{\mu}{}_{(\eta)} \, \mathrm{d}S_{\mu}, \tag{2.14}$$

where $\partial\Omega$ is the boundary of the region Ω and $\mathrm{d}S_{\mu}$ represents the oriented surface area element[7], guarantees that the inner product of $\mathcal{Q}_{(\eta)}$ with $d\mathbf{S}$ must sum to zero over the boundary of Ω. There are essentially two ways this can happen.

[4]A tensor density of weight w is the product of a physical tensor and $\sqrt{-g}^{w}$. It is called a tensor density because of its unique transformation properties. A tensor density of weight w transforms like a tensor, but with an additional factor of the Jacobian to the w^{th} power. $\mathcal{I}^{\mu\cdots}_{\nu\cdots} = \left|\frac{\partial x^{(\mu)}}{\partial x^{(\nu)}}\right|^{w} \frac{\partial x^{\mu}}{\partial x^{\alpha}} \cdots \frac{\partial x^{\beta}}{\partial x^{\nu}} \cdots \mathcal{I}^{\alpha\cdots}_{\beta\cdots}$.

[5]The parentheses around the η's are used to emphasize the fact that η is *not* a tensor index; that is, the complete set of field equations does not compose a single tensor equation—indeed, there are five equations, but only four dimensions.

[6]The local principles illustrated with this example are valid for any general relativistic metric since the equivalence principle implies that any four-dimensional Lorentzian manifold approaches Minkowski in a small enough region.

[7]The oriented surface area element is just the differential 3-volume of the boundary $\partial\Omega$ oriented outward. On the top boundary of Ω it is the final instantaneous differential 3-volume of the hypercube (directed forward in time), and on the bottom boundary it is the initial instantaneous differential 3-volume (directed backward in time). On the side boundaries it is the product of a differential cross-sectional area and a differential interval of time (directed out of the region in a spacelike direction).

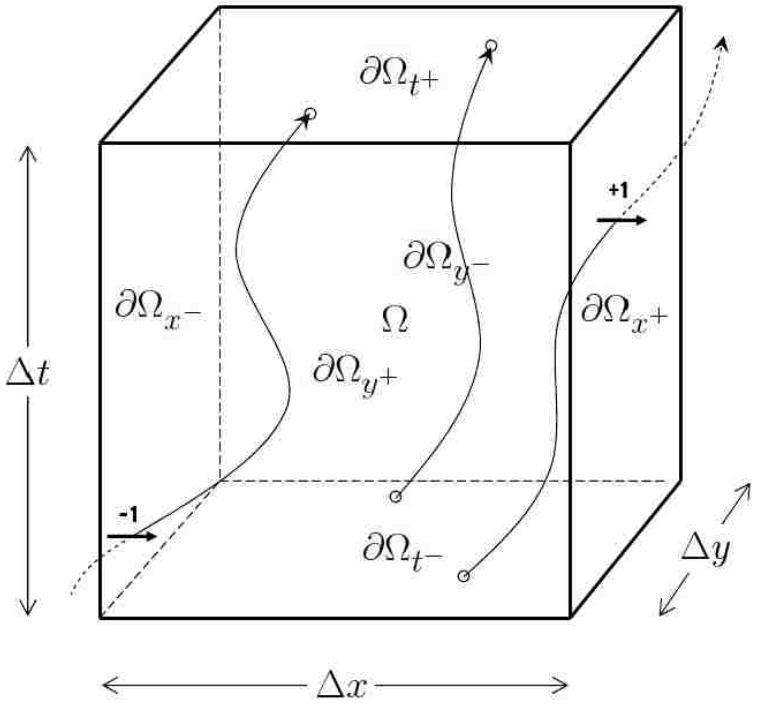

Figure 2.1: Diagram of control volume with zero net flux. The vertical direction in this diagram represents the timelike dimension, and the two horizontal directions spacelike dimensions. (The third spacelike dimension is suppressed.) For the sake of visualization, contributions to the global conservative variable are here represented by discrete "particles" that can enter and exit the region Ω. "Particles" that exit through a side boundary are labeled '+1' to emphasize the fact that this represents a positive flux out of a hypersurface of Ω, whereas "particles" that enter through a side boundary are labeled '-1' to emphasize the fact that this represents a negative flux out of a hypersurface of Ω. "Particles" that enter and exit Ω through the bottom and top boundaries do not represent fluxes, but rather contributions to the global conservative variable within the region at the beginning and end of the indicated time interval. In the case illustrated by this figure, the flux directed inward through the side boundaries equals the flux outward through the side boundaries, so the net flux is zero and the global conservative variable remains unchanged – namely, '+2' – within the region during the relevant interval of time.

1. The contributions to this inner product sum through the top and bottom boundaries could exactly cancel, along with any contributions through the side boundaries (in which case the integral of $\mathcal{Q}^{\mu}{}_{(\eta)}\ \mathrm{d}S_{\mu}$ taken over the control volume – known as the global conservative variable – remains unchanged during the time interval spanned by Ω, as in Figure 2.1).

2. Otherwise, the nonzero net contribution from the top and bottom boundaries could

cancel with the opposite-in-sign, but equal-in-magnitude, nonzero net contribution through the side boundaries (in which case the global conservative variable changes over the time interval spanned by Ω corresponding to the nonzero contribution through the side boundaries, as in Figure 2.2).

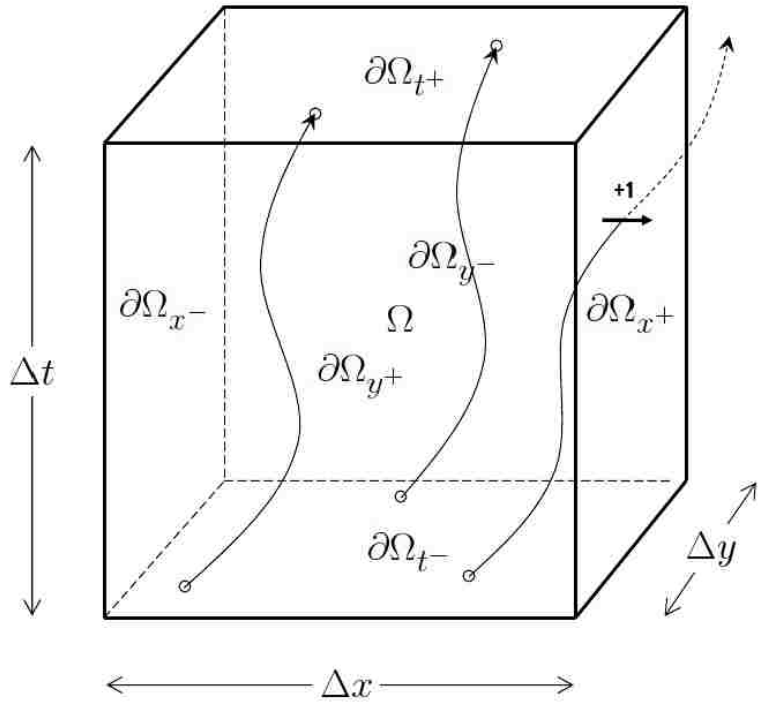

Figure 2.2: Diagram of control volume with non-zero net flux. This figure is analogous to Figure 2.1, but now there is a positive net flux outward through the side boundaries of Ω, so the conservative variable within the region must decrease correspondingly — from '+3' to '+2' in this case. Similarly, if there were a negative net flux out through the side boundaries, then the conservative variable would increase inside Ω.

If we should further suppose that the quantity $\mathcal{Q}_{(\eta)}$ is proportional to the 4-velocity $\mathbf{u}$, such that

$$\mathcal{Q}^{\mu}{}_{(\eta)} \equiv \sqrt{-g}\ \psi_{(\eta)}\ u^{\mu}, \tag{2.15}$$

where g is the determinant of the metric and $\psi_{(\eta)}$ is any scalar function, then it becomes possible to view $\mathcal{Q}^{\mu}{}_{(\eta)}\ \mathrm{d}S_{\mu}$ as a more conventional differential flux — that is, as the product of a velocity, a differential area element, a local conservative variable (represented by the

"particles" in Figs. 2.1 and 2.2), and a differential interval of time.

$$\mathcal{Q}^{\mu}{}_{(\eta)}\, \mathrm{d}S_{\mu} = \underbrace{W\psi_{(\eta)}}_{\substack{\text{conservative}\\ \text{state}\\ \text{variable}}} \cdot \underbrace{\frac{\sqrt{\gamma}}{\sqrt{\gamma\{j\}}}\left(v^{j} - c\beta^{j}/\alpha\right)}_{\substack{\text{transport}\\ \text{velocity}}} \cdot \underbrace{\sqrt{\gamma\{j\}}\,\frac{\mathrm{d}S_{j}}{dx^{0}}}_{\substack{\text{differential}\\ \text{area}\\ \text{element}}} \cdot \underbrace{\alpha/c\; dx^{0}}_{\substack{\text{differential}\\ \text{time}\\ \text{interval}}}, \tag{2.16}$$

where W is the relativistic Lorentz factor $(1 - v^2/c^2)^{-1/2}$, γ is the determinant of the induced 3-metric over the control volume, $\gamma\{j\}$ is the determinant of the entity that results from deleting the j^{th} row and column of the induced metric[8], $\mathbf{v}$ is the 3-velocity through the control volume, β is the shift vector[9], and α is the lapse[10]. This convenient factorization of the flux in its most general form will be explored through the introduction of a series of increasingly complex examples in §2.6.

Since the global conservative variable in a given region can now decrease only if some of it exits through the boundary of the region, and it can only increase if some of it enters through the boundary, the global conservative variable is a quantity that can now neither be created nor destroyed. This is the definition of a conserved quantity, and the reason for the variable's name.[11]

The only mathematical conditions that were required to provide exact local conservation of the conservative variable were:

1. That the source $\mathcal{S}_{(\eta)}$ be zero, and

2. That Eq. (2.12) be satisfied by some quantity $\mathcal{Q}_{(\eta)} \equiv \sqrt{-g}\; \psi_{(\eta)}\; \mathbf{u}$.

If, on the other hand, we should consider the case when the source is *not* zero, it can now be thought of as giving rise to the spontaneous creation or destruction of the local conservative variable $W\psi_{(\eta)}$. One prominent physical example of this comes from a perfectly

[8]Effectively, $\gamma\{j\}$ is the determinant of the 2-metric on a bounding face of the control volume.

[9]The shift vector is an important part of the Arnowitt-Deser-Misner (ADM) decomposition of the metric (detailed in Subsection 7.1.2) and essentially represents the 3-velocity of the coordinates.

[10]The lapse function is also a critical component of the ADM decomposition of the metric (detailed in Subsection 7.1.2) and can be thought of as the local time dilation factor – which identifies the ratio of the rate at which time passes as measured by a local observer to the rate at which time passes as measured by an observer at infinity – scaled by the speed of light c.

[11]The name of the conservative variable holds even when the source $\mathcal{S}_{(\eta)}$ is nonzero. "Conservative" is understood to mean that the variable is the unique quantity associated with a particular equation that will be conserved whenever the source vanishes.

balanced, spherically symmetric star in equilibrium called a TOV star[12]. The star maintains an equilibrium configuration because the inward gravitational force perfectly balances the outward pressure force at every layer within the star. If a small imbalance should develop such that a net radial force acts on a layer of the star, then this net force must give rise to a time rate of change of momentum in the radial direction since

$$\mathbf{F} = \frac{\mathrm{d}\mathbf{p}}{\mathrm{d}t}. \tag{2.17}$$

Mathematically, the imbalance will appear as a source term on the R.H.S. of the radial Euler equation, and it will give rise to the spontanteous creation (if pressure overpowers gravity) or destruction (if gravity overpowers pressure) of radial momentum.

At first glance, this may seem strange since it is a central tenet of physics that things like mass, momentum, and energy can never be created nor destroyed within an isolated system. This is true, and the resolution is that within the context of special relativity, it is actually the 4-momentum that is conserved, and not its individual components. Individual components of this quantity are conserved only when the coordinates possess certain special symmetry properties, which will be discussed in detail in Chapter 3. In our example, radial momentum is not conserved because the radial coordinate does not possess this symmetry property.

2.4 Interpretation

Having explained the physical meaning of equations in the form of (2.12), we are now in a position to interpret the terms that appear in the field equations (2.9) and (2.10 or 2.11). Substituting the definitions of **J** (Eq. 2.3) and **T** (Eq. 2.4) into the field equations, we find that

$$\frac{1}{\sqrt{-g}}\,\partial_\mu\left(\sqrt{-g}\;\rho u^\mu\right) = 0 \tag{2.18}$$

$$\frac{1}{\sqrt{-g}}\,\partial_\mu\left[\sqrt{-g}\;\left(\rho h u_i\; u^\mu + P\delta^\mu{}_i\right)\right] = \rho h u_\alpha u^\mu \Gamma^\alpha_{\mu i} + P\Gamma^\mu_{\mu i} \tag{2.19}$$

$$\frac{1}{\sqrt{-g}}\,\partial_\mu\left[\sqrt{-g}\;\left(\rho h u^0\; u^\mu + g^{\mu 0}P\right)\right] = -\rho h u^\mu u^\alpha \Gamma^0_{\mu\alpha} - P g^{\mu\alpha}\Gamma^0_{\mu\alpha}, \tag{2.20}$$

[12] A Tolman-Oppenheimer-Volkoff (TOV) star is a fully-relativistic, spherically symmetric star in static equilibrium. Its equation of state is (2.6). For more details, see [80], [53], and [81].

where Greek indices range over all dimensions and Latin indices range over spacelike dimensions only. Here, for reasons that will yet be explained, we have chosen to base the momentum equations upon (2.11) and the energy equation upon (2.10).

While each of the field equations is in the form of Eq. (2.12), it is now apparent that the momentum and energy equations have $\mathcal{Q}$'s that are not in the form of (2.15). This means that, in their current form, we will not be able to think of the flux terms arising from the momentum and energy equations as traditional physical fluxes and, consequently, it will not be obvious how to physically interpret these equations. In order to further investigate the exact meaning of these equations it will be necessary to use the product rule to pull any pressure terms outside the partial derivatives on the L.H.S. This will leave $\mathcal{Q}$'s that are in the form necessary to produce a traditional physical flux, but it has the drawback of producing additional terms involving the pressure that will appear in isolation outside the partial derivatives on the L.H.S.

$$\frac{1}{\sqrt{-g}}\,\partial_\mu\left(\sqrt{-g}\;\rho u^\mu\right) = 0 \tag{2.21}$$

$$\frac{1}{\sqrt{-g}}\,\partial_\mu\left(\sqrt{-g}\;\rho h u_i\;u^\mu\right) + \partial_i P + P\Gamma^\mu_{\mu i} = \rho h u_\alpha u^\mu \Gamma^\alpha_{\mu i} + P\Gamma^\mu_{\mu i} \tag{2.22}$$

$$\frac{1}{\sqrt{-g}}\,\partial_\mu\left(\sqrt{-g}\;\rho h u^0\;u^\mu\right) + g^{\mu 0}\partial_\mu P - P g^{\mu\alpha}\Gamma^0_{\mu\alpha} = -\rho h u^\mu u^\alpha \Gamma^0_{\mu\alpha} - P g^{\mu\alpha}\Gamma^0_{\mu\alpha}. \tag{2.23}$$

It is not insignificant that Eq. (2.21) is still in the form of (2.12). Furthermore, it has no source, and the term inside the differential operator takes the form of (2.15). This implies that proper mass density[13] will necessarily be conserved.

The momentum and energy equations (2.22 and 2.23) no longer appear in the form of (2.12). This was the cost of pulling the pressure terms outside the partial derivatives and obtaining $\mathcal{Q}$'s in the form of (2.15) so that the fluxes would be more physically meaningful.

If we now separate key spacelike terms from timelike terms, we find that the continuity equation becomes

$$\frac{1}{\sqrt{-g}}\,\partial_0\left(\sqrt{-g}\;\rho u^0\right) + \frac{1}{\sqrt{-g}}\,\partial_j\left(\sqrt{-g}\;\rho u^j\right) = 0. \tag{2.24}$$

[13]More precisely, the proper baryon number density will be conserved since mass is an ambiguous quantity in general relativity. Nevertheless, we will tend to refer to this quantity as (the more familiar) mass.

The first term represents the time-rate-of-change of proper mass density. The second is the net (outward) flux of mass density. By moving the second term to the R.H.S. so that

$$\frac{1}{\sqrt{-g}}\,\partial_0\left(\sqrt{-g}\;\rho u^0\right) = -\frac{1}{\sqrt{-g}}\,\partial_j\left(\sqrt{-g}\;\rho u^j\right), \tag{2.25}$$

we see that any time-variation in the proper mass density can only be caused by a net flux. A decrease in mass density will occur if the net (outward) flux at that location is positive, and an increase in mass density will occur if the net (outward) flux is negative. The minus sign on the R.H.S. can be thought of as owing to the fact that flux is defined as being an outward quantity that tends to diminish the mass density. It is no coincidence that the source for this conservative quantity is always zero. This can be thought of as owing to the fact that the fundamental conserved quantity is baryon number — a scalar quantity which has no components (and consequently, no symmetry constraints on the coordinates) to contend with.

The momentum equations, on the other hand, now take the form

$$\begin{aligned}\frac{1}{\sqrt{-g}}\,\partial_0\left(\sqrt{-g}\;\rho h u_i\; u^0\right) \;&+\; \frac{1}{\sqrt{-g}}\,\partial_j\left(\sqrt{-g}\;\rho h u_i\; u^j\right) + \partial_i P + P\Gamma^\mu_{\mu i} \\ &= \rho h u_\alpha u^\mu \Gamma^\alpha_{\mu i} + P\Gamma^\mu_{\mu i}.\end{aligned} \tag{2.26}$$

The first term on the L.H.S. is the time-rate-of-change of one component of the proper momentum density — clearly a coordinate-dependent quantity. The second term on the left is the (outward) flux of this particular component of the proper momentum density. Next is the corresponding component of the pressure gradient. The first term on the R.H.S. is a coordinate artifact associated with the curvature of the metric and represents the local force density of gravity. Each of these terms corresponds to an important physical quantity that plays a role in the natural evolution of the fluids these field equations model. The remaining term, in contrast, appears on both sides of Eq. (2.26) and is entirely unphysical. We will hereafter refer to this term as the *naked pressure term* since P appears outside any derivatives.

Finally, the energy equation becomes

$$\begin{aligned} \frac{1}{\sqrt{-g}}\,\partial_0\left(\sqrt{-g}\;\rho h u^0\;u^0\right) \;&+\; \frac{1}{\sqrt{-g}}\,\partial_j\left(\sqrt{-g}\;\rho h u^0\;u^j\right) + g^{\mu 0}\partial_\mu P - P g^{\mu\alpha}\Gamma^0_{\mu\alpha} \\ &= \; -\rho h u^\mu u^\alpha \Gamma^0_{\mu\alpha} - P g^{\mu\alpha}\Gamma^0_{\mu\alpha}. \end{aligned} \tag{2.27}$$

Once again, the first term on the left is the time-rate-of-change of the conservative variable — in this case, the total energy density. The second term is the (outward) flux of total energy density, and the third term is the time-rate-of-change of pressure measured by a coordinate observer. The first term on the right can essentially be viewed as the rate at which gravity does work on the fluid, and the last term on either side is the unphysical naked pressure term associated with the energy equation.

2.5 The Valencia Formulation

In order to further emphasize the exact conservative nature of the field equations, the Valencia group [10] has demonstrated that Eq. (2.9) and each of the four equations represented by expression (2.10 or 2.11) can be cast into the form of a hyperbolic conservation law — one which is stable and converges to the correct solution as the grid resolution is improved. Specifically, in the Valencia formulation the equations governing the conservation of baryon number, conservation of the three components of the fluid momentum, and conservation of energy may be written collectively as,

$$\frac{1}{\alpha\sqrt{\gamma}}\left(\partial_0\;\sqrt{\gamma}\;\mathcal{F}^0{}_{(\eta)} + \partial_j\;\alpha\sqrt{\gamma}\;\mathcal{F}^j{}_{(\eta)}\right) = \mathcal{S}_{(\eta)}, \tag{2.28}$$

where the index, $\eta = 1 \rightarrow 5$, tags each of the five governing equations. The relevant five-component state vector[14] is,

$$\mathcal{F}^0{}_{(\eta)} \;\equiv\; \left(D, S_i, \tau\right)^T\,, \tag{2.29}$$

where,

$$D \;\equiv\; \rho W\,, \tag{2.30a}$$

$$S_i \;\equiv\; \rho h W u_i = \rho h W^2 v_i, \tag{2.30b}$$

$$\tau \;\equiv\; \rho h c W \alpha u^0 - P - c^2 D = \rho h c^2 W^2 - P - c^2 D\,; \tag{2.30c}$$

[14] In reality, this is just a collection of state variables. One can think of it as a pseudovector.

the respective fluxes are,

$$\mathcal{F}^{j}{}_{(\eta)} \equiv \left(D\frac{u^j}{\alpha u^0} \ , \ S_i\frac{u^j}{\alpha u^0} + \frac{P}{c}\delta^j{}_i \ , \ \tau\frac{u^j}{\alpha u^0} + \frac{P}{c}v^j \right)^T ; \tag{2.31}$$

and the respective sources are,

$$\mathcal{S}_{(\eta)} \equiv \begin{pmatrix} 0 \\ T^{\mu\nu}\left(\partial_\mu g_{\nu i} - \Gamma^\delta_{\mu\nu} g_{\delta i}\right)/c \\ \alpha\left(T^{\mu 0}\partial_\mu \ln\alpha - T^{\mu\nu}\Gamma^0_{\mu\nu}\right) \end{pmatrix} . \tag{2.32}$$

For a detailed derivation showing how the fundamental field equations, (2.1 and 2.2), can be manipulated to yield Eq. (2.28), see Appendix B.

It is worth pointing out that the energy equation in the Valencia formulation — obtained by specifying $\eta = 5$ in Eq. (2.28) — is not derived directly from the $\nu = 0$ component of Eq. (2.10). Instead, it is obtained by constructing an appropriate linear combination of the $\nu = 0$ component of Eq. (2.10) and the continuity equation (2.9). The energy conservation equation obtained in this manner is deemed more suitable for numerical implementation because the rest-mass energy — which can be orders of magnitude larger than any of the other components of the total energy — does not appear in the definition of the energy density τ. Our proposed modifications and generalization of the Valencia formulation (which will be detailed in the following chapter) should be viewed in a similar light.

2.6 Flux Terms

2.6.1 Implementation Issues

Following custom, the design of a finite-volume algorithm should begin by integrating the Valencia equations (2.28) over the 3-volume of a grid cell and over the time interval spanned by a given timestep. We will call this hypervolume Ω in analogy to the hypervolume of §2.3. Then (2.28) becomes

$$\frac{1}{\alpha\sqrt{\gamma}}\int_\Omega \partial_0\left(\sqrt{\gamma}\ \mathcal{F}^0{}_{(\eta)}\right)\ \mathrm{d}\Omega + \frac{1}{\alpha\sqrt{\gamma}}\int_\Omega \partial_j\left(\alpha\sqrt{\gamma}\ \mathcal{F}^j{}_{(\eta)}\right)\ \mathrm{d}\Omega = \frac{1}{\alpha\sqrt{\gamma}}\int_\Omega \alpha\sqrt{\gamma}\ \mathcal{S}_{(\eta)}\ \mathrm{d}\Omega, \tag{2.33}$$

where $\mathrm{d}\Omega \equiv \mathrm{d}x^1\ \mathrm{d}x^2\ \mathrm{d}x^3\ \mathrm{d}x^0$. In order to convert the two terms on the L.H.S. into flux integrals over the boundary of the hypervolume, we next invoke the divergence theorem

(Eq. 2.14), where $\mathrm{d}S_\mu \equiv \mathrm{d}x^1\,\mathrm{d}x^2\,\mathrm{d}x^3\,\mathrm{d}x^0/\mathrm{d}x^\mu$ and $\mathcal{Q}_{(\eta)}$ is chosen such that $\mathcal{Q}^0{}_{(\eta)} = \sqrt{\gamma}\,\mathcal{F}^0{}_{(\eta)}$ and $\mathcal{Q}^j{}_{(\eta)} = \alpha\sqrt{\gamma}\,\mathcal{F}^j{}_{(\eta)}$. This produces

$$\frac{1}{\alpha\sqrt{\gamma}}\oint_{\partial\Omega}\left(\sqrt{\gamma}\,\mathcal{F}^0{}_{(\eta)}\right)\,\mathrm{d}S_0 + \frac{1}{\alpha\sqrt{\gamma}}\oint_{\partial\Omega}\left(\alpha\sqrt{\gamma}\,\mathcal{F}^j{}_{(\eta)}\right)\,\mathrm{d}S_j = \frac{1}{\alpha\sqrt{\gamma}}\int_\Omega \alpha\sqrt{\gamma}\,\mathcal{S}_{(\eta)}\,\mathrm{d}\Omega. \quad (2.34)$$

To aid in numerical implementation, it proves instructive (at least in the case of the continuity and momentum equations) to factor the various terms in this expression as indicated by Eq. (2.16).

$$\begin{aligned}\frac{1}{\alpha\sqrt{\gamma}}\oint_{\partial\Omega}\mathcal{F}^0{}_{(\eta)}\,\left(\sqrt{\gamma}\,\mathrm{d}S_0\right) \;+\; & \frac{1}{\alpha\sqrt{\gamma}}\oint_{\partial\Omega}\mathcal{F}^0{}_{(\eta)}\left(\frac{\sqrt{\gamma}}{\sqrt{\gamma\{j\}}}\,\frac{\mathcal{F}^j{}_{(\eta)}}{\mathcal{F}^0{}_{(\eta)}}\,c\right)\left(\sqrt{\gamma\{j\}}\,\frac{\mathrm{d}S_j}{\mathrm{d}x^0}\right)\,\left(\alpha/c\;\mathrm{d}x^0\right) \\ = \;& \frac{1}{\alpha\sqrt{\gamma}}\int_\Omega c\mathcal{S}_{(\eta)}\,\left(\sqrt{\gamma}\,\frac{\mathrm{d}\Omega}{\mathrm{d}x^0}\right)\,\left(\alpha/c\;\mathrm{d}x^0\right), \end{aligned} \quad (2.35)$$

where $\gamma\{j\}$ refers to the cofactor associated with the (j,j) element of the induced metric; that is, it is the determinant of the 2-metric that results from deleting the j^{th} row and j^{th} column of the induced 3-metric. Following the lead of Stone & Norman [74], it furthermore proves instructive to label the various terms in this expression after plugging in expressions for the state variables from (2.29) and the fluxes from (2.31).

$$\begin{aligned}\overbrace{\frac{1}{\alpha\sqrt{\gamma}}\oint_{\partial\Omega}S_{(\eta)}\left(\sqrt{\gamma}\,\mathrm{d}S_0\right)}^{\text{time\_update}} \;+\; & \overbrace{\frac{1}{\alpha\sqrt{\gamma}}\oint_{\partial\Omega}S_{(\eta)}\left(\frac{\sqrt{\gamma}}{\sqrt{\gamma\{j\}}}\,W^2(v^j - c\beta^j/\alpha)\right)\left(\sqrt{\gamma\{j\}}\,\frac{\mathrm{d}S_j}{\mathrm{d}x^0}\right)\,\left(\alpha/c\;\mathrm{d}x^0\right)}^{\text{flux (transport)}} \\ = \;& \underbrace{\frac{1}{\alpha\sqrt{\gamma}}\int_\Omega c\mathcal{S}_{(\eta)}\,\left(\sqrt{\gamma}\,\frac{\mathrm{d}\Omega}{\mathrm{d}x^0}\right)\,\left(\alpha/c\;\mathrm{d}x^0\right)}_{\text{source}}. \end{aligned} \quad (2.36)$$

Each of the separately identified factors inside the integrals on the L.H.S. of Eq. (2.36) has a particular physical significance. The first factor that appears inside the integral in both the time_update term and the flux term is the conservative state variable—analogous to the Newtonian variable referred to as q by Stone & Norman [74]. The second factor inside the integral of the flux term is the transport velocity; it is the component of the fluid 3-velocity normal to the cell face, as measured by the Eulerian observer, and is constructed by subtracting the appropriate component of the grid velocity from the corresponding component of the fluid velocity, each as measured by a stationary (hypersurface-orthogonal[15])

[15] A hypersurface-orthogonal observer is one whose world line is everywhere orthogonal to the hypersurfaces it pierces.

observer. The third factor inside the integral of the flux term is the differential area element on the boundary of the hypervolume as measured by the Eulerian observer; the analogous area element in the Stone & Norman presentation is referred to by the variable $\tilde{A}$. The last factor inside the integral of the flux term is a differential interval of time as measured by the Eulerian observer. Finally, the last factor inside the time_update term is analogous to what Stone & Norman refer to as the control volume (really a differential control volume as per §2.3 of this dissertation), τ.

It is useful to keep in mind the physical significance of each of these factors when developing a numerical algorithm to perform a discrete time-integration of Eq. (2.35). As Stone & Norman [74] point out – see especially the discussion associated with the concept of "consistent transport" in their §4.4 – improved local as well as global conservation of the state variable can be achieved if care is taken to formulate a spatial interpolation (between, for example, discrete cell centers and cell faces) that is separately appropriate for each of the factors in the flux term. We note in particular that the area element at each cell face may already be known and therefore will require no interpolation once the metric (grid geometry) has been specified. Similarly, each instance of $\alpha\sqrt{\gamma}$, which arises from integrating over a cell volume and over an interval of time, depends only on the chosen grid structure. Related issues have also been discussed in [66]. For a term-by-term expansion of the momentum equations, showing the form that the divergence term takes on each face of a grid cell, see Appendix C.

2.6.2 Examples

Our examples are prefaced with a brief description of the metric and the two basic pieces of information that it contains:

1. Information about the inherent geometry of the manifold, and

2. Information about the coordinate system that is chosen to describe the manifold.

To illustrate, first consider a simple example of two Eulerian flat-space metrics,

$$g_{ij} = \begin{pmatrix} 1 & 0 & 0 \\ 0 & 1 & 0 \\ 0 & 0 & 1 \end{pmatrix} \qquad \text{and} \qquad \tilde{g}_{ij} = \begin{pmatrix} 1 & 0 & 0 \\ 0 & r^2 & 0 \\ 0 & 0 & r^2 \sin^2\theta \end{pmatrix}. \tag{2.37}$$

Although these both describe exactly the same geometry, they are *not* the same metric. The first metric g_{ij} describes an intrinsically flat manifold and specifies Cartesian coordinates. The second metric $\tilde{g}_{ij}$ describes the same intrinsically flat manifold, but specifies spherical coordinates rather than Cartesian. One can also express $\tilde{g}_{ij}$ in terms of the Cartesian coordinates, but it still describes the manifold from the point of view of a spherical coordinate system.

$$\tilde{g}_{ij} = \begin{pmatrix} 1 & 0 & 0 \\ 0 & x^2+y^2+z^2 & 0 \\ 0 & 0 & x^2+y^2 \end{pmatrix} \neq \begin{pmatrix} 1 & 0 & 0 \\ 0 & 1 & 0 \\ 0 & 0 & 1 \end{pmatrix} = g_{ij}. \tag{2.38}$$

Here $\tilde{g}_{ij}$ is expressed in terms of purely Cartesian coordinates, but it clearly is not the Cartesian-coordinate metric g_{ij}. This illustrates the fact that two metrics describing the same physical spacetime – but in terms of distinct coordinates bases – are *not* the same metric and *cannot* be used interchangeably. (Though, they can each be expressed in terms of the alternative coordinate system.)

The next point I want to make is that it is not possible to describe two distinct manifold geometries using the same coordinate system. Any coordinate system that covers one manifold cannot possibly cover the other — it does not fit. So, while it is possible to describe the same manifold with distinct coordinate systems, it is *never* possible to describe two manifolds with distinct geometries using the same set of coordinates.[16] One inescapable repercussion of this is that there are more distinct coordinate systems than there are distinct manifold geometries. Since the metric specifies not only the geometry, but also a particular coordinate system, there is an n-parameter family (where n is the dimension of the manifold) of metrics all describing the same manifold geometry.

[16] One may, however, be able to draw analogies between two similar sets of coordinate systems describing distinct manifolds. The coordinates used to describe Minkowski spacetime and those used to describe perturbations over Minkowski spacetime, for example, may appear to have identical forms, but they are distinct in the sense that the metrics required to describe them are not identical. Additional terms appear in the perturbed metric.

In this sense, there is an important distinction between Cartesian coordinates on an intrinsically flat manifold and Cartesian coordinates on an intrinsically curved manifold, a difference between spherical coordinates on a flat manifold and spherical coordinates on a curved manifold, and so forth. In fact, it becomes important to specify what one means by spherical coordinates (or cylindrical coordinates, or any other type of coordinates) in the first place. Each of these types of coordinate systems is defined in terms of its inherent symmetries. A spherical coordinate system, by definition, exhibits spherical symmetry (and consequently can only exist on a spherically symmetric manifold). Schwarzschild coordinates, for example, are spherical coordinates that are adapted to the Schwarzschild geometry.

One question that naturally arises from this discussion is how one can determine if two distinct metrics both describe the same manifold. If both metrics describe the same manifold, then it must be possible to transform between the two corresponding coordinate systems; there must be an equivalence between the two line elements. Since there are $\frac{1}{2}n(n+1)$ degrees of freedom in the metric[17], and n of them are associated with the choice of coordinates, the remaining $\frac{1}{2}n(n-1)$ must be associated with the geometry of the manifold. This implies the existence of an anti-symmetric second-rank tensor that contains all the information about the geometry and no information about the coordinate choice. It turns out that if such a tensor can be constructed from a vector field ξ such that

$$\nabla_\mu \xi_\nu + \nabla_\nu \xi_\mu = 0_{\mu\nu}, \tag{2.39}$$

then ξ is a Killing vector, and identifies a particular symmetry of the manifold. The set of relations described by Eq. (2.39) are known as Killing's equations. Certainly, in order for any two metrics to describe the same manifold, they must give rise to equivalent Killing spaces; that is, equivalent solution spaces to Killing's equations. We will discuss Killing vectors and their relevance to this work in more detail in Chapter 3.

There are six properties that can be used to classify different types of coordinate systems. Each of these properties has the potential to be predetermined by the geometry of the manifold. (For example, given a highly dynamic spacetime, it may not be possible to find

[17]This is because the metric is a symmetric, n-dimensional, second-rank tensor.

an orthogonal coordinate system.) If the geometry alone does not predetermine whether the coordinate map can possess a given attribute, then the choice of coordinates will. Each of these properties adds a degree of generalization and complexity. They can be summarized with the following six questions:

1. Are the coordinates Cartesian? (i.e., "Are they rectangular?")
2. Are the coordinates orthogonal?
3. Are the coordinates static? (i.e., "Is the shift vector zero?")
4. Are the coordinates non-deforming?
5. Is the manifold intrinsically flat?
6. Is the manifold static? (i.e., "Does there exist any coordinate system in which the shift vector is everywhere zero?")

Answers to each of the first three questions will have an impact on the way we think about what a transport velocity, a cell face area, an interval of time, and a cell volume mean to an Eulerian observer. Answers to the last three questions will introduce additional complexity, but, somewhat surprisingly, they will not have an impact on how we think about each of the aforementioned quantities.

The examples detailed in this section include:

1. Advection of a fluid 3-velocity normal to the cell face on a Cartesian grid in Minkowski spacetime;
2. Advection of a fluid with a 3-velocity with an arbitrary orientation relative to the cell face on a Cartesian grid in Minkowski spacetime;
3. Advection of a fluid with a 3-velocity with an arbitrary orientation relative to the cell face on a cylindrical grid in Minkowski spacetime;
4. Advection of a fluid with a 3-velocity with an arbitrary orientation relative to the cell face on a non-orthogonal grid in Minkowski spacetime;

5. Advection of a fluid with a 3-velocity with an arbitrary orientation relative to the cell face on a rotating cylindrical grid in Minkowski spacetime;

6. Advection of a fluid with a 3-velocity with an arbitrary orientation relative to the cell face on a spherically symmetric, infalling grid in Minkowski spacetime;

7. Advection of a fluid with a 3-velocity with an arbitrary orientation relative to the cell face on a static spherical grid in Schwarschild spacetime;

Example 1: Advection of a fluid with a 3-velocity normal to the cell face on a Cartesian grid in Minkowski spacetime

Cartesian coordinates in Minkowski spacetime[18] give rise to the simplest grid structure through which advection can be performed. The coordinates and metric are

$$x^{\mu} \equiv \begin{pmatrix} t \\ x \\ y \\ z \end{pmatrix}, \quad g_{\mu\nu} \equiv \begin{pmatrix} -c^2 & 0 & 0 & 0 \\ 0 & 1 & 0 & 0 \\ 0 & 0 & 1 & 0 \\ 0 & 0 & 0 & 1 \end{pmatrix}. \tag{2.40}$$

Appealing to the ADM relations detailed in Subsection 7.1.2, we can read directly from the metric

$$\begin{array}{rclcrcl} \alpha & = & c. & & \sqrt{\gamma\{x\}} & = & 1. \\ \beta & = & \mathbf{0}. & & \sqrt{\gamma\{y\}} & = & 1. \\ \sqrt{\gamma} & = & 1. & & \sqrt{\gamma\{z\}} & = & 1. \end{array}$$

Assuming we want to advect across the x^+ cell face, the advection variable, transport velocity, face area, interval of time, and cell volume, each as given by (2.16), are

$$\begin{aligned} \text{advection variable} &= \mathcal{F}^0{}_{(\eta)} = W\psi_{(\eta)}. \\ \text{transport velocity} &= \frac{\sqrt{\gamma}}{\sqrt{\gamma\{x\}}}\left(v^x - c\beta^x/\alpha\right) = v. \\ \text{face area} &= \sqrt{\gamma\{x\}}\,\frac{\Delta^3 x}{\Delta x^x} = \Delta y\ \Delta z. \\ \text{interval of time} &= \frac{\alpha}{c}\,\Delta x^0 = \Delta t. \\ \text{cell volume} &= \sqrt{\gamma}\,\Delta^3 x = \Delta x\ \Delta y\ \Delta z. \end{aligned}$$

By cross-referencing the illustration in Figure 2.3, one can quickly verify that each of these quantities is in accordance with what one would expect. Since (for a small enough

[18]Minkowski spacetime is the flat, Lorentzian spacetime of special relativity. It has no gravity and no intrinsic curvature.

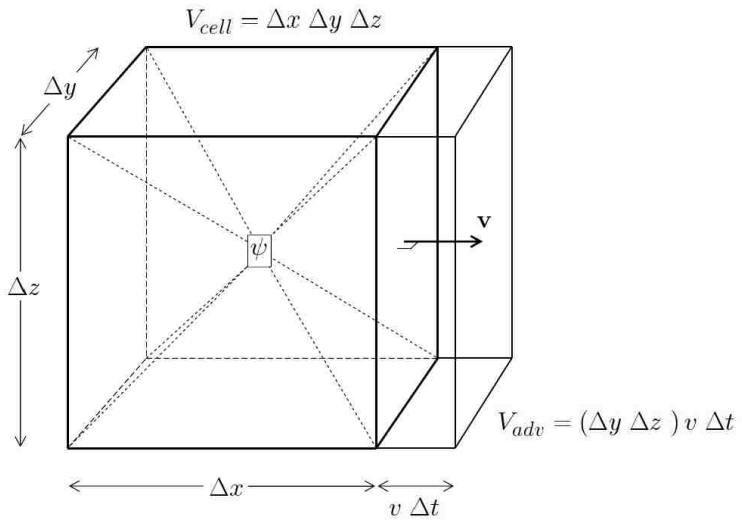

Figure 2.3: Advection on a Cartesian grid with a fluid 3-velocity normal to the cell face. If the fluid 3-velocity is normal to the x^+ cell face, then the area of the cuboid of fluid advected through the x^+ cell face is just the product of the area of the face and the magnitude of the fluid 3-velocity times time.

cell volume) the state variable $\mathcal{F}^0{}_{(\eta)}$ will be almost homogeneous throughout the cell, the complete advection term (given by Eq. 2.16) should measure the amount of $\mathcal{F}^0{}_{(\eta)}$ that is carried out of the cell through each cell face in a given time Δt. In this simplest example, the fluid velocity at a given cell face will be normal to that face, as indicated in Figure 2.3. Then $\mathbf{v} = v^x\ \mathbf{e}_x$. The ratio of the volume of $\mathcal{F}^0{}_{(\eta)}$ advected through the x^+ cell face to the volume of the grid cell will be the fraction of $\mathcal{F}^0{}_{(\eta)}$ carried out of the cell through the given cell face.

$$\frac{\Delta_{x^+}\left(\mathcal{F}^0{}_{(\eta)}\right)}{\mathcal{F}^0{}_{(\eta)}} = \left(\frac{\text{volume of } \mathcal{F}^0{}_{(\eta)} \text{ that leaves through the } x^+ \text{ face in time } \Delta t}{\text{volume of the grid cell}}\right). \quad (2.41)$$

So the total amount of $\mathcal{F}^0{}_{(\eta)}$ that is carried out of the cell through this face is the product of this ratio and the state variable $\mathcal{F}^0{}_{(\eta)}$ measured at the cell face,

$$\Delta_{x^+}\left(\mathcal{F}^0{}_{(\eta)}\right) = \left(\frac{\text{volume of } \mathcal{F}^0{}_{(\eta)} \text{ that leaves through the } x^+ \text{ face in time } \Delta t}{\text{volume of the grid cell}}\right)\ \mathcal{F}^0{}_{(\eta)}\big|_{x^+}\,. \quad (2.42)$$

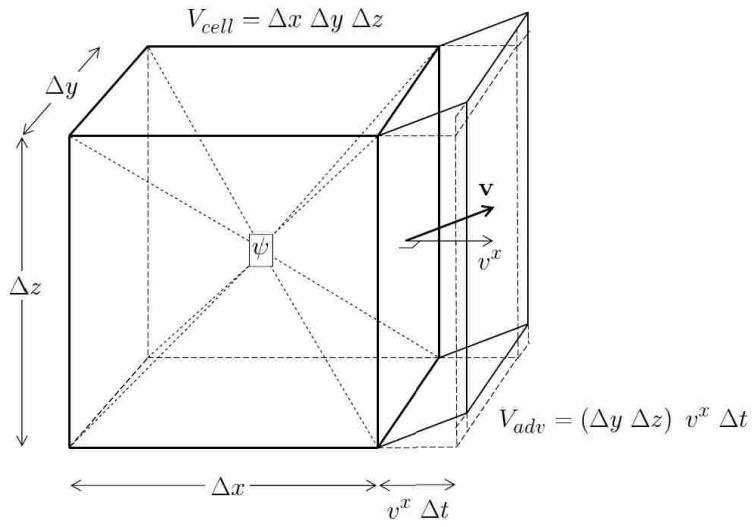

Figure 2.4: Advection on a Cartesian grid with a fluid 3-velocity that is not normal to the cell face. Since the fluid 3-velocity is no longer normal to the x^+ cell face, the volume of fluid advected through the x^+ cell face is now a parallelepiped. The volume of the parallelepiped is given by the product of the area of the x^+ cell face and the x-component of the 3-velocity times time.

Since the volume of ${\mathcal{F}^0}_{(\eta)}$ that leaves the cell through the indicated face is equal to the face area times the transport velocity times the interval of time, we find that

$$\Delta_{x^+}\left({\mathcal{F}^0}_{(\eta)}\right) = \frac{V_{adv}}{V_{cell}} \cdot {\mathcal{F}^0}_{(\eta)} = \frac{(\Delta y\ \Delta z) \cdot v \cdot \Delta t}{\Delta x\ \Delta y\ \Delta z}\ {\mathcal{F}^0}_{(\eta)}\Big|_{x^+} .$$

Example 2: Advection of a fluid with a 3-velocity with an arbitrary orientation relative to the cell face on a Cartesian grid in Minkowski spacetime

In the more general case (when the fluid velocity is not normal to the given cell face), the amount of ${\mathcal{F}^0}_{(\eta)}$ advected will still be given by (2.42). The only difference is that now the volume advected (see Figure 2.4) is a parallelepiped, rather than a cuboid. But the volume of ${\mathcal{F}^0}_{(\eta)}$ that leaves through the x^+ will still equal the face area times the transport velocity times the interval of time, and the transport velocity will now just be v^x, the physical component of the velocity normal to the cell face.

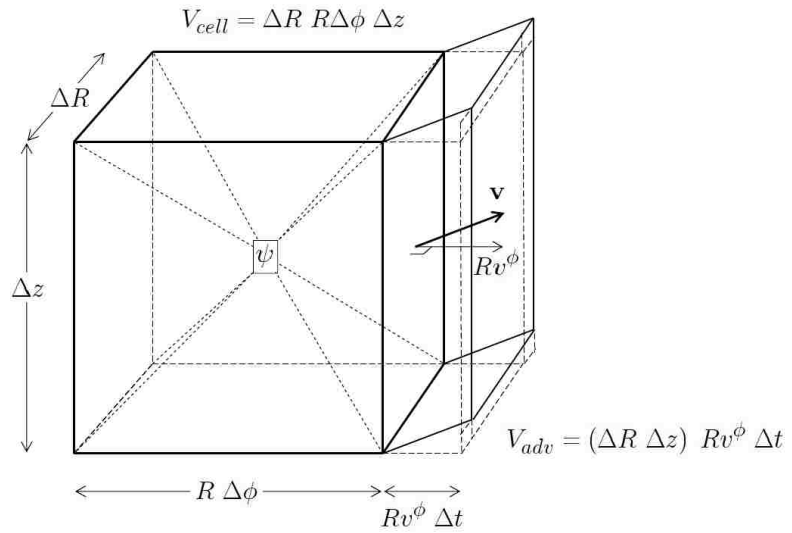

Figure 2.5: Advection on a cylindrical grid. Since the ϕ coordinate is not normalized in this example, v^ϕ must necessarily be scaled by R to produce the transport velocity.

Example 3: Advection of a fluid with a 3-velocity with an arbitrary orientation relative to the cell face on a cylindrical grid in Minkowski spacetime

The cylindrical coordinates and metric are

$$x^\mu \equiv \begin{pmatrix} t \\ R = \sqrt{x^2+y^2} \\ \phi = \arctan(y/x) \\ z \end{pmatrix}, \quad g_{\mu\nu} \equiv \begin{pmatrix} -c^2 & 0 & 0 & 0 \\ 0 & 1 & 0 & 0 \\ 0 & 0 & R^2 & 0 \\ 0 & 0 & 0 & 1 \end{pmatrix}. \tag{2.43}$$

And the ADM relations give

$$\begin{aligned} \alpha &= c. & \sqrt{\gamma\{R\}} &= R. \\ \beta &= \mathbf{0}. & \sqrt{\gamma\{\phi\}} &= 1. \\ \sqrt{\gamma} &= R. & \sqrt{\gamma\{z\}} &= R. \end{aligned}$$

Suppose we want to advect $\mathcal{F}^0{}_{(\eta)}$ in the azimuthal direction, as shown in Figure 2.5. Then,

$$\begin{aligned} \text{advection variable} &= \mathcal{F}^0{}_{(\eta)} = W\psi_{(\eta)}. \\ \text{transport velocity} &= \frac{\sqrt{\gamma}}{\sqrt{\gamma\{\phi\}}}\left(v^\phi - c\beta^\phi/\alpha\right) = Rv^\phi. \\ \text{face area} &= \sqrt{\gamma\{\phi\}}\,\frac{\Delta^3 x}{\Delta x^\phi} = \Delta R\ \Delta z. \\ \text{interval of time} &= \frac{\alpha}{c}\,\Delta x^0 = \Delta t. \\ \text{cell volume} &= \sqrt{\gamma}\ \Delta^3 x = R\ \Delta R\ \Delta\phi\ \Delta z. \end{aligned}$$

The advection term for this face, then, is

$$\Delta_{\phi^+}\left(\mathcal{F}^0{}_{(\eta)}\right) = \frac{(\Delta R\ \Delta z)\cdot\left(Rv^\phi\right)\cdot\Delta t}{R\ \Delta R\ \Delta\phi\ \Delta z}\ \mathcal{F}^0{}_{(\eta)}\Big|_{\phi^+},$$

where v^ϕ is the contravariant component of the fluid velocity in the ϕ-direction, and Rv^ϕ is the physical component of the fluid velocity in the ϕ-direction. Meanwhile, $\Delta R\ \Delta z = \sqrt{\gamma\{\phi\}}\ \Delta R\ \Delta z$ is the cell face area, and $R\ \Delta R\ \Delta\phi\ \Delta z = \sqrt{\gamma}\ \Delta R\ \Delta\phi\ \Delta z$ is the grid cell volume. Also, while γ is the determinant of the induced metric, $\gamma\{\phi\}$ refers to the determinant of the 2-metric on the cell face—that is, the determinant of the entity that is left when the row and column associated with ϕ are deleted from the 3-metric. This is

$$\gamma\{\phi\} = \begin{vmatrix} 1 & 0 \\ 0 & 1 \end{vmatrix} = 1.$$

Once again, referring to Figure 2.5, the advection term can be thought of as

$$\Delta_{\phi^+}\left(\mathcal{F}^0{}_{(\eta)}\right) = \left(\frac{\text{volume of } \mathcal{F}^0{}_{(\eta)} \text{ that leaves through the } \phi^+ \text{ face in time } \Delta t}{\text{volume of the grid cell}}\right)\ \mathcal{F}^0{}_{(\eta)}\big|_{\phi^+}.$$

Example 4: Advection of a fluid with a 3-velocity with an arbitrary orientation relative to the cell face on a non-orthogonal grid in Minkowski spacetime

The skewed coordinates that we will select and corresponding metric are non-orthogonal[19].

$$x^\mu \equiv \begin{pmatrix} t \\ x' = x \\ y' = y - x \\ z \end{pmatrix}, \quad g_{\mu\nu} \equiv \begin{pmatrix} -c^2 & 0 & 0 & 0 \\ 0 & 2 & 1 & 0 \\ 0 & 1 & 1 & 0 \\ 0 & 0 & 0 & 1 \end{pmatrix}. \tag{2.44}$$

Then the ADM quantities become

$$\begin{array}{rclcrcl} \alpha & = & c. & & \sqrt{\gamma\{x'\}} & = & 1. \\ \beta & = & \mathbf{0}. & & \sqrt{\gamma\{y'\}} & = & \sqrt{2}. \\ \sqrt{\gamma} & = & 1. & & \sqrt{\gamma\{z\}} & = & 1. \end{array}$$

This time we will advect $\mathcal{F}^0{}_{(\eta)}$ across an x' = constant cell face, as shown in Figure 2.6. From (2.36), we have

[19] In orthogonal coordinate systems, each of the basis vectors is everywhere orthogonal to each of the other basis vectors. This is manifest by a metric with no off-diagonal terms. (There are some manifolds that cannot be mapped by an orthogonal coordinate system.)

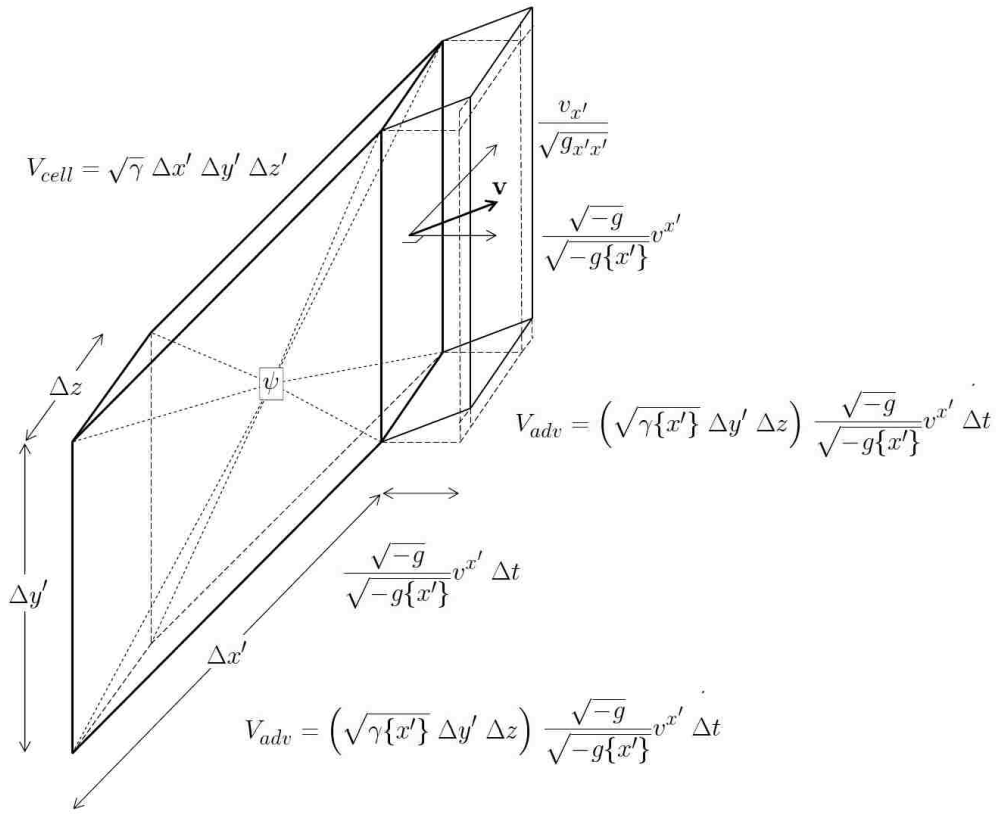

Figure 2.6: Advection on a non-orthogonal grid. The transport velocity is the component of the 3-velocity that is normal to the x'^{+} cell face, not the one that points in the direction of the x' coordinate. The transport velocity is the necessary component for the construction of the appropriate advection term.

$$\begin{aligned}
\text{advection variable} &= \mathcal{F}^0{}_{(\eta)} = W\psi_{(\eta)}. \\
\text{transport velocity} &= \frac{\sqrt{\gamma}}{\sqrt{\gamma\{x'\}}}\left(v^{x'} - c\beta^{x'}/\alpha\right) = v^{x'}. \\
\text{face area} &= \sqrt{\gamma\{x'\}}\ \frac{\Delta^3 x}{\Delta x^{x'}} = \Delta y'\ \Delta z. \\
\text{interval of time} &= \frac{\alpha}{c}\ \Delta x^0 = \Delta t. \\
\text{cell volume} &= \sqrt{\gamma}\ \Delta^3 x = \Delta x'\ \Delta y'\ \Delta z.
\end{aligned}$$

The advection term for this face, then, is

$$\Delta_{x'^{+}}\left(\mathcal{F}^0{}_{(\eta)}\right) = \frac{(\Delta y'\ \Delta z)\cdot\left(v^{x'}\right)\cdot\Delta t}{\Delta x'\ \Delta y'\ \Delta z}\ \mathcal{F}^0{}_{(\eta)}\Big|_{x'^{+}}.$$

The advection term will still be the ratio of the volume of ${\mathcal{F}^0}_{(\eta)}$ advected through the x'^+ cell face to the grid cell volume, times ${\mathcal{F}^0}_{(\eta)}$. But because the contravariant components of a vector field v^μ are generally used with the coordinate basis vectors $\mathbf{e}_\mu$, and the covariant components of a vector field v_μ are generally used with the covectors $\mathbf{e}^\mu$, at first glance it would appear that $v^{x'}$ is not the transport velocity, but the component of the fluid 3-velocity pointing in the x'-direction (which is not normal to the cell face). (For an explanation detailing why this is not the case, see Appendix A.) Nonetheless, it turns out that the *covariant* components v_μ are needed to give the physical components in the direction of the *basis vectors* $\mathbf{e}_\mu$, and the *contravariant* components v^μ are needed to give the physical components in the direction of the *covectors* $\mathbf{e}^\mu$! Apparently, this is just one of the features that emerge from the deep complexities of duality.

This can be shown as follows. In order to obtain the physical components of a vector field in the direction of the covectors $\mathbf{e}^\mu$, one needs to project the vector field onto the unit covectors,

$$v(\mu) = \mathbf{v} \cdot \hat{\mathbf{e}}^\mu = \mathbf{v} \cdot \frac{\mathbf{e}^\mu}{|\mathbf{e}^\mu|} = \mathbf{v} \cdot \frac{\mathbf{e}^\mu}{\sqrt{\mathbf{e}^\mu \cdot \mathbf{e}^\mu}} = \frac{v^\mu}{\sqrt{g^{\mu\mu}}}.$$

The contravariant component of the metric that appears in the denominator can be expressed in terms of the more standard covariant components of the metric by recalling that the contravariant components of the metric form a matrix that is the inverse of the matrix formed by the covariant components of the metric. For that reason, the contravariant components of the metric are sometimes referred to collectively as the "inverse metric". Further, recall from linear algebra that the components of an inverse matrix can be obtained from the determinant of the matrix, and the collection of cofactors.

$$(A^{-1})_{ij} = \frac{1}{\det A} C_{ji}, \tag{2.45}$$

where C_{ji} is the cofactor associated with the (j, i) element of A. In an analogous fashion, $g^{\mu\mu}$ can then be expressed as

$$g^{\mu\mu} = \frac{1}{g} g\{\mu\} = \frac{-g\{\mu\}}{-g}, \tag{2.46}$$

where g is the determinant of the metric and $g\{\mu\}$ is the determinant of the entity that is obtained by deleting the μ row and column of the metric. Or, in other words, $g\{\mu\}$ is the

cofactor associated with the (μ,μ) component of the metric. All together, then, we have

$$v(\mu) = \frac{\sqrt{-g}}{\sqrt{-g\{\mu\}}}\ v^{\mu}, \tag{2.47}$$

for the physical component of $\mathbf{v}$ in the direction normal to the μ^+ cell face. Because the chosen coordinates are not moving, the factor of $\sqrt{-g}/\sqrt{-g\{\mu\}}$ appearing in front of v^μ in (2.47) reduces to the factor of $\sqrt{\gamma}/\sqrt{\gamma\{i\}}$ appearing in front of $W^2(v^i - c\beta^i/\alpha)$ in Eq. (2.36). For a description of why the latter is the more general expression for the transport velocity measured by an Eulerian observer, see the next example. It involves a moving coordinate system.

Example 5: Advection of a fluid with a 3-velocity with an arbitrary orientation relative to the cell face on a rotating cylindrical grid in Minkowski spacetime

The coordinates and metric components are stationary[20] in this case.

$$x^\mu \equiv \begin{pmatrix} t' = t \\ R \\ \phi' = \phi - \omega t \\ z \end{pmatrix}, \quad g_{\mu\nu} \equiv \begin{pmatrix} -\left(c^2 - R^2\omega^2\right) & 0 & R^2\omega & 0 \\ 0 & 1 & 0 & 0 \\ R^2\omega & 0 & R^2 & 0 \\ 0 & 0 & 0 & 1 \end{pmatrix}. \tag{2.48}$$

The inverse metric, then, becomes

$$g^{\mu\nu} = \begin{pmatrix} -1/c^2 & 0 & \omega/c^2 & 0 \\ 0 & 1 & 0 & 0 \\ \omega/c^2 & 0 & \frac{c^2 - R^2\omega^2}{c^2 R^2} & 0 \\ 0 & 0 & 0 & 1 \end{pmatrix}, \quad \gamma^{ij} = \begin{pmatrix} 1 & 0 & 0 \\ 0 & 1/R^2 & 0 \\ 0 & 0 & 1 \end{pmatrix}, \tag{2.49}$$

and the ADM quantities are

$$\begin{array}{rclcrcl} \alpha & = & c. & & \sqrt{\gamma\{R\}} & = & R. \\ \beta & = & \omega\ \mathbf{e}_{\phi'} = R^2\omega\ \mathbf{e}^{\phi'}. & & \sqrt{\gamma\{\phi'\}} & = & 1. \\ \sqrt{\gamma} & = & R. & & \sqrt{\gamma\{z\}} & = & R. \end{array}$$

If we construct an advection term in the azimuthal direction, it will be very similar to the term we constructed for the static cylindrical coordinates. The only difference is that now the moving coordinates are chasing down the fluid. As a result, we will need to subtract the 3-velocity of the coordinates from the fluid 3-velocity.

[20]Static coordinates are motionless, whereas stationary coordinates can be moving as long as their global structure never changes. The shift vector is a measure of this coordinate motion. The physical components of the 3-velocity of the coordinates, given by (7.13), are directly proportional to the shift vector.

$$\begin{aligned}
\text{advection variable} &= \mathcal{F}^0{}_{(\eta)} = W\psi_{(\eta)}. \\
\text{transport velocity} &= \frac{\sqrt{\gamma}}{\sqrt{\gamma\{\phi'\}}}\left(v^{\phi'} - c\beta^{\phi'}/\alpha\right) = R\left(v^{\phi'} - \omega\right). \\
\text{face area} &= \sqrt{\gamma\{\phi'\}}\,\frac{\Delta^3 x}{\Delta x^{\phi'}} = \Delta R\;\Delta z. \\
\text{interval of time} &= \frac{\alpha}{c}\,\Delta x^0 = \Delta t'. \\
\text{cell volume} &= \sqrt{\gamma}\;\Delta^3 x = R\;\Delta R\;\Delta\phi'\;\Delta z.
\end{aligned}$$

The advection term for this face, then, is

$$\Delta_{\phi'+}\left(\mathcal{F}^0{}_{(\eta)}\right) = \frac{(\Delta R\;\Delta z)\cdot\left(R\big(v^{\phi'} - \omega\big)\right)\cdot\Delta t'}{R\;\Delta R\;\Delta\phi'\;\Delta z}\;\mathcal{F}^0{}_{(\eta)}\Big|_{\phi'+}.$$

Since the grid is moving in this example, the physical component of $\mathbf{v}$ pointing in the direction of $\mathbf{e}^{\phi'}$ is no longer tangent to the spatial hypersurface. This is because the covector is normal to the t' coordinate, which moves along with the grid. Consequently, the covector must have a nonzero timelike component. As a result, the physical component of $\mathbf{v}$ in the $\mathbf{e}^{\phi'}$-direction is no longer the transport velocity measured by the Eulerian observer. She can measure only hypersurface tangent components.

In the previous example, we demonstrated that the projection of the 3-velocity onto $\hat{\mathbf{e}}^i$ is

$$\frac{\sqrt{-g}}{\sqrt{-g\{i\}}}\;v^i.$$

Now we want to find what part of this is tangent to the hypersurface. One can imagine what $\hat{\mathbf{e}}^i$ would look like if t' were deleted as a coordinate. The remaining coordinates would span the hypersurface only. Then $\hat{\mathbf{e}}^i$ would lie tangent to the $t' = \text{const.}$ hypersurface. Replacing the 4-metric $g_{\mu\nu}$ with the induced 3-metric γ_{ij} on the hypersurface, the above expression becomes

$$\frac{\sqrt{\gamma}}{\sqrt{\gamma\{i\}}}\;v^i.$$

Finally, subtracting off the 3-velocity of the coordinates, we arrive at the transport velocity given by Eq. (2.36),

$$\text{transport velocity} = \frac{\sqrt{\gamma}}{\gamma\{i\}}W^2\left(v^i - c\beta^i/\alpha\right). \tag{2.50}$$

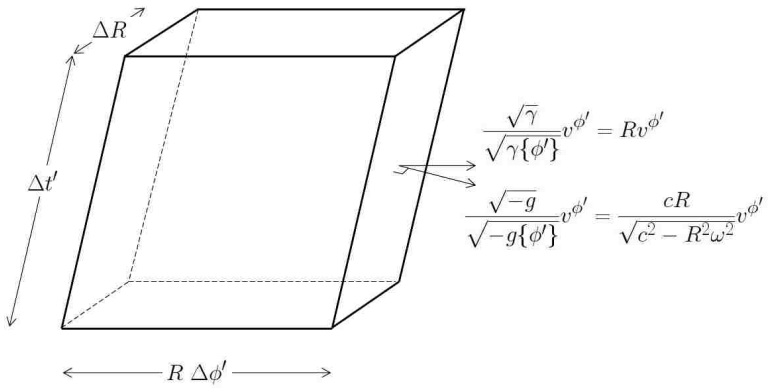

Figure 2.7: Advection on a moving grid. Since the transport velocity is measured by the Eulerian observer, it must be tangent to the hypersurface of constant t'. But since the grid is moving in this example, the component of the 4-velocity that is normal to the ϕ'^{+} hyperface, $(\sqrt{-g}/\sqrt{-g\{\phi'\}}\ )\ v^{\phi'}$, is not tangent to the hypersurface; consequently, it cannot be the transport velocity. The transport velocity is the part of this that is tangent to the hypersurface. It is obtained by replacing $-g$ with γ, which lies exclusively in the hypersurface. Thus, $(\sqrt{\gamma}/\sqrt{\gamma\{\phi'\}}\ )\ v^{\phi'}$ becomes the transport velocity.

Notice that the transport velocity is normal to the spatial 2-face, but not to the hyperface, as shown in Figure 2.7.

Example 6: Advection of a fluid with a 3-velocity with an arbitrary orientation relative to the cell face on a spherically symmetric, infalling grid in Minkowski spacetime

The concept of infalling coordinates[21] can be applied to a number astrophysical phenomenae. In general, the infall speed of the coordinates is $\tilde{v}\,(t)$. This results in a metric that

[21]Non-deforming coordinates can move, but only along a Killing vector field. (This, of course, implies that there are some geometries—geometries that do not admit any Killing vector field—where non-deformable coordinates are not possible.) Any non-Killing motion of the coordinates will result in a time-dependent deformation of the grid cells. This can be measured by checking to see if the 4-velocity of the coordinates (given by Eq. 7.14), satisfies the Killing equations (4.2). The rotating cylindrical coordinates discussed above, for example, have a 4-velocity of

$$\mathbf{u}_{\text{coords}} = \frac{c\ \mathbf{e}_0}{\sqrt{c^2 - R^2\omega^2}}.$$

One can check that this vector field does in fact satisfy Killing's equations. Consequently, rotating cylindrical coordinates do not deform.

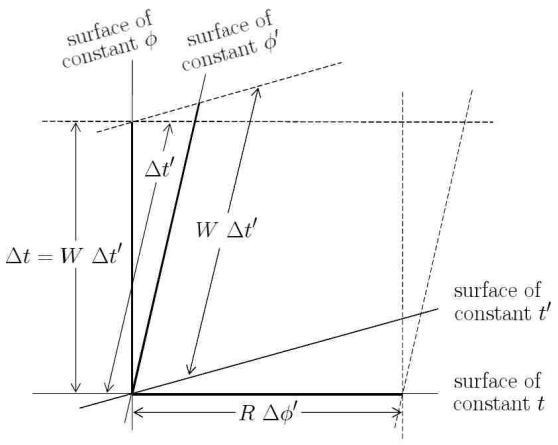

Figure 2.8: Relationship between $\Delta t'$ and Δt for a moving grid. One should not be alarmed that the interval $\Delta t = W\ \Delta t'$ appears shorter in Figure 2.7 than does $\Delta t'$. This is an illusion that can be explained away by the Lorentzian character of the metric. Making use of the principle of relativity of simultaneity, here one can see that, in fact, $\Delta t = W\ \Delta t'$ is a longer interval than $\Delta t'$, as would be expected.

takes the form

$$x^{\mu} \equiv \begin{pmatrix} t \\ r' = r + \tilde{r}\,(t) \\ \theta \\ \phi \end{pmatrix}, \quad g_{\mu\nu} \equiv \begin{pmatrix} \tilde{v}^2\,(t) - c^2 & -\tilde{v}\,(t) & 0 & 0 \\ -\tilde{v}\,(t) & 1 & 0 & 0 \\ 0 & 0 & r'^2 & 0 \\ 0 & 0 & 0 & r'^2 \sin^2\theta \end{pmatrix}. \tag{2.51}$$

We also have

$$\begin{array}{rclcrcl} \alpha & = & c. & & \sqrt{\gamma\{r'\}} & = & r'^2 \sin\theta. \\ \beta & = & -\tilde{v}\,(t)\ \mathbf{e}_{r'} = -\tilde{v}\,(t)\ \mathbf{e}^{r'}. & & \sqrt{\gamma\{\theta\}} & = & r' \sin\theta. \\ \sqrt{\gamma} & = & r'^2 \sin\theta. & & \sqrt{\gamma\{\phi\}} & = & r'. \end{array}$$

The 4-velocity of the coordinates will, of course, not satisfy Killing's equations in this case because of the squashing that happens as the coordinates fall inward. Despite this, there is nothing new here with respect to constructing an advection term. So let us construct the advection term out of the $+r'$ face.

$$\begin{array}{rcl} \text{advection variable} & = & \mathcal{F}^0{}_{(\eta)} = W\psi_{(\eta)}. \\ \text{transport velocity} & = & \dfrac{\sqrt{\gamma}}{\sqrt{\gamma\{r'\}}}\left(v^{r'} - c\beta^{r'}/\alpha\right) = v^{r'} - \tilde{v}\,(t)\,. \\ \text{face area} & = & \sqrt{\gamma\{r'\}}\ \dfrac{\Delta^3 x}{\Delta x^{r'}} = r'^2 \sin\theta\ \Delta\theta\ \Delta\phi. \end{array}$$

$$\begin{aligned}
\text{interval of time} &= \frac{\alpha}{c}\,\Delta x^0 = \Delta t. \\
\text{cell volume} &= \sqrt{\gamma}\;\Delta^3 x = r'^2 \sin\theta\;\Delta r'\;\Delta\theta\;\Delta\phi. \\
\Delta_{r'+}\left(W\psi\right) &= W\psi\left(v^{r'} - \tilde{v}\left(t\right)\right)\left(r'^2 \sin\theta\;\Delta\theta\;\Delta\phi\right)\frac{\Delta t}{r'^2 \sin\theta\;\Delta\theta\;\Delta\phi}\bigg|_{r'+}.
\end{aligned}$$

Example 7: Advection of a fluid with a 3-velocity with an arbitrary orientation relative to the cell face on a static spherical grid in Schwarschild spacetime

The Schwarzschild spacetime is curved[22], but spherically symmetric. Its coordinates and metric are

$$\xi^\mu \equiv \begin{pmatrix} t \\ r \\ \theta \\ \phi \end{pmatrix}, \quad g_{\mu\nu} \equiv \begin{pmatrix} -c^2\left(1 - 2GM/rc^2\right) & 0 & 0 & 0 \\ 0 & \left(1 - 2GM/rc^2\right)^{-1} & 0 & 0 \\ 0 & 0 & r^2 & 0 \\ 0 & 0 & 0 & r^2 \sin^2\theta \end{pmatrix}, \quad (2.52)$$

which implies that

$$\begin{aligned}
\alpha &= c\,\sqrt{1 - 2GM/rc^2}. & \sqrt{\gamma\{r\}} &= r^2 \sin\theta. \\
\beta &= \mathbf{0}. & \sqrt{\gamma\{\theta\}} &= \tfrac{r\sin\theta}{\sqrt{1-2GM/rc^2}}. \\
\sqrt{\gamma} &= \tfrac{r^2\sin\theta}{\sqrt{1-2GM/rc^2}}. & \sqrt{\gamma\{\phi\}} &= \tfrac{r}{\sqrt{1-2GM/rc^2}}.
\end{aligned}$$

The only complications arising from advecting on a curved manifold are conceptual. Gravitational time dilation scales the interval of time, and gravitational length contraction scales the face area and cell volume. All of this occurs naturally inside the metric and requires no generalization in the construction of the advection term. In this example, we shall advect across the θ^- cell face. We find that,

$$\begin{aligned}
\text{advection variable} &= \mathcal{F}^0{}_{(\eta)} = W\psi_{(\eta)}. \\
\text{transport velocity} &= -\frac{\sqrt{\gamma}}{\sqrt{\gamma\{\theta\}}}\left(v^\theta - c\beta^\theta/\alpha\right) = -rv^\theta. \\
\text{face area} &= \sqrt{\gamma\{\theta\}}\,\frac{\Delta^3 x}{\Delta x^\theta} = \frac{r\sin\phi}{\sqrt{1 - 2GM/rc^2}}\;\Delta r\;\Delta\phi. \\
\text{interval of time} &= \frac{\alpha}{c}\,\Delta x^0 = \sqrt{1 - 2GM/rc^2}\;\Delta t. \\
\text{cell volume} &= \sqrt{\gamma}\;\Delta^3 x = \frac{r^2\sin\theta}{\sqrt{1 - 2GM/rc^2}}\;\Delta r\;\Delta\theta\;\Delta\phi. \\
\Delta_{\theta^-}\left(W\psi\right) &= -\,W\psi\left(rv^\theta\right)\left(\frac{r\sin\theta}{\sqrt{1 - 2GM/rc^2}}\;\Delta r\;\Delta\phi\right)\frac{\sqrt{1 - 2GM/rc^2}\;\Delta t}{\frac{r^2\sin\theta}{\sqrt{1-2GM/rc^2}}\;\Delta r\;\Delta\theta\;\Delta\phi}\bigg|_{\theta^-}.
\end{aligned}$$

[22]Flat manifolds have no intrinsic curvature, which means that all the components of the Riemann tensor are zero.

There are two distinct ways of thinking about where the minus sign comes from in this case. First, one can think of advecting across the θ^- cell face in the $-\theta$ direction so that the relevant physical component of the velocity is $-rv^\theta$ and the oriented face area is $\sqrt{\gamma\{\theta\}}\ \Delta r\ \Delta\phi$. Or second, one can think of advecting across the θ^- cell face in the $+\theta$ direction. Then the relevant physical component of the velocity is $+rv^\theta$, but the oriented cell face area is $-\sqrt{\gamma\{\theta\}}\ \Delta r\ \Delta\phi$. Either way, the necessary minus sign is produced.

2.7 The Naked Pressure Term

We return to dwell on the appearance of the naked pressure term $P\Gamma^\mu_{\mu i}$ on both sides of the momentum equations (2.26). Analytically this unphysical term presents no formal problems because it appears on both sides of the equation and therefore can be canceled. But numerical implementations of the governing fluid equations in this standard form – such as elements $\eta = 2,\ 3,\ \&\ 4$ of expression (2.28) in the Valencia formulation – are subject to numerical errors associated with the failure of the naked pressure terms to cancel. It is difficult for the terms to cancel numerically because the finite-difference expressions that are used to approximate derivatives that appear in the source term on the R.H.S. generally are different from the numerical expressions used to approximate derivatives on the L.H.S.

It is apparent that the error made by not removing the naked pressure terms will vanish whenever the Christoffel symbols are zero (like when Cartesian coordinates are used on a flat manifold), and that it is greatest in regions where the Christoffel symbols are large (that is, wherever the basis vectors change rapidly from one point to the next—like near coordinate poles[23]).

Neilsen & Choptuik [49] encountered this problem in their study of the critical collapse of spherically symmetric perfect fluids. Because they carried out their simulations on a spherical coordinate grid, the naked pressure term explicitly contained a factor of $1/r$. They

[23]It is useful to understand that the Christoffel symbols identify the rate at which the basis vectors change as you move along a given coordinate. (Test it, for example, in cylindrical coordinates where the only nonzero connection coefficients are $\Gamma^R_{\phi\phi} = -R$ and $\Gamma^\phi_{R\phi} = R^{-1} = \Gamma^\phi_{\phi R}$ and see if you get what you expect.) This can be seen by considering the relationship $\partial_\mu \mathbf{e}_\nu = \Gamma^\alpha_{\mu\nu}\mathbf{e}_\alpha$. [46] For the *unit* vectors this becomes $\partial_\mu \hat{\mathbf{e}}_\nu = \frac{\sqrt{g_{\alpha\alpha}}}{\sqrt{g_{\nu\nu}}}\ \Gamma^\alpha_{\mu\nu}\hat{\mathbf{e}}_\alpha$ $(\alpha \neq \nu)$. Incidentally, note that, with these relations, it is very straightforward to take the total time derivatives of the basis vectors or of the unit vectors.

found (see the discussion in their Appendix B) that the lack of perfect cancelation of the source term with the pressure term in the flux induced errors that became quite large near the origin of their grid. The explicit divergent $(1/r)$ behavior of the naked pressure term that was encountered by Neilsen & Choptuik can be avoided if a dynamical simulation is carried out in Cartesian coordinates. But even on a Cartesian coordinate grid, curvature in the metric can cause the naked pressure term to be large.

Consider trying to model, for example, the dynamical behavior of a near-equilibrium neutron star represented by a spherically symmetric TOV star. In near-equilibrium, pressure gradients will almost balance gravity throughout the star; that is, at all radii,

$$\frac{\rho h u^\mu u_\alpha \Gamma^\alpha_{\mu(x)}}{\partial_x P} \approx 1 \,. \tag{2.53}$$

How large will the naked pressure term be in such a configuration? To illustrate, consider a numerical scheme in which an $n_R{}^{\text{th}}$-order accurate finite-difference stencil is used to evaluate derivatives on the R.H.S. – in which case the error introduced in each term is $\mathcal{O}(\Delta x^{n_R+1})$ – and a lower $n_L{}^{\text{th}}$-order flux reconstruction scheme is used to perform one-dimensional advection in a smooth region of some simulation domain – in which case a numerical evaluation of each term involving spatial derivatives on the L.H.S. introduces an error $\mathcal{O}(\Delta x^{n_L+1})$. The numerical error ϵ_P that results from a lack of cancelation of the naked-pressure terms will be dominated by the lower-order treatment on the L.H.S.; that is,

$$\begin{aligned} \epsilon_P = \left| P\Gamma^\mu_{\mu(x)}\Big|_{\text{RHS}} - P\Gamma^\mu_{\mu(x)}\Big|_{\text{LHS}} \right| &= P\Gamma^\mu_{\mu(x)} \left| \left(1 + \mathcal{O}\left(\Delta x^{n_R+1}\right)\right) - \left(1 + \mathcal{O}\left(\Delta x^{n_L+1}\right)\right) \right| \\ &= P\Gamma^\mu_{\mu(x)} \cdot \mathcal{O}\left(\Delta x^{n_L+1}\right) \,. \end{aligned} \tag{2.54}$$

The numerical error ϵ_{adv} introduced by the advection term on the L.H.S. is of this same order; that is,

$$\epsilon_{\text{adv}} = \partial_x \left(\rho u^2\right) \cdot \mathcal{O}\left(\Delta x^{n_L+1}\right) . \tag{2.55}$$

Therefore, the error associated with evaluation of the naked pressure terms will be more significant than the error associated with advection *unless*,

$$P\Gamma^\mu_{\mu(x)} < \partial_x \left(\rho u^2\right) \,. \tag{2.56}$$

But in near-equilibrium we expect dynamical motion to be small so that

$$\frac{\partial_x \left(\rho u^2\right)}{\partial_x P} \ll 1 \,. \tag{2.57}$$

Condition (2.56) will therefore be violated when modeling the near-equilibrium behavior of a given neutron star configuration if, in any region of the flow, the dimensionless ratio

$$\sigma_{(x)} \equiv \frac{P\Gamma^{\mu}_{\mu(x)}}{\partial_x P} = \frac{\Gamma^{\mu}_{\mu(x)}}{\partial_x \left(\ln P\right)} \,, \tag{2.58}$$

is not small (meaning, $\ll 1$). The panel on the left of Figure 2.9 shows how the magnitude of $\sigma_{(x)}$ (implying the use of Cartesian coordinates) varies with position inside individual, spherically symmetric $\Gamma = 2$ TOV stars that have different total masses. (See Appendix E for a detailed derivation of $\sigma_{(x)}$ within a TOV star.) The panel on the right of Figure 2.9 shows how the maximum value of $\sigma_{(x)}$ varies with GM/c^2R (where M is the total mass of the TOV star and R is its radius) for a wide range of TOV masses. It is evident that $\left|\sigma_{(x)}\right|$ becomes increasingly relevant as one moves deeper into the relativistic regime, growing to values of order unity near the center of the most massive stars.

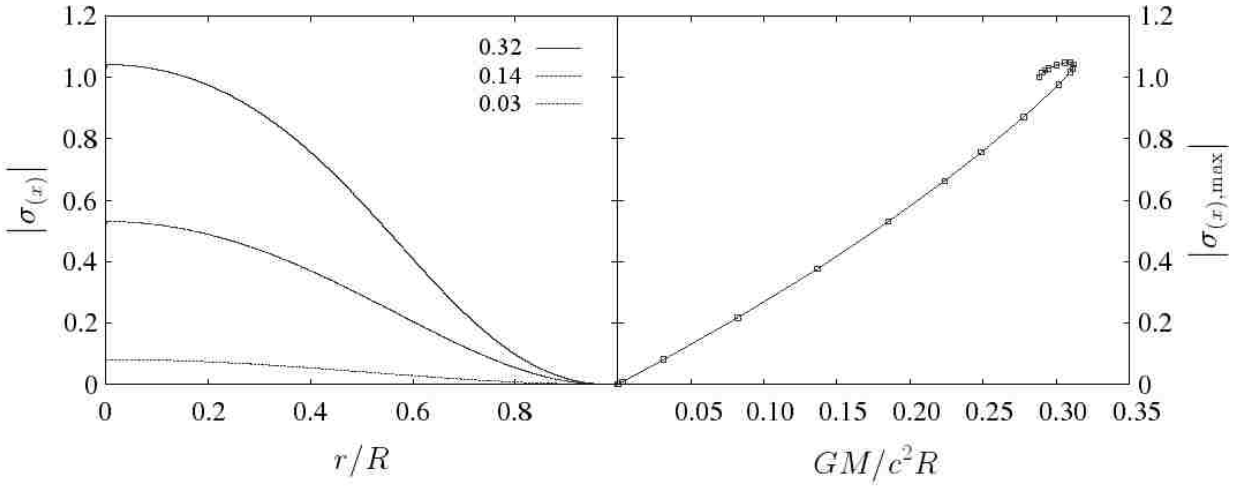

Figure 2.9: Naked pressure term (normalized to the pressure gradient) inside several TOV stars. The left panel shows how $\left|\sigma_{(x)}\right|$ (as defined in Eq. 2.58) varies with radius inside $\Gamma = 2$ TOV stars having total masses $GM/c^2R = 0.03, 0.14$, and 0.32. The right panel shows the relationship between $\left|\sigma_{(x),\max}\right|$ and GM/c^2R for TOV stars having a wide range of masses.

To illustrate this point more concretely, we have numerically determined the net acceleration that would be felt at various locations inside one of our static, equilibrium TOV stars

(the one with $GM/c^2R = 0.31$) according to Eq. (2.10), assuming the advection term on the L.H.S. is evaluated using the Colella & Woodward PPM[24] reconstruction scheme [23]. The acceleration resulting from a lack of cancelation of the naked pressure terms, normalized to the equilibrium pressure gradient, is shown as a function of position r/R in the left panel of Figure 2.10 for three different adopted grid resolutions — 64, 128, and 256 zones. Because pressure balances gravity to a very high degree of precision in the TOV star (which was constructed using Mathematica and a grid containing thousands of radial zones) and the velocity everywhere is zero, the net acceleration should be many orders of magnitude smaller than what is displayed.

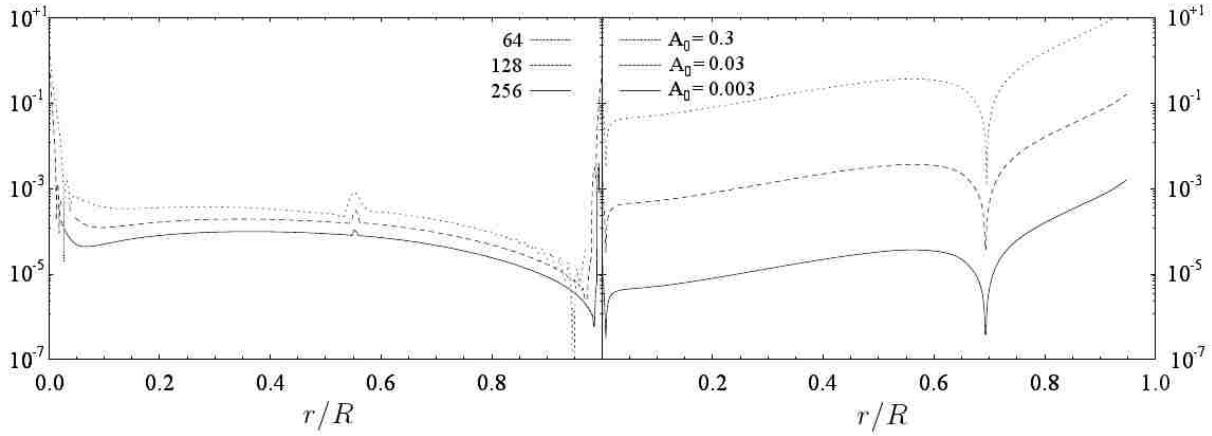

Figure 2.10: Comparison of spurious numerical accelerations with momentum updates from flux terms for a moderately relativistic, near-equilibrium TOV star. *Left panel:* Spurious radial accelerations that result from a lack of cancelation of the naked pressure terms inside a TOV star having $GM/c^2R = 0.3$. Curves show resulting spurious accelerations, normalized to the local pressure gradient and plotted as a function of radius, when a PPM scheme is used to reconstruct fluxes according to Eq. (2.10) for three different radial grid resolutions — 64 (dotted), 128 (dashed), and 256 (solid) zones. *Right panel:* The Eulerian time-rate-of-change of the radial momentum density that should actually be produced inside the same TOV star when various radial velocity flow fields defined by Eq. (2.59) are introduced. Curves show results, normalized to the local pressure gradient and plotted as a function of radius, when the velocity amplitude $A_0 = 0.3$ (dotted), 0.03 (dashed), and 0.003 (solid).

To assess how errors introduced by the naked pressure terms might affect the evolution of models that are near but not precisely in hydrostatic balance, we imprinted a radial velocity

[24]Piecewise parabolic method.

flow field of the form,

$$\frac{v_r}{c} \;=\; A_0\left(\frac{r}{R}\right), \tag{2.59}$$

where A_0 is a constant, onto the equilibrium structure of our 128-zone TOV star. Then, using the same PPM reconstruction scheme as before but a form of the momentum conservation equation in which the naked pressure terms have been canceled analytically — specifically, Eq. (2.60a) introduced below — we again numerically determined the Eulerian-frame time-rate-of-change of the radial momemtum density throughout the star. The right panel of Figure 2.10 shows these results, normalized to the equilibrium pressure gradient, for three different adopted values of A_0: 0.3, 0.03, and 0.003. These are not spurious accelerations; they arise due to the properties of our prescribed nonequilibrium flow field and are free of errors arising from naked pressure terms. Had we used Eq. (2.10) instead, our determination of the net acceleration would have included errors on the order of the spurious accelerations shown in the left panel of Figure 2.10. For velocity amplitudes A_0 on the order of 0.01, or smaller, these errors would have corrupted our attempt to accurately determine the Eulerian-frame time variation of the radial momentum density shown in the right panel of the figure.

To avoid this unnecessary source of numerical error (ϵ_P), we propose that the Valencia formulation be modified to ensure cancelation of the unphysical naked pressure terms. Specifically, we propose that the term, $P\delta^i{}_j/c$, that appears inside the fluxes associated with all three components of the momentum in Eq. (2.31) be moved to the R.H.S. of the momentum conservation equation and be considered part of the source. With this objective in mind, rather than developing a relativistic formulation of the fluid equations that is built upon Eq. (2.26), we will base our subsequent discussion and derivations on a momentum conservation equation of the form,

$$\begin{aligned}
&\frac{1}{\sqrt{-g}}\,\partial_0\left(\sqrt{-g}\;\rho h u_i\; u^0\right) \\
&+\frac{1}{\sqrt{-g}}\,\partial_j\left(\sqrt{-g}\;\rho h u_i\; u^j\right) + \partial_i P \;&=\;& \rho h u^\mu u_\alpha \Gamma^\alpha_{\mu i} &\text{(2.60a)}\\
&&=\;& (T^\mu{}_\alpha - P\delta^\mu{}_\alpha)\Gamma^\alpha_{\mu i}\,. &\text{(2.60b)}
\end{aligned}$$

2.8 The Pressure Gradient

In addition to strategically removing the naked pressure terms, there are benefits that can be realized when the remaining pressure gradient is moved to the R.H.S. (For the energy equation, though, we will keep the pressure term on the L.H.S. inside the expression for the flux since it is not clear how to take explicit partial derivatives of the pressure with respect to time.)

$$\begin{aligned} &\frac{1}{\sqrt{-g}}\,\partial_0\left(\sqrt{-g}\;\rho h u_i\;u^0\right) \\ +&\frac{1}{\sqrt{-g}}\,\partial_j\left(\sqrt{-g}\;\rho h u_i\;u^j\right) &= \rho h u^\mu u_\alpha \Gamma^\alpha_{\mu i} - \partial_i P &\text{(2.61a)} \\ &&= (T^\mu{}_\alpha - P\delta^\mu{}_\alpha)\Gamma^\alpha_{\mu i} - \partial_i P\,. &\text{(2.61b)} \end{aligned}$$

First, moving the pressure gradient to the R.H.S. reduces the magnitude of both the source and the divergence term in regions of near steady-state flow — minimizing the numerical cancelation that needs to take place between the flux and source terms. The magnitude of the source will be minimized because, in steady state, pressure can be expected to nearly balance gravity; the magnitude of the divergence term will be minimized as well because very little net fluid actually passes from one cell to another. We will elaborate further on this point in Chapter 3.

Second, note that if we raise the i-index on both sides of (2.61a), the L.H.S. is the total time derivative of a coordinate 4-momentum. Consequently, the R.H.S. can be thought of as a coordinate 4-force — that is, the physical component of a 4-force pointing in the direction of u^i, plus a pseudo 4-force associated with the local acceleration of the x^i coordinate. The source will be zero if a fluid element experiences the same acceleration as the coordinate system; otherwise it provides a measure of the deviation of the fluid element's acceleration from the acceleration of the coordinates. Because the unphysical naked pressure term does not appear in these last expressions, and because the pressure gradient is now included on the R.H.S. and thought of as a source, we will henceforth call the R.H.S. of Eqs. (2.61a) and

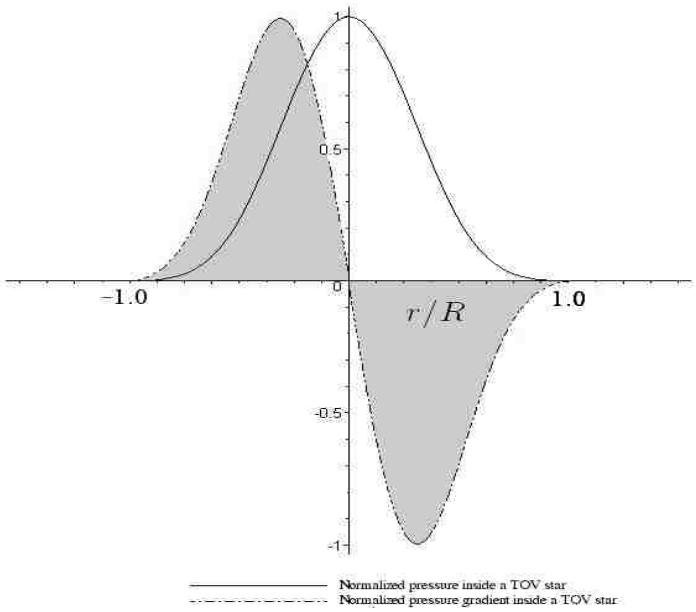

Figure 2.11: Pressure and pressure gradient curves for a 1.4 solar-mass neutron star. This figure shows visually that a pressure gradient cannot produce a global change in momentum. The highlighted area under the pressure gradient curve represents the total integrated pressure force. As long as the pressure itself tends to zero asymptotically, then the highlighted area under the curve must necessarily add to zero. In fact, in one dimension this is just a restatement of the Fundamental Theorem of Calculus, $\int_a^b [-F(x)]\ \mathrm{d}x = P(b) - P(a)$, where $dP/dx \equiv -F(x)$. In multiple dimensions, it is the Divergence Theorem, $\int_\Omega \nabla_\mu P^\mu(\mathbf{x}) = \oint_{\partial\Omega} F^\mu(\mathbf{x})\ \mathrm{d}S_\mu$.

(2.61b) the *physical source*, whereas we will henceforth refer to the R.H.S. of Eqs. (2.10) and (2.11) as the *standard source*.

It is also worth noting that from an analytic point of view, by moving the pressure gradient into the source we have in no way spoiled the conservative nature of the evolution equations. Given the appropriate boundary conditions, the gradient of the pressure must add to zero globally, so its appearance on the R.H.S. cannot have an impact on global conservation.

In fact, any vector (including the 4-force) can be expressed as the sum of a gradient and a curl,

$$\mathbf{F} = \nabla\Phi + \nabla \times \mathbf{A}, \tag{2.62}$$

(see, e.g., [37]). As pointed out in Figure 2.11, any gradient must sum to zero globally whenever the corresponding potential function (pressure, in the context of this discussion) goes to zero at the boundaries. So only a nonzero curl piece can spoil conservation (see

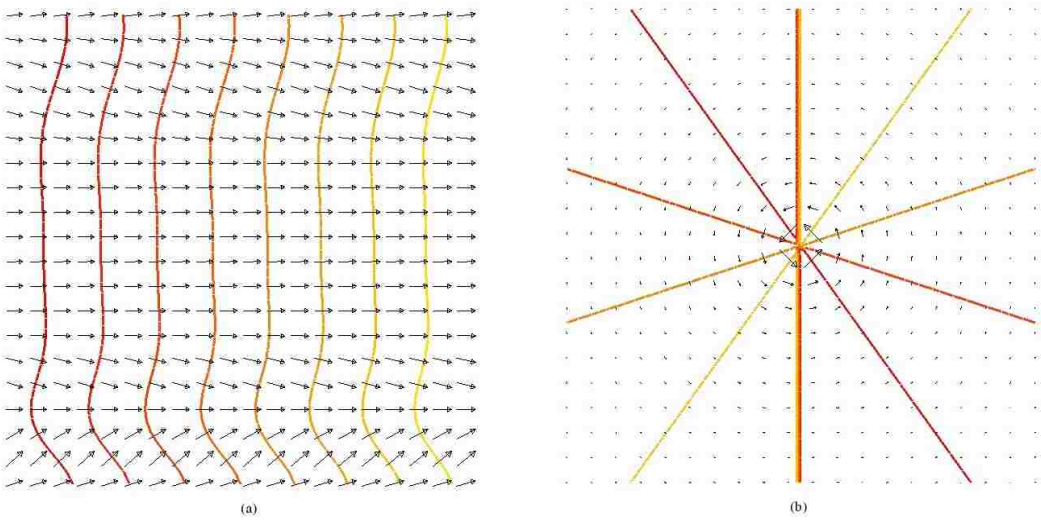

Figure 2.12: Two vector fields and contour lines of constant potential. (a) A curl-less vector field has a potential representation because path integrals depend only on endpoints, and closed path integrals are zero. (b) Any curl contributing to a vector field cannot have the traditional potential representation because path integrals now depend on the choice of path, and closed path integrals are not necessarily zero.

Figure 2.12). And the deviation of $\nabla \times \mathbf{A}$ from zero is a good measure of the degree to which global conservation is lost.

We should make it clear that by separating the $\partial_i P$ term from the flux term on the L.H.S. of the Euler equations – or even by including $\partial_i P$ on the R.H.S. as part of the source – we are not suggesting that the effects of the pressure should be ignored when determining the characteristic structure of the hydrodynamic flow. In Godunov schemes, for example, pressure is a critical element of any Riemann solver that is used to compute accurate approximations to the fluxes of conserved quantities. We are suggesting instead that the geometry factors that give rise to the naked pressure term be strategically extracted before spatial derivatives of the pressure are evaluated on the L.H.S. (or on the R.H.S.), in a manner analogous to the approach that Neilsen & Choptuik [49] adopted (see their Appendix B) to eliminate the naked pressure terms in their numerical study of the critical collapse of spherically symmetric perfect fluids. In particular, the manner in which values of the pressure are reconstructed at cell interfaces before spatial derivatives of the pressure

are evaluated should be in accordance with the manner in which values of key conserved variables are reconstructed.

3. Generalized State Variables

3.1 Construction

The central feature of the generalized formalism we are proposing is its ability to handle generalized state variables, and thereby hopefully reduce the magnitude of the corresponding sources. A weighted linear combination of the Euler equations (in the standard form of either expression 2.10 or 2.11, where the pressures are still buried inside the L.H.S.) can be taken in an attempt to manage the source term. The weighting is accomplished by contracting the Euler equations with a vector field that will characterize some new state variable. As a result, we will call this the *characteristic vector*, $\mathbf{C}$. Since this will result in a single Euler equation, we will require four independent characteristic vectors $\mathbf{C}_{(\eta)}$ to produce four independent Euler equations.

Contracting expression (2.11) with this characteristic vector, we find that

$$\frac{1}{\sqrt{-g}}\, C^{\nu}{}_{(\eta)}\, \partial_{\mu}\left(\sqrt{-g}\; T^{\mu}{}_{\nu}\right) = C^{\nu}{}_{(\eta)}\; T^{\mu}{}_{\alpha}\Gamma^{\alpha}_{\mu\nu}.$$

The weighting factor, $C^{\nu}{}_{(\eta)}$, appearing on the L.H.S. should be brought inside the partial derivative, using the product rule. This, of course, produces an additional term.

$$\frac{1}{\sqrt{-g}}\, \partial_{\mu}\left(\sqrt{-g}\; T^{\mu}{}_{\nu} C^{\nu}{}_{(\eta)}\right) - T^{\mu}{}_{\nu}\; \partial_{\mu} C^{\nu}{}_{(\eta)} = C^{\nu}{}_{(\eta)}\; T^{\mu}{}_{\alpha}\Gamma^{\alpha}_{\mu\nu}.$$

The extra term that is produced should then be moved to the R.H.S. and included as part of the source so that our new Euler equation will assume the conservative form of Eq. (2.12) with $T^{\mu}{}_{\nu}C^{\nu}{}_{(\eta)}$ now becoming the new $\mathcal{Q}^{\mu}{}_{(\eta)}$ for this particular Euler equation. It is important to recognize that while the new state variable we will produce – associated with $T^{\mu}{}_{\nu}C^{\nu}{}_{(\eta)}$ – is just a linear combination of the old state variables, the term we are moving to the R.H.S. will supplement the linear combination of old sources we have constructed.

$$\frac{1}{\sqrt{-g}}\, \partial_{\mu}\left(\sqrt{-g}\; T^{\mu}{}_{\nu} C^{\nu}{}_{(\eta)}\right) = T^{\mu}{}_{\nu}\left(\partial_{\mu} C^{\nu}{}_{(\eta)} + \Gamma^{\nu}_{\mu\alpha} C^{\alpha}{}_{(\eta)}\right).$$

The source material inside the parentheses now fits the definition of an exact covariant derivative (see, for example, [46] or [25]), so our new Euler equation can be written simply as

$$\frac{1}{\sqrt{-g}}\,\partial_\mu\left(\sqrt{-g}\;T^\mu{}_\nu C^\nu{}_{(\eta)}\right) = T^\mu{}_\nu \nabla_\mu C^\nu{}_{(\eta)}. \tag{3.1}$$

If we had started instead with Eq. (2.10), we would have obtained the equivalent form,

$$\frac{1}{\sqrt{-g}}\,\partial_\mu\left(\sqrt{-g}\;T^{\mu\nu} C_{\nu(\eta)}\right) = T^{\mu\nu} \nabla_\mu C_{\nu(\eta)}\,. \tag{3.2}$$

Papadopoulos and Font were the first to show [58] (see also [32, 33, 34]) that this procedure could be used to form a weighed linear combination of the Euler equations in their standard form.[1] This Euler equation can also be expressed in physical form by substituting in the definition of the stress-energy tensor from expression (2.4) and separating the pressure terms from the other terms. Doing so produces

$$\begin{aligned}\frac{1}{\sqrt{-g}}\,\partial_\mu\left(\sqrt{-g}\;\rho h u_\nu C^\nu{}_{(\eta)}\;u^\mu\right) \;&+\; \frac{1}{\sqrt{-g}}\,\partial_\mu\left(\sqrt{-g}\;P C^\mu{}_{(\eta)}\right) \\ &= \rho h u^\mu u_\nu\;\nabla_\mu C^\nu{}_{(\eta)} + P\;\nabla_\mu C^\mu{}_{(\eta)}.\end{aligned} \tag{3.3}$$

We can now use the product rule to break apart the second term on the L.H.S., and the definition of covariant differentiation to break apart the second term on the R.H.S.,

$$\begin{aligned}\frac{1}{\sqrt{-g}}\,\partial_\mu\left(\sqrt{-g}\;\rho h u_\nu C^\nu{}_{(\eta)}\;u^\mu\right) \;&+\; P\;\partial_\mu C^\mu{}_{(\eta)} + P\Gamma^\mu_{\mu\nu} C^\nu{}_{(\eta)} + C^\mu{}_{(\eta)}\;\partial_\mu P \\ &= \rho h u^\mu u_\nu\;\nabla_\mu C^\nu{}_{(\eta)} + P\;\partial_\mu C^\mu{}_{(\eta)} + P\Gamma^\mu_{\mu\nu} C^\nu{}_{(\eta)}.\end{aligned} \tag{3.4}$$

The naked pressure term now comes in two pieces (the second and third terms on either side of 3.4), but could be written more succinctly as $P\;\nabla_\mu C^\mu{}_{(\eta)}$. Cancelling these terms leaves us with the analytically-equivalent physical expression,

$$\frac{1}{\sqrt{-g}}\,\partial_\mu\left(\sqrt{-g}\;\rho h u_\nu C^\nu{}_{(\eta)}\;u^\mu\right) = \rho h u^\mu u_\nu\;\nabla_\mu C^\nu{}_{(\eta)} - C^\mu{}_{(\eta)}\;\partial_\mu P \tag{3.5a}$$

$$= \left(T^\mu{}_\nu - P\delta^\mu{}_\nu\right)\;\nabla_\mu C^\nu{}_{(\eta)} - C^\mu{}_{(\eta)}\;\partial_\mu P\,. \tag{3.5b}$$

$$= T^\mu{}_\nu \nabla_\mu C^\nu - \nabla_\mu P C^\mu \tag{3.5c}$$

[1] While Papadopoulos and Font were considering this from the context in which **C** is chosen to be a Killing vector (in which case the R.H.S. vanishes entirely), one is not necessarily required to make that choice.

Separating spacelike pieces from timelike pieces, it again becomes possible to give a physical interpretation to each term appearing in Eq. (3.5a).

$$\overbrace{\frac{1}{\sqrt{-g}}\,\partial_0\left(\sqrt{-g}\;\rho h u_\nu C^\nu{}_{(\eta)}\;u^0\right)}^{\substack{\text{time-rate-of-change of}\\ \text{generalized state variable}}} + \overbrace{\frac{1}{\sqrt{-g}}\,\partial_j\left(\sqrt{-g}\;\rho h u_\nu C^\nu{}_{(\eta)}\;u^j\right)}^{\substack{\text{traditional flux of}\\ \text{generalized state variable}}} = \underbrace{\rho h u^\mu u_\nu\;\nabla_\mu C^\nu{}_{(\eta)}}_{\substack{\text{gravity ``force''}\\ \text{impacting generalized}\\ \text{state variable}}}\;\underbrace{-C^\mu{}_{(\eta)}\;\partial_\mu P}_{\substack{\text{pressure ``force''}\\ \text{impacting generalized}\\ \text{state variable}}}\;. \tag{3.6}$$

Here the word "force" really means a *generalized force*. Depending on the geometric character of the chosen state variable, it may actually be a force component, a torque component, or even a power.

$$\frac{\mathrm{d}p^i}{\mathrm{d}t} = F^i \qquad \frac{\mathrm{d}L^i}{\mathrm{d}t} = \tau^i \qquad \frac{\mathrm{d}E}{\mathrm{d}t} = \mathcal{P}$$

In practice, this generalized approach amounts to specifying a generalized momentum density or energy density, $\psi_{(\eta)} \equiv \rho h u_\nu C^\nu{}_{(\eta)}$, that one wants to advect during a given numerical simulation. The choice of characteristic vector fields is restricted only by smoothness conditions. Papadopoulos and Font pointed out that the R.H.S. of Eq. (3.1) vanishes if $\mathbf{C}_{(\eta)}$ is chosen to be a Killing vector. In Chapter 4 we explore how the properties of various physical flows can motivate other choices of $\mathbf{C}_{(\eta)}$.

3.2 Generalized Valencia Formulation

With a generalized Euler equation now in hand, it is possible to construct a generalized Valencia formulation to reflect the free choice of state variable. In so doing, we also modify the original Valencia formulation (as suggested in §§2.7 and 2.8) by first extracting all the pressure terms from the L.H.S. of the original momentum equations (2.26), thereby leaving them in the physical form of (2.61a). But recall that we do not remove pressure terms from the L.H.S. of the energy equation (2.27); it is left in standard form. Fundamentally our derivation is not new (except in its treatment of pressure terms) since Papadopoulos and Font [58] already have shown how Eq. (3.1) can be expressed as a set of hyperbolic conservation laws.

Before presenting the fully-generalized Valencia formulation, we present a simplified version of the generalized Valencia formulation that allows for the intermixing of momentum equations, but not with the energy equation, by choosing three characteristic vectors that satisfy the conditions,

$$C^0{}_{(i')} = 0 \,, \tag{3.7a}$$

$$C^i{}_{(i')} = \tilde{C}^j{}_{(i')} \,, \tag{3.7b}$$

where $i' \rightarrow 2$, 3, or 4. This avoids the complication of mixing three equations that are in physical form with an equation that is in standard form.

In this simplified version of the generalized Valencia forulation, the field equations can still be written in the form of Eq. (2.28),

$$\frac{1}{\alpha\sqrt{\gamma}}\left(\partial_0 \, \sqrt{\gamma} \, \tilde{\mathcal{F}}^0{}_{(\eta)} + \partial_j \, \alpha\sqrt{\gamma} \, \tilde{\mathcal{F}}^j{}_{(\eta)}\right) = \tilde{\mathcal{S}}_{(\eta)}, \tag{3.8}$$

but the relevant state vector,

$$\tilde{\mathcal{F}}^0{}_{(\eta)} \equiv \left(D, \tilde{S}_{(i')}, \tau\right)^T, \tag{3.9}$$

now takes the form,

$$D \equiv \rho W \,, \tag{3.10a}$$

$$\tilde{S}_{(i')} \equiv \rho h W u_j \tilde{C}^j{}_{(i')} = \rho h W^2 v_j \tilde{C}^j{}_{(i')} \,, \tag{3.10b}$$

$$\begin{aligned} \tau &\equiv \rho h c W \alpha u^0 - P - c^2 D \\ &= \rho h c^2 W^2 - P - c^2 D \,. \end{aligned} \tag{3.10c}$$

As one would expect, only the momentum state variables have been redefined. Here the i subscript (which counts momentum equations) is primed to emphasize the fact that this momentum equation is *not* equivalent to the momentum equation identified by the unprimed subscript i in the original Valencia formulation. The fluxes become,

$$\tilde{\mathcal{F}}^j{}_{(\eta)} \equiv \left(D\frac{u^j}{\alpha u^0} \;,\; \tilde{S}_{(i')}\frac{u^j}{\alpha u^0} \;,\; \tau\frac{u^j}{\alpha u^0} + \frac{P}{c}v^j\right)^T, \tag{3.11}$$

and the sources become,

$$\tilde{\mathcal{S}}_{(\eta)} \equiv \begin{pmatrix} 0 \\ \left(T^{\mu\beta} - Pg^{\mu\beta}\right)\left(g_{\beta j}\ \partial_\mu \tilde{C}^j{}_{(i')} + \left(\partial_\mu g_{j\beta} - \Gamma^\delta_{\mu\beta} g_{\delta j}\right)\tilde{C}^j{}_{(i')}\right)/c - \tilde{C}^j{}_{(i')}\ \partial_j P/c \\ \alpha\left(T^{\mu 0}\ \partial_\mu \ln\alpha - T^{\mu\nu}\Gamma^0_{\mu\nu}\right) \end{pmatrix}. \tag{3.12}$$

The quantity $v_j \tilde{C}^j{}_{(i')}$ that appears in Eq. (3.10b) represents the component of the 3-velocity that points along $\tilde{\mathbf{C}}_{(i')}$. In this formulation the ψ's appearing in Eq. (2.12) are

$$\psi_{(1)} = \rho\ , \tag{3.13a}$$

$$\psi_{(i')} = \rho h u_j \tilde{C}^j{}_{(i')}\ , \tag{3.13b}$$

$$\psi_{(5)} = \rho h u^0\ . \tag{3.13c}$$

For the sake of convenience, we will tend to call these the *advection variables*, and they are directly related to the conservative state variables as follows,

$$D \equiv W\psi_{(1)}\,, \tag{3.14a}$$

$$\tilde{S}_{(i')} \equiv W\psi_{(i')}\,, \tag{3.14b}$$

$$\tau \equiv cW\alpha\psi_{(5)} - P - c^2 W\psi_{(1)}\,. \tag{3.14c}$$

Since $W \equiv (1 - v^2/c^2)^{-1/2}$ is the Lorentz factor relating the fluid frame and the coordinate frame, and since $\psi_{(i')}/W \equiv \rho h v_j \tilde{C}^j{}_{(i')}$ is the generalized momentum density as measured by a comoving observer (that is, the proper generalized momentum density), the product $W\psi_{(i')}$ represents the generalized momentum density as measured by an Eulerian observer. (The first Lorentz factor scales up the relativistic mass, and the second takes care of length contraction—both tend to increase the momentum density.) Note that the original Valencia formulation, as presented here in §2.5, can be retrieved from our generalized formulation by choosing our three characteristic vectors to be the Cartesian basis vectors, $\tilde{\mathbf{C}}_{(i')} = \mathbf{e}_i = \beta_i \mathbf{e}^0 + \gamma_{ij}\mathbf{e}^j$, and reintroducing naked pressure terms.

Our fully-generalized Valencia formulation is not as clean as the original Valencia formulation. This is because our weighted linear combination mixes (or has the potential to mix, given an appropriate characteristic vector) momentum and energy equations and, con-

sequently, involves pieces that are in physical form and other pieces that are in standard form. (For a full derivation, see Appendix B.)

The field equations can still be written as Eq. (2.28),

$$\frac{1}{\alpha\sqrt{\gamma}}\left(\partial_0\ \sqrt{\gamma}\ \hat{\mathcal{F}}^0{}_{(\eta)} + \partial_j\ \alpha\sqrt{\gamma}\ \hat{\mathcal{F}}^j{}_{(\eta)}\right) = \hat{\mathcal{S}}_{(\eta)}, \tag{3.15}$$

but the relevant state vector,

$$\hat{\mathcal{F}}^0{}_{(\eta)} \equiv \left(D, \hat{S}_{(i')}, \hat{\tau}\right)^T, \tag{3.16}$$

takes the form,

$$D \equiv \rho W\,, \tag{3.17a}$$

$$\hat{S}_{(i')} \equiv \tilde{S}_{(i')} + C^0{}_{(i')}\frac{\tau}{\alpha} = \rho h W^2 v_j C^j{}_{(i')} + \frac{1}{\alpha}C^0{}_{(i')}\left(\rho h c^2 W^2 - P - c^2 D\right), \tag{3.17b}$$

$$\hat{\tau} \equiv \tau + cS_j C^j{}_{(5)} = \left(\rho h c^2 W^2 - P - c^2 D\right)(c/\alpha)\, C^0{}_{(5)} + \rho h c W^2 v_j C^j{}_{(5)}\,. \tag{3.17c}$$

Only the continuity state variable maintains its original definition. The sources, though, are by far the messiest, and can be expressed most easily as,

$$\hat{\mathcal{S}}_{(\eta)} \equiv \begin{pmatrix} 0 \\ \tilde{\mathcal{S}}_{(i')} + \frac{1}{c}\,\tilde{\mathcal{S}}_{(5)}\Big|_{C^0{}_{(5)}\to C^0{}_{(i')}} \\ \tilde{\mathcal{S}}_{(5)} + c\,\tilde{\mathcal{S}}_{(i')}\Big|_{C^j{}_{(i')}\to C^j{}_{(5)}} \end{pmatrix}. \tag{3.18}$$

Fundamentally, the nonlinear nature of the three components of the momentum equation arises from the product of velocities that appears inside the flux term. However, it is clear from the form of Eq. (2.35) that the two velocities that make up this product carry different physical interpretations. One is the transport velocity and the other is intimately connected with the conservative state variable $\hat{S}_{(i')}$, that is, the generalized momentum density of the fluid. While it has been customary to evolve components of the fluid momentum defined by the same set of basis vectors that is used to specify the grid geometry (and, consequently, the transport velocities [74, 10]), this is not necessary. There are a variety of reasons why, in a given numerical simulation, it may be desirable to evolve components of the momentum corresponding to some other set of basis vectors. In what follows, we highlight several such examples and, in each case, outline an approach that can be taken to identify the appropriate

set of characteristic vector fields $\mathbf{C}_{(\eta)}$. Through the definition of $\hat{S}_{(i')}$ given by Eq. (3.17b), our generalized Valencia formulation provides a structure through which such state variables can be evolved.

3.3 Generalized Flux Terms

While it is possible, using our generalized formalism, to evolve state variables defined by characteristic vectors that are independent of the chosen coordinates/grid geometry, one difficulty associated with choosing a state variable that is independent of the grid geometry is that it can be very confusing to construct the fluxes that compose the divergence term.

Expressing the state variables and fluxes explicitly in terms of the primitives (blue) which depend on the choice of coordinates and not the generalized advection variables, and the conservatives (red) which depend on the choice of generalized advection variables and not the coordinates, the continuity equation becomes,

$$\begin{aligned} &\frac{1}{\alpha\sqrt{\gamma}}\oint_{\partial\Omega} W\psi_{(1)}\,\left(\sqrt{\gamma}\,\mathrm{d}S_0\right) \\ +\;&\frac{1}{\alpha\sqrt{\gamma}}\oint_{\partial\Omega} W\psi_{(1)}\left[\frac{\sqrt{\gamma}}{\sqrt{\gamma\{i\}}}\left(v^i-c\beta^i/\alpha\right)\right]\left(\sqrt{\gamma\{i\}}\,\frac{\mathrm{d}S_i}{\mathrm{d}x^0}\right)\left(\alpha/c\;\mathrm{d}x^0\right)=0, \end{aligned} \tag{3.19a}$$

the three momentum equations become,

$$\begin{aligned} &\frac{1}{\alpha\sqrt{\gamma}}\oint_{\partial\Omega} W\psi_{(i')}\,\left(\sqrt{\gamma}\,\mathrm{d}S_0\right) \\ +\;&\frac{1}{\alpha\sqrt{\gamma}}\oint_{\partial\Omega} W\psi_{(i')}\left[\frac{\sqrt{\gamma}}{\sqrt{\gamma\{i\}}}\left(v^i-c\beta^i/\alpha\right)\right]\left(\sqrt{\gamma\{i\}}\,\frac{\mathrm{d}S_i}{\mathrm{d}x^0}\right)\left(\alpha/c\;\mathrm{d}x^0\right) \\ =\;&\frac{1}{\alpha\sqrt{\gamma}}\int_{\Omega}\left\{\left(T^{\mu\beta}-Pg^{\mu\beta}\right)\left[g_{\beta\nu}\partial_\mu C^{\nu}{}_{(j')}+\left(\partial_\mu g_{\alpha\beta}-\Gamma^{\delta}_{\mu\beta}g_{\delta\alpha}\right)C^{\alpha}{}_{(j')}\right]-C^{\mu}{}_{(j')}\partial_\mu P\right\} \\ &\qquad\cdot\left(\sqrt{\gamma}\,\frac{\mathrm{d}\Omega}{\mathrm{d}x^0}\right)\left(\alpha/c\;\mathrm{d}x^0\right), \end{aligned} \tag{3.19b}$$

and the energy equation becomes,

$$
\begin{aligned}
& \frac{1}{\alpha\sqrt{\gamma}} \oint_{\partial\Omega} \left(cW\alpha\ \psi_{(5)} + \alpha^2 P C^0{}_{(5)} - c^2 W\ \psi_{(1)}\right)\ \left(\sqrt{\gamma}\ \mathrm{d}S_0\right) \\
+ & \frac{1}{\alpha\sqrt{\gamma}} \oint_{\partial\Omega} \left(cW\alpha\ \psi_{(5)} + \alpha^2 P C^0{}_{(5)} - c^2 W\ \psi_{(1)}\right) \left[\frac{\sqrt{\gamma}}{\sqrt{\gamma\{i\}}}\left(v^i - c\beta^i/\alpha\right)\right] \\
& \qquad \cdot \left(\sqrt{\gamma\{i\}}\ \frac{\mathrm{d}S_i}{\mathrm{d}x^0}\right)\left(\alpha/c\ \mathrm{d}x^0\right) \\
- & \frac{1}{\alpha\sqrt{\gamma}} \oint_{\partial\Omega} \frac{\sqrt{\gamma}}{\sqrt{\gamma\{i\}}} \left(\alpha^2 P C^0{}_{(5)} v^i - c\alpha P \gamma^{ij} C_{j\,(5)}\right)\left(\sqrt{\gamma\{i\}}\ \frac{\mathrm{d}S_i}{\mathrm{d}x^0}\right)\left(\alpha/c\ \mathrm{d}x^0\right) \\
= & \frac{1}{\alpha\sqrt{\gamma}} \int_{\Omega} c\alpha T^{\mu\nu} \left(C_{\nu(5)}\partial_\mu \ln\alpha + \partial_\mu C_{\nu(5)} - \Gamma^\beta_{\mu\nu} C_{\beta(5)}\right)\left(\sqrt{\gamma}\ \frac{\mathrm{d}\Omega}{\mathrm{d}x^0}\right)\left(\alpha/c\ \mathrm{d}x^0\right).
\end{aligned}
\tag{3.19c}
$$

The sources are very complicated hybrid expressions. While the numerical value of the sources does not depend on the choice of coordinates, some of the pieces used to construct the sources do depend on the coordinates. For example, anything involving the metric depends on the coordinates. Apparently, the coordinate-dependent pieces must combine in just such a way as to eliminate all coordinate-dependence from the sources.

4. The Characteristic Vector

The potential uses for this generalized formalism (involving generalized Euler equations) that we have recommended are numerous. Perhaps this can best be appreciated through the presentation of various approaches in choosing a characteristic vector. Each option presented herein is motivated by the potential for improved numerical accuracy in standard finite volume codes.

4.1 Coordinate Basis Vectors

Without the aid of a generalized formalism, sets of state variables have customarily been chosen in a manner that is consistent with the chosen grid geometry; this seems like the obvious thing to do. This approach is equivalent to choosing characteristic vectors that equal the coordinate basis vectors; that is, it is equivalent to setting

$$\mathbf{C}_{(\eta)} = \mathbf{e}_{\eta}. \tag{4.1}$$

By adopting this definition of $\mathbf{C}_{(j')}$, the set of conservative variables from the original Valencia formulation is recovered. And if the basis vectors define a curvilinear coordinate system — see, for example, the variety of orthogonal curvilinear basis sets accommodated in Stone & Norman's ZEUS code [74] — then via Eq. (3.13b) the characteristic vector field assignment (4.1) will produce a new set of conservative variables that corresponds to the geometry of that chosen coordinate system. For example, setting $\mathbf{C} = \mathbf{e}_R$ produces cylindrical radial momentum as one of the state variables, and its physical source will of course *not* be zero except in equilibrium when pressure exactly counterbalances gravity.

A more strategic selection of the characteristic vector fields $\mathbf{C}_{(\eta)}$ can result in a minimization – if not a complete elimination – of the source terms associated with Eq. (3.15). Such a selection would be advantageous because, as we have already discussed, global and/or local conservation of key physical quantities can be ensured when source terms are zero.

It is desirable to set the standard source to zero because this ensures global conservation of the chosen conservative state variable, as long as the gradient of the pressure is zero on

the computational boundary, and no advection occurs through the boundary. The situation is even more desirable if the physical source can be set to zero because, beyond global conservation, this produces local conservation everywhere. (Eliminating the standard source does not produce local conservation because the pressure is mixed inside the advected flux.) In the following three sections, we outline three options toward eliminating the source.

4.2 Killing Vectors

It is straightforward to show, as Papadopoulos and Font did [58], that if any of the characteristic vectors is chosen to be a Killing vector — that is, a vector that satisfies Killing's equations,

$$\nabla_\mu C_\nu + \nabla_\nu C_\mu = 0_{\mu\nu}, \tag{4.2}$$

then the standard source (the R.H.S. of Eq. 3.2 or, equivalently, of Eq. 3.1) vanishes.[1] This is because the stress-energy tensor is symmetric while, by requirement of Killing's equations, $\nabla\mathbf{C}$ is exclusively antisymmetric. Owing to the stress-energy tensor's symmetry, the standard source can be rewritten as,

$$T^{\mu\nu}\left(\nabla_\mu C_{\nu(\eta)} + \nabla_\nu C_{\mu(\eta)}\right).$$

And by requirement of Killing's equations, the term is parentheses is explicitly zero.

But generally speaking, unless the problem being studied is embedded in a highly symmetric manifold, it will not be possible to find even one global vector field that satisfies Eq. (4.2). On the other hand, if a problem is being studied in which certain symmetries are being imposed — for example, a spherically symmetric or axisymmetric manifold — then it likely will not be necessary to solve Killing's equations as the imposed symmetries will identify the appropriate Killing vector(s) *a priori*. Once one or more Killing vectors have been identified, the associated conservative variable(s) can be constructed by using Eqs. (3.17b)

[1] The physical source may also vanish, but this is not guaranteed. For example, consider a near-equilibrium problem carried out on an axisymmetric background metric. Due to the background metric's axisymmetry, there will be no gravitational forces in the azimuthal direction, but rather an azimuthal Killing vector. Consequently, the standard source associated with the angular momentum Euler equation will be zero. But if the azimuthal component of the pressure gradient is not identically zero everywhere, then the physical source will be nonzero—despite the existence of an azimuthal Killing vector.

and (3.17c). But some other approach will be needed to construct any remaining conservative quantities. We will present additional alternatives to choosing characteristic vectors in the following sections, but first we pause to dwell on the richness of the Killing vector.

4.2.1 Meaning of a Killing Vector

A Killing vector field represents a metric-preserving transformation. That is, if a transformation is performed on the metric such that the coordinates are all shifted infinitesimally along the Killing vector field,

$$\mathbf{x} \to \mathbf{x}' = \mathbf{x} + \alpha \mathbf{C}, \tag{4.3}$$

then the metric will remain unchanged up to first order in the infinitesimal parameter α. Physically, this means the Killing vector represents a symmetry in the geometry of the manifold.

Another way of thinking about a Killing vector field is to say that it describes a coordinate transformation that is rigid in the sense that it does not stretch or squash any region of the manifold. When a Killing vector field exists, weighted linear combinations of the Euler equations can be taken to produce an energy or a momentum conservation law. So Killing vector fields also give rise to conserved quantities associated with energy and momentum.

4.2.2 Derivation of Killing's Equations

We now show how Killing's equations are derived directly from the metric. The covariant components of the metric transform as

$$g_{\mu\nu}(\mathbf{x}) = \frac{\partial x'^{\alpha}}{\partial x^{\mu}} \frac{\partial x'^{\beta}}{\partial x^{\nu}} g'_{\alpha\beta}(\mathbf{x}'). \tag{4.4}$$

This gives the relationship between the functional dependence of the old metric g on the old coordinates $\mathbf{x}$ and the functional dependence of the new metric g' on the new coordinates $\mathbf{x}'$. Of course, in order for $\mathbf{C}$ to be a Killing vector, we must require that ${g'}_{\mu\nu}$ have the same functional dependence on $\mathbf{x}'$ as $g_{\mu\nu}$ has on $\mathbf{x}$. Then we have the following requirement for $\mathbf{C}$ to be a Killing vector field,

$$g_{\mu\nu}(\mathbf{x}) = \frac{\partial x'^{\alpha}}{\partial x^{\mu}} \frac{\partial x'^{\beta}}{\partial x^{\nu}} g_{\alpha\beta}(\mathbf{x} + \alpha \mathbf{C}). \tag{4.5}$$

Using Taylor's theorem (up to first order in α) on the metric, and noting that

$$\frac{\partial x'^{\alpha}}{\partial x^{\mu}} = \partial_{\mu}\left(x^{\alpha} + \alpha C^{\alpha}\right) = \delta^{\alpha}{}_{\mu} + \alpha \partial_{\mu} C^{\alpha}, \tag{4.6}$$

we find that

$$g_{\mu\nu}\left(\mathbf{x}\right) = \left(\delta^{\alpha}{}_{\mu} + \alpha \partial_{\mu} C^{\alpha}\right)\left(\delta^{\beta}{}_{\nu} + \alpha \partial_{\nu} C^{\beta}\right)\Big(g_{\alpha\beta}\left(\mathbf{x}\right) + \alpha C^{\sigma}\partial_{\sigma} g_{\alpha\beta}\left(\mathbf{x}\right)\Big). \tag{4.7}$$

Expanding this, and neglecting any remaining second order terms in α brings us to

$$g_{\mu\nu} = g_{\mu\nu} + \alpha\left(g_{\alpha\nu}\partial_{\mu}C^{\alpha} + g_{\mu\beta}\partial_{\nu}C^{\beta} + C^{\sigma}\partial_{\sigma}g_{\mu\nu}\right). \tag{4.8}$$

Cancelling the $g_{\mu\nu}$ on either side leaves us with

$$g_{\alpha\nu}\partial_{\mu}C^{\alpha} + g_{\mu\beta}\partial_{\nu}C^{\beta} + C^{\sigma}\partial_{\sigma}g_{\mu\nu} = 0_{\mu\nu} \tag{4.9}$$

If we do not mind picking up a few additional terms, we can write this expression using covariant derivatives rather than partials.

$$g_{\alpha\nu}\nabla_{\mu}C^{\alpha} - g_{\alpha\nu}\Gamma^{\alpha}_{\mu\beta}C^{\beta} + g_{\mu\beta}\nabla_{\nu}C^{\beta} - g_{\mu\beta}\Gamma^{\beta}_{\nu\alpha}C^{\alpha} + C^{\sigma}\nabla_{\sigma}g_{\mu\nu} + C^{\sigma}\Gamma^{\alpha}_{\sigma\mu}g_{\alpha\nu} + C^{\sigma}\Gamma^{\alpha}_{\sigma\nu}g_{\mu\alpha} = 0_{\mu\nu} \tag{4.10}$$

Fortunately, all the terms involving Christoffel symbols cancel, and the covariant derivative of the metric is identically zero. That leaves just two terms on the L.H.S. Moving the metric inside the covariant derivative, and using it to lower the index on $\mathbf{C}$ in each of those terms gives us

$$\nabla_{\mu}C_{\nu} + \nabla_{\nu}C_{\mu} = 0_{\mu\nu}. \tag{4.11}$$

These are Killing's equations as they appear in expression (4.2).

4.2.3 Common Examples of Some Killing Vectors

Let

$$g_{\mu\nu} = \begin{pmatrix} -c^2 & 0 & 0 & 0 \\ 0 & 1 & 0 & 0 \\ 0 & 0 & R^2 & 0 \\ 0 & 0 & 0 & 1 \end{pmatrix} \quad \text{and} \quad x^{\mu} = \begin{pmatrix} t \\ R \\ \phi \\ z \end{pmatrix},$$

so that

$$ds^2 = -c^2\ dt^2 + dR^2 + R^2\ d\phi^2 + dz^2.$$

The azimuthal Killing vector for this metric is

$$\mathbf{C}_{(\phi)} = \mathbf{e}_{\phi}.$$

It implies the following coordinate transformation,

$$\left.\begin{array}{ccccc} t & \rightarrow & t' & = & t \\ R & \rightarrow & R' & = & R \\ \phi & \rightarrow & \phi' & = & \phi + \alpha \\ z & \rightarrow & z' & = & z \end{array}\right\} \quad \Longrightarrow \quad ds^2 \rightarrow ds'^2 = -c^2\ dt'^2 + dR'^2 + R'^2 + d\phi'^2 + dz'^2$$

This means that

$$g'_{\mu\nu} = \begin{pmatrix} -c^2 & 0 & 0 & 0 \\ 0 & 1 & 0 & 0 \\ 0 & 0 & R'^2 & 0 \\ 0 & 0 & 0 & 1 \end{pmatrix}.$$

These are new coordinates, but the transformed metric has the same dependence on these as the old metric had on the old coordinates. This is what it means for the transformation to "preserve the metric."

Consider the same Killing symmetry as before, but now from within the framework of Cartesian coordinates. Now,

$$g_{\mu\nu} = \begin{pmatrix} -c^2 & 0 & 0 & 0 \\ 0 & 1 & 0 & 0 \\ 0 & 0 & 1 & 0 \\ 0 & 0 & 0 & 1 \end{pmatrix}, \quad \text{and} \quad x^{\mu} = \begin{pmatrix} t \\ x \\ y \\ z \end{pmatrix},$$

so that

$$ds^2 = -c^2\ dt^2 + dx^2 + dy^2 + dz^2.$$

The azimuthal Killing vector now takes the form

$$\mathbf{C}_{(\phi)} = -y\ \mathbf{e}_x + x\ \mathbf{e}_y,$$

which implies the following coordinate transformation,

$$\begin{array}{ccccc} t & \rightarrow & t' & = & t, \\ x & \rightarrow & x' & = & x - \alpha y, \\ y & \rightarrow & y' & = & y + \alpha x, \\ z & \rightarrow & z' & = & z. \end{array}$$

Inverting this system of equations leads to

$$\left.\begin{array}{rcl} t &=& t' \\ x &=& \dfrac{x' + \alpha y'}{1+\alpha^2} \\ y &=& \dfrac{y' - \alpha x'}{1+\alpha^2} \\ z &=& z' \end{array}\right\} \quad \Longrightarrow \quad \left\{\begin{array}{rcl} dt &=& dt' \\ dx &=& \dfrac{dx' + \alpha\ dy'}{1+\alpha^2} \\ dy &=& \dfrac{dy' - \alpha\ dx'}{1+\alpha^2} \\ dz &=& dz' \end{array}\right.$$

Again, keeping only first-order terms in α, the line element now becomes

$$ds^2 \to ds'^2 = -c^2\ dt'^2 + \left(dx'^2 + 2\alpha\ dx'\ dy'\right) + \left(dy'^2 - 2\alpha\ dx'\ dy'\right) + dz'^2.$$

Cancelling cross-terms, again we see that the metric maintains its original functional dependence on the new coordinates,

$$ds^2 \to ds'^2 = -c^2\ dt'^2 + dx'^2 + dy'^2 + dz'^2.$$

4.2.4 A Counterexample

It may be instructive to include a counterexample. Vectors that do *not* satisfy Killing's equations will produce coordinate transformations that do *not* preserve the metric to first order in the variational parameter. Choose,

$$\mathbf{C}_{(\tilde{\phi})} = \frac{\mathbf{e}_\phi}{R},$$

which implies the following coordinate transformation,

$$\begin{array}{rcccl} t & \to & t' &=& t, \\ R & \to & R' &=& R, \\ \phi & \to & \phi' &=& \phi + \dfrac{\alpha}{R}, \\ z & \to & z' &=& z. \end{array}$$

Inverting this system of equations leads to

$$\left.\begin{array}{rcl} t &=& t' \\ R &=& R' \\ \phi &=& \phi' - \dfrac{\alpha}{R'} \\ z &=& z' \end{array}\right\} \quad \Longrightarrow \quad \left\{\begin{array}{rcl} dt &=& dt' \\ dR &=& dR' \\ d\phi &=& d\phi' + \dfrac{\alpha}{R'^2}\ dR' \\ dz &=& dz' \end{array}\right.$$

Again, keeping only first-order terms in α, the line element now becomes

$$ds^2 \rightarrow ds'^2 = -c^2\ dt'^2 + dR'^2 + R'^2\ d\phi'^2 + 2\alpha\ dR' d\phi' + dz'^2.$$

This time, the first-order term in α does not vanish. So, despite the fact that $\mathbf{e}_\phi/R$ points in the same direction as the Killing vector $\mathbf{e}_\phi$, its $1/R$ scaling precludes it from satisfying Killing's equations and, consequently, from producing a conserved quantity. (Angular momentum is conserved, but azimuthal momentum is not.)

4.3 Quasi-Killing Vectors

In many cases, near-equilibrium problems – involving perturbations over an underlying symmetry – are of particular interest. In these cases, one may be able to take advantage of the quasi-symmetry, despite the fact that the true metric of the problem does not produce any Killing vectors. Quasi-symmetries give rise to quasi-Killing vectors. We will now show, through the application of variational calculus, how this can be done.

Before employing variational calculus to define and determine a quasi-Killing vector, we will introduce the approach and techniques of variational calculus by presenting the derivation of Lagrange's equations.

4.3.1 Lagrange's Equations

I hope the reader will forgive this somewhat-lengthy digression, but building a firm understanding of the derivation of Lagrange's equations will endow us with a better understanding of the quasi-Killing vector problem, and a reference from which to draw guidance. The action, as defined by Hamilton's principle (see e.g., [38]) is

$$S \equiv \int_{t_1}^{t_2} \mathcal{L}\Big(\mathbf{x}(t), \dot{\mathbf{x}}(t), t\Big)\ \mathrm{d}t, \quad \text{where } \mathcal{L} \equiv T - V. \tag{4.12}$$

A unique path is specified by the functions $x^i(t)$. This path can be varied slightly by defining new functional dependences of the coordinates on t, infinitesimally distinct from the previous ones,

$$x^i(t, \alpha) = x^i(t, 0) + \alpha\eta^i(t), \tag{4.13}$$

where here α is a one-dimensional infinitesimal parameter and the $\eta^i(t)$ are functions of t that are arbitrary everywhere except at the endpoints t_1 and t_2; their values are required to be zero at the endpoints since the endpoints of the path are fixed as the path is varied. Notice that as α approaches zero, the varied path approaches the original path. With an expression for the varied path in hand, we can now write the dependence of the action on the variational parameter α,

$$S(\alpha) = \int_{t_1}^{t_2} \mathcal{L}\Big(\mathbf{x}(t,\alpha), \dot{\mathbf{x}}(t,\alpha), t\Big)\, \mathrm{d}t. \tag{4.14}$$

The requirement for a path to be an extremum path is that $S(\alpha) = S(0) + \mathcal{O}(\alpha^2)$. This is the requirement we will use to check our result in a simple physical example once we have finished deriving Lagrange's equations.

Meanwhile, now that we've managed to quantify the path variation in terms of a one-dimensional parameter α, we can talk about differentiating the action with respect to this parameter. The extremum path we seek will be the one that yields a stationary action,

$$\left.\frac{\mathrm{d}S(\alpha)}{\mathrm{d}\alpha}\right|_{\alpha=0} = 0. \tag{4.15}$$

We can move this differentiation inside the action integral because the operations of differentiation with respect to the variational parameter and differentiation with respect to the coordinates do not see each other. Then, using the chain rule, we find that

$$\left.\frac{\mathrm{d}S(\alpha)}{\mathrm{d}\alpha}\right|_{\alpha=0} = \int_{t_1}^{t_2} \left(\frac{\partial \mathcal{L}}{\partial x^i}\frac{\partial x^i}{\partial \alpha} + \frac{\partial \mathcal{L}}{\partial \dot{x}^i}\frac{\partial \dot{x}^i}{\partial \alpha} + \frac{\partial \mathcal{L}}{\partial t}\frac{\partial t}{\partial \alpha}\right)\, \mathrm{d}t, \tag{4.16}$$

where repeated indices imply summation as is customary. The final term is zero since the indepenedent parameter t does not depend on the variational parameter α. Next we apply integration by parts to the second term. (The summation does not preclude us from doing this since integration by parts can be performed independently on each term in the summation.) We have,

$$\left.\frac{\mathrm{d}S(\alpha)}{\mathrm{d}\alpha}\right|_{\alpha=0} = \int_{t_1}^{t_2} \left(\frac{\partial \mathcal{L}}{\partial x^i}\frac{\partial x^i}{\partial \alpha}\, dt\right) + \left.\frac{\partial \mathcal{L}}{\partial \dot{x}^i}\frac{\partial x^i}{\partial \alpha}\right|_{t_1}^{t_2} - \int_{t_1}^{t_2} \left(\frac{d}{dt}\left(\frac{\partial \mathcal{L}}{\partial \dot{x}^i}\right)\frac{\partial x^i}{\partial \alpha}\, \mathbf{d}t\right). \tag{4.17}$$

The middle term is zero since $\partial x^i/\partial\alpha = \eta^i$, which vanish at the endpoints. Combining the two remaining integrals and factoring out the common term, then, leaves us with the

condition

$$\left.\frac{\mathrm{d}s\left(\alpha\right)}{\mathrm{d}\alpha}\right|_{\alpha=0}=\int_{t_1}^{t_2}\left(\frac{\partial\mathcal{L}}{\partial x^i}-\frac{d}{dt}\frac{\partial\mathcal{L}}{\partial\dot{x}^i}\right)\ \eta^i\ \mathbf{d}t=0. \tag{4.18}$$

Recall that this condition must be simultaneously met for all vector functions $\eta\left(t\right)$ that vanish at the endpoints. The only way to do this is by setting the quantity in parentheses to zero. Thus we obtain Lagrange's equations,

$$\frac{\partial\mathcal{L}}{\partial x^i}-\frac{\mathrm{d}}{\mathrm{d}t}\frac{\partial L}{\partial\dot{x}^i}=0_i. \tag{4.19}$$

Now, the promised example. Consider the simple case of a point particle in free fall in one dimension. The kinetic energy is $T=\frac{1}{2}m\dot{z}^2$, and the potential energy is $V=mgz$. Then the Lagrangian is $\mathcal{L}\equiv T-V=\frac{1}{2}m\dot{z}^2-mgz$. The appropriate derivatives of the Lagrangian are:

$$\frac{\partial\mathcal{L}}{\partial z}=-mg \tag{4.20}$$

$$\frac{\partial\mathcal{L}}{\partial\dot{z}}=m\dot{z}. \tag{4.21}$$

So Lagrange's equation gives,

$$\frac{\partial\mathcal{L}}{\partial z}-\frac{\mathrm{d}}{\mathrm{d}t}\frac{\partial\mathcal{L}}{\partial\dot{z}}=-mg-m\ddot{z}=0. \tag{4.22}$$

The general solution for this equation is, of course,

$$z\left(t\right)=-\frac{1}{2}gt^2+v_0t+z_0. \tag{4.23}$$

A small variation around this solution, then, is

$$z\left(t,\alpha\right)=-\frac{1}{2}gt^2+v_0t+z_0+\alpha\eta\left(t\right). \tag{4.24}$$

Now, as a check of Lagrange's equation in this example, we'll verify that in fact the variation of the action does not contain first-order terms in α if $z\left(t\right)$ is taken to be $-\frac{1}{2}gt^2+v_0t+z_0$, as required by Lagrange's equation.

$$S\left(\alpha\right)=\int_{t_1}^{t_2}\left[\frac{1}{2}m\Big(-gt+v_0+\alpha\dot{\eta}\left(t\right)\Big)^2-mg\left(-\frac{1}{2}gt^2+v_0+z_0+\alpha\eta\left(t\right)\right)\right]\ \mathrm{d}t. \tag{4.25}$$

Expanding and organizing in powers of α up to first order, we have

$$S(\alpha) = m\int_{t_1}^{t_2}\left[\left(g^2t^2 - 2v_0gt + \left(\frac{1}{2}{v_0}^2 - gz_0\right)\right) + \alpha\Big(\left(-gt + v_0\right)\ \dot{\eta}(t) - g\eta(t)\Big)\right]\ \mathrm{d}t. \tag{4.26}$$

Notice that the coefficient of the α-term, $\left(-gt + v_0\right)\ \dot{\eta}(t) - g\eta(t)$, is an exact differential, $\mathrm{d}/\mathrm{d}t\ \Big(\left(-gt + v_0\right)\ \eta(t)\Big)$. Integrating gives

$$S(\alpha) = m\left[\left(\frac{1}{3}g^2t^3 - v_0gt^2 + \left(\frac{1}{2}{v_0}^2 - gz_0\right)t\right) + \alpha\Big(-gt + v_0\Big)\ \eta(t)\right]_{t_1}^{t_2} + \mathcal{O}\left(\alpha^2\right). \tag{4.27}$$

Notice that the α-term indeed vanishes since η is zero at the endpoints. Consequently, we see that in this case Lagrange's equation does, in fact, specify a path that yields a stationary value for the action.

Suppose, instead, that we had taken $z(t)$ to be vt, clearly not a path specified by Lagrange's equation. Varying the action with respect to this (wrong) path will contribute a nonzero first-order term in α. The variation of the action now gives

$$S(\alpha) = \int_{t_1}^{t_2}\left[\frac{1}{2}m\Big(v + \alpha\dot{\eta}(t)\Big)^2 - mg\Big(vt + \alpha\eta(t)\Big)\right]\ \mathrm{d}t. \tag{4.28}$$

Expanding and keeping only terms up to first-order in α, we find that

$$S(\alpha) = m\int_{t_1}^{t_2}\left[\left(-vgt + \frac{1}{2}v^2\right) + \alpha\Big(v\dot{\eta}(t) - g\eta(t)\Big) + \mathcal{O}\left(\alpha^2\right)\right]\ \mathrm{d}t. \tag{4.29}$$

This time the α coefficient is not an exact differential, but we can write it as an exact differential and a remainder,

$$S(\alpha) = m\int_{t_1}^{t_2}\left[\left(-vgt + \frac{1}{2}v^2\right) + \alpha\frac{d}{dt}v\eta(t) - \alpha g\eta(t) + \mathcal{O}\left(\alpha^2\right)\right]\ \mathrm{d}t. \tag{4.30}$$

Finally, we perform the integration.

$$S(\alpha) = m\left[\left(-\frac{1}{2}vgt^2 + \frac{1}{2}v^2t\right)\Big|_{t_1}^{t_2} + \alpha\ \Big(v\eta(t)\Big)\Big|_{t_1}^{t_2} - \alpha g\int_{t_1}^{t_2}\eta(t)\ \ dt\right] + \mathcal{O}\left(\alpha^2\right). \tag{4.31}$$

Recognize that the second term will evaluate to zero at the endpoints, but the third term, which is also first-order in α will not evaluate to zero for all functions $\eta(t)$. This demonstrates that when we choose the wrong path, the action is not stationary.

Before parting from our one-dimensional example and from our review of the derivation of Lagrange's equations, let us do one more thing. Let us check that the condition given on the path by setting the first-order term in α to zero is identical to the condition given by Lagrange's equation. We'll do this by taking the variation of the action with repect to an arbitrary function $z\left(t\right)$.

$$S\left(\alpha\right)=\int_{t_1}^{t_2}\left[\frac{1}{2}m\Big(\dot{z}\left(t\right)+\alpha\dot{\eta}\left(t\right)\Big)^2-mg\Big(z\left(t\right)+\alpha\eta\left(t\right)\Big)\right]\,\mathrm{d}t. \tag{4.32}$$

Once again factoring into powers of α up to first order,

$$S\left(\alpha\right)=\int_{t_1}^{t_2}\left[\left(\frac{1}{2}\dot{z}^2\left(t\right)-gz\left(t\right)\right)+\alpha\Big(\dot{z}\left(t\right)\dot{\eta}\left(t\right)-g\eta\left(t\right)\Big)+\mathcal{O}\left(\alpha^2\right)\right]\,\mathrm{d}t. \tag{4.33}$$

For the same reasons that were outlined in the last two examples, the first-order term will vanish upon integration and evaluation if the first-order coefficient is an exact differential of $f\left(t\right)\eta\left(t\right)$, where f can be any function of t. Taking advantage of the product rule, we can see that this will only be the case if $\ddot{z}\left(t\right)=-g$. Bingo, this is precisely Lagrange's equation. Now, let us see how the calculus of variations can help us with *our* problem!

4.3.2 Quasi-Killing Equations

Other than a few subtle departures due to tensor transformation rules and the dimensionality of the action integral, this calculation will be identical to the treatment in the last section. At the end of the day, we will end up with a set of differential equations constraining $\mathbf{C}$ which are analogous to the Lagrange equations just derived.

Analogous to the role played by the action in the previous section, we begin by constructing an action for which we will seek stationary values. For the purpose of finding approximate symmetries, our action will be

$$S=\int_{\Omega}\epsilon^2\Big(\mathbf{C}\left(\mathbf{x}\right),\nabla\mathbf{C}\left(\mathbf{x}\right),\mathbf{x}\Big)\,\sqrt{-g}\,\mathrm{d}\Omega \tag{4.34}$$

where $\epsilon^2\equiv(\nabla_\mu C_\nu)(\nabla_n uC_\mu)$ is the scalar quantity we wish to minimize. We wish to extremize ϵ^2 in the region Ω by varying the vector field $\mathbf{C}$. The factor of $\sqrt{-g}$ is included because $\sqrt{-g}\,\mathrm{d}\Omega$ is the volume element.[2]

[2]Tensor densities do not transform as tensors; an additional factor – the w^{th} power of the Jacobian, where

Our next step is to define an infinitesimal variation of our vector $\mathbf{C}$. We'll do this just as before.

$$C_\nu\left(\mathbf{x},\alpha\right)=C_\nu\left(\mathbf{x},0\right)+\alpha\ \eta_\nu\left(\mathbf{x}\right), \tag{4.35}$$

where η is an arbitrary vector function everywhere except on the boundary of the region in question $\partial\Omega$, where it must be zero. Then the variation of the action will become

$$S\left(\alpha\right)=\int_\Omega \epsilon^2\Big(\mathbf{C}\left(\mathbf{x},\alpha\right),\nabla\mathbf{C}\left(\mathbf{x},\alpha\right)\mathbf{x}\Big)\ \sqrt{-g}\ \mathrm{d}\Omega. \tag{4.36}$$

The condition for obtaining a stationary action is, once again, that

$$\left.\frac{\mathrm{d}S}{\mathrm{d}\alpha}\right|_{\alpha=0}=0. \tag{4.37}$$

Now we move the differentiation with respect to α inside the action integral, since differentiation with respect to α is independent of differentiation with respect to the coordinates. Then we use the chain rule as before to obtain

$$\left.\frac{\mathrm{d}S\left(\alpha\right)}{\mathrm{d}\alpha}\right|_{\alpha=0}=\int_\Omega\left(\frac{\partial\epsilon^2}{\partial C_\nu}\frac{\partial C_\nu}{\partial\alpha}+\frac{\partial\epsilon^2}{\partial C_{\nu;\mu}}\frac{\partial C_{\nu;\mu}}{\partial\alpha}+\frac{\partial\epsilon^2}{\partial x^\rho}\frac{\partial x^\rho}{\partial\alpha}\right)\ \sqrt{-g}\ \mathrm{d}\Omega. \tag{4.38}$$

Since ϵ^2 does not depend explicitly on either $\mathbf{C}$ or $\mathbf{x}$, only the $\nabla\mathbf{C}$ term will contribute to the L.H.S. And for the same reason that we were permitted to bring the α-derivative inside the integral, we can now reverse the order of differentiation on $\mathbf{C}$ so that

$$\left.\frac{\mathrm{d}S\left(\alpha\right)}{\mathrm{d}\alpha}\right|_{\alpha=0}=\int_\Omega\frac{\partial\epsilon^2}{\partial C_{\nu;\mu}}\left(\nabla_\mu\frac{\partial C_\nu}{\partial\alpha}\right)\ \sqrt{-g}\ \mathrm{d}\Omega. \tag{4.39}$$

The next step is to integrate by parts.

$$\left.\frac{\mathrm{d}S\left(\alpha\right)}{\mathrm{d}\alpha}\right|_{\alpha=0}=\int_\Omega\nabla_\mu\left(\frac{\partial\epsilon^2}{\partial C_{\nu;\mu}}\frac{\partial C_\nu}{\partial\alpha}\sqrt{-g}\right)\ \mathrm{d}\Omega-\int_\Omega\frac{\partial C_\nu}{\partial\alpha}\nabla_\mu\left(\frac{\partial\epsilon^2}{\partial C_{\nu;\mu}}\sqrt{-g}\right)\mathrm{d}\Omega. \tag{4.40}$$

We will start by dealing with the first term. The object inside the parentheses is a contravariant vector field tensor density of weight +1. The covariant divergence of a contravariant vector field tensor density of weight +1 is equal to the ordinary divergence of the same

w is the weight of the tensor density – is required. As a consequence of their transformation properties, only true tensors ($w=0$) can be integrated over a macroscopic region. Consequently, the appearance of $\sqrt{-g}$ in the volume element is necessary because $\mathrm{d}\Omega$ is a tensor density of weight -1. Since $\sqrt{-g}$ is a tensor density of weight -1, their product is a true tensor and can therefore be integrated.

vector field [81], [25], $\nabla_\alpha \mathcal{I}^\alpha = \partial_\alpha \mathcal{I}^\alpha$. In other words, the additional terms in the covariant derivative arising from the connection coefficients vanish.

Following the pattern of the last section, the next step is to perform and evaluate the integral on the first term. The multidimensional analog of evaluating a function at its endpoints is provided by the divergence theorem. In our notation, the divergence theorem can be written

$$\int_\Omega \partial_\alpha \mathcal{I}^\alpha \, \mathrm{d}\Omega = \oint_{\partial\Omega} \mathcal{I}^\alpha \, \mathrm{d}S_\alpha, \tag{4.41}$$

where $\mathrm{d}\mathbf{S}$ is the oriented differential area element of the boundary. Applying this theorem to our first term, and recognizing that $\partial C_j / \partial \alpha = \eta_j$ by definition, produces the term

$$\oint_{\partial\Omega} \frac{\partial \epsilon^2}{\partial C_{\nu;\mu}} \eta_\nu \, \sqrt{-g} \, \mathrm{d}S_\mu, \tag{4.42}$$

which must be identically zero since η is required to be zero everywhere on the boundary. That just leaves us with the second term on the R.H.S. of (4.40) in our condition for extremizing the action. The $\sqrt{-g}$ can be taken outside the covariant derivative because $\nabla_\mu \, \sqrt{-g} = 0_\mu$. Once that is done, we have

$$\left. \frac{\mathrm{d}S\,(\alpha)}{\mathrm{d}\alpha} \right|_{\alpha=0} = -\int_\Omega \eta_\nu \, \nabla_\mu \left(\frac{\partial \epsilon^2}{\partial C_{\nu;\mu}} \right) \, \sqrt{-g} \, \mathrm{d}\Omega = 0. \tag{4.43}$$

The only way this condition can hold for all vector fields η that are zero on the boundary, is if the term in parentheses is itself zero. What we have arrived at is analogous to Lagrange's equations.

$$\nabla_\mu \frac{\partial \epsilon^2}{\partial C_{\nu;\mu}} = 0^\nu. \tag{4.44}$$

In the Lagrangian formulation, the dependence of $\mathcal{L}$ on the coordinates and conjugate momenta is not specified until a particular problem is outlined. But in our case, the dependence of ϵ^2 on the vector field $\mathbf{C}$ and its covariant derivative is outlined *a priori*,

$$\epsilon^2 \equiv \epsilon_{\mu\nu}\epsilon^{\mu\nu} = \left(\nabla_\mu C_\nu + \nabla_\nu C_\mu\right)\left(\nabla_\rho C_\sigma + \nabla_\sigma C_\rho\right) g^{\mu\rho} g^{\nu\sigma}. \tag{4.45}$$

Consequently, we were able to identify early on that ϵ^2 has no explicit dependence on $\mathbf{C}$. If we had not discarded the term arising from such a dependence, equation (4.44) would have

been identical in form to Lagrange's equations.

$$\frac{\partial \epsilon^2}{\partial C_\nu} - \nabla_\mu \frac{\partial \epsilon^2}{\partial C_{\nu;\mu}} = 0^\nu. \tag{4.46}$$

Since we do know the dependence of ϵ^2 in the general case, we can actually continue on by substituting in to the indicated partial derivative.

$$\frac{\partial \epsilon^2}{\partial C_{\nu;\mu}} = \left[\left(\delta^\mu_\alpha \delta^\nu_\beta + \delta^\mu_\beta \delta^\nu_\alpha\right)\left(\nabla_\gamma C_\rho + \nabla_\rho C_\gamma\right) + \left(\nabla_\alpha C_\beta + \nabla_\beta C_\alpha\right)\left(\delta^\mu_\gamma \delta^\nu_\rho + \delta^\mu_\rho \delta^\nu_\gamma\right)\right] g^{\alpha\gamma} g^{\beta\rho}. \tag{4.47}$$

Performing the indicated contractions and reorganizing a little bit, we obtain the expression,

$$\frac{\partial \epsilon^2}{\partial C_{\nu;\mu}} = 4\left(\nabla^\mu C^\nu + \nabla^\nu C^\mu\right) = 4\epsilon^{\mu\nu}. \tag{4.48}$$

Ultimately, then, we find that the condition for $\mathbf{C}$ to minimize the action, as given by (4.37), is

$$\nabla_\mu \left(\nabla^\mu C^\nu + \nabla^\nu C^\mu\right) = 0^\nu. \tag{4.49}$$

Thus we have arrived at the desired set of equations. It is immediately apparent that any vector field satisfying the first-order Killing equations will also satisfy these second-order equations. While these equations are second-order, they can be treated one derivative at a time by expressing them in terms of the ϵ tensor,

$$\nabla_\mu \epsilon^{\mu\nu} = 0^\nu, \tag{4.50}$$

Interestingly, this is identical in form to the Euler equations (2.2).

Time for a much-needed example that is both simple and informative. Consider a flat two-dimensional manifold with Cartesian coordinates. Our objective is to find all vector fields that satisfy Killing's equations, as well as those that solve the quasi-Killing equations. Then we will verify that all Killing vector fields ξ give rise to an action that is both stationary and zero, that all quasi-Killing vector fields $\mathbf{C}$ not satisfying Killing's equations give rise to a nonzero, but stationary, action, and that all vector fields $\mathbf{C}$ not satisfying the quasi-Killing equations give rise to a stationary action. We will do this by varying the action and expanding it in powers of α, just as we did in the previous section. If the zeroth-order term is zero, then the action is zero; if the first-order term is zero, then the action is stationary; we will largely ignore higher order terms.

For the given problem, the metric is the 2×2 identity matrix,

$$g_{ij} = \begin{pmatrix} 1 & 0 \\ 0 & 1 \end{pmatrix} \tag{4.51}$$

There are no non-zero connection coefficients. Killing's equations become

$$\partial_x \xi_x = 0 \tag{4.52}$$

$$\partial_y \xi_y = 0 \tag{4.53}$$

$$\partial_x \xi_y + \partial_y \xi_x = 0. \tag{4.54}$$

Whereas the quasi-Killing equations become

$$2C^x_{,xx} + C^y_{,xy} + C^x_{,yy} = 0 \tag{4.55}$$

$$C^y_{,xx} + C^x_{,xy} + 2C^y_{,yy} = 0. \tag{4.56}$$

From Killing's equations, we can immediately see that

$$\xi_x = f(y) \tag{4.57}$$

$$\xi_y = g(x) \tag{4.58}$$

$$g'(x) = -f'(y) = \lambda_0, \tag{4.59}$$

where $f(y)$ and $g(x)$ are arbitrary functions, except for the constraint placed on them by (4.59). Solving (4.59) leads to the following solutions:

$$f(y) = -\lambda_0 y + \lambda_1 \tag{4.60}$$

$$g(x) = \lambda_0 x + \lambda_2, \tag{4.61}$$

where the λ's are all arbitrary constants of integration. The most general Killing vector field, then, for this geometry is given by

$$\xi = \mathbf{g} \cdot \xi = (-\lambda_0 + \lambda_1) \frac{\partial}{\partial x} + (\lambda_0 x + \lambda_2) \frac{\partial}{\partial y}. \tag{4.62}$$

Varying this vector field gives,

$$\xi_x(x, y, \alpha) = \lambda_0 y + \lambda_1 + \alpha\ \eta_x(x, y) \tag{4.63}$$

$$\xi_y(x, y, \alpha) = \lambda_0 x + \lambda_2 + \alpha\ \eta_y(x, y). \tag{4.64}$$

Now we're in a position to compute ϵ^2,

$$\epsilon^2 = \Big(\partial_\mu \left(\xi_\nu + \alpha\ \eta_\nu\right) + \partial_\nu \left(\xi_\mu + \alpha\ \eta_\mu\right)\Big)\Big(\partial_\sigma \left(\xi_\tau + \alpha\ \eta_\tau\right) + \partial_\tau \left(\xi_\sigma + \alpha\ \eta_\sigma\right)\Big) g^{\mu\sigma} g^{\nu\tau}. \tag{4.65}$$

Performing the indicated contractions leaves us with

$$\epsilon^2 = 4\left(\xi_{x,x} + \alpha\ \eta x, x\right)^2 + 2\left(\xi_{x,y} + \alpha\ \eta_{x,y} + \xi_{y,x} + \alpha\ \eta_{y,x}\right)^2 + 4\left(\xi_{y,y} + \alpha\ \eta_{y,y}\right)^2. \tag{4.66}$$

Multiplying all this out and dropping second-order terms is the next step.

$$\begin{aligned}\epsilon^2 &= 4\left(\xi_{x,x}^2 + 2\alpha\xi_{x,x}\eta_{x,x}\right) + 2\left(\xi_{x,y}^2 + 2\xi_{x,y}\xi_{y,x} + \xi_{y,x}^2 + 2\alpha\xi_{x,y}\eta_{y,x} + 2\alpha\xi_{y,x}\eta_{x,y} + 2\alpha\xi_{y,x}\eta_{y,x}\right) \\ &\quad +4\left(\xi_{y,y}^2 + 2\alpha\xi_{y,y}\eta_{y,y}\right) + \mathcal{O}\left(\alpha^2\right).\end{aligned} \tag{4.67}$$

Noting that $\xi_{x,x}$ and $\xi_{y,y}$ are zero, and organizing into powers of α, we have

$$\epsilon^2 = 2\left(\xi_{x,y}^2 + 2\xi_{x,y}\xi_{y,x} + \xi_{y,x}^2\right) + 4\alpha\left(\xi_{x,y}\eta_{x,y} + \eta_{x,y}\xi_{y,x} + \xi_{y,x}\eta_{x,y} + \xi_{y,x}\eta_{y,x}\right) + \mathcal{O}\left(\alpha^2\right). \tag{4.68}$$

Finally, plugging in the values from (4.63) and (4.64),

$$\epsilon^2 = 2\left({\lambda_0}^2 + {\lambda_0}^2 - 2{\lambda_0}^2\right) + 4\alpha\Big(-\lambda_0\left(\eta_{x,y} + \eta_{y,x}\right) + \lambda_0\left(\eta_{x,y} + \eta_{y,x}\right)\Big) + \mathcal{O}\left(\alpha^2\right) = \mathcal{O}\left(\alpha^2\right). \tag{4.69}$$

Clearly, then, the action is both stationary and zero, as expected:

$$S\left(\alpha\right) = \int_\Omega \mathcal{O}\left(\alpha^2\right)\ \sqrt{-g}\ \mathrm{d}\Omega = \mathcal{O}\left(\alpha^2\right). \tag{4.70}$$

Next, consider the quasi-Killing vector field

$$\mathbf{C} = x\mathbf{e}_x \tag{4.71}$$

It is not hard to see that this vector field satisfies the quasi-Killing equations (4.55) and (4.56). It also satisfies the last two of Killing's three equations (4.53) and (4.54), but it does not satisfy the first (4.52). Accordingly, it cannot be a Killing vector field. An infinitesimal variation of this vector field is given by

$$C_x\left(x, y, \alpha\right) = x + \alpha\ \eta_x\left(x, y\right) \tag{4.72}$$

$$C_y\left(x, y, \alpha\right) = \alpha\ \eta_y\left(x, y\right). \tag{4.73}$$

We can proceed just as before. Plugging the appropriate quantities into equation (4.45) quickly gives

$$\epsilon^2 = 4 + \alpha\left(8\eta_{x,x}\right) + \mathcal{O}\left(\alpha^2\right). \tag{4.74}$$

Consequently, the action is

$$S\left(\alpha\right) = \int_\Omega \left(4 + 8\alpha\eta_{x,x} + \mathcal{O}\left(\alpha^2\right)\right)\ \mathrm{d}x\ \mathrm{d}y. \tag{4.75}$$

An integration over x can be performed on the middle term to obtain

$$S\left(\alpha\right) = 4\int_\Omega \mathrm{d}x\ \mathrm{d}y + 8\alpha\int_\Omega \eta_x|_{x_{\text{lower bdry}}}^{x_{\text{upper bdry}}}\ \mathrm{d}y + \mathcal{O}\left(\alpha^2\right). \tag{4.76}$$

But η_x is zero at $x_{\text{upper bdry}}$ and $x_{\text{lower bdry}}$. Accordingly, the middle term vanishes. All together, then, the variation of the action is

$$S\left(\alpha\right) = 4\int_\Omega \mathrm{d}x\ \mathrm{d}y + \mathcal{O}\left(\alpha^2\right) \tag{4.77}$$

for the given quasi-Killing vector field. The zeroth-order term is non-zero because this vector field does not satisfy Killing's equations. The first-order term *is* zero because the vector field *does* satisfy the quasi-Killing equations.

The fundamental result of this section is Eq. (4.49), the condition for a quasi-Killing vector. Again, however, it generally will not be necessary to solve Eq. (4.49) because in many situations the underlying symmetry can be assumed in advance.

4.4 Vanishing Vectors

Suppose the goal is to define a set of vector fields that will ensure that the source vanishes. Recall that a Killing vector causes the standard source to vanish[3], so as long as we are talking about the standard source, a Killing vector is also a vanishing vector. But are there any other vectors (*not* satisfying Killing's equations) that can cause the source to vanish?

Yes, but generally, this will require a brute-force solution of the expression,

$$T^{\mu\nu}\left(\nabla_\mu C_\nu + \nabla_\nu C_\mu\right) = 0, \tag{4.78}$$

[3]And it *may* also cause the physical source to vanish; particularly, if the pressure possesses the same symmetries as the metric.

if one wants the standard source to vanish, or

$$\rho h u^{\mu} u_{\nu} \nabla_{\mu} C^{\nu} - C^{\mu} \, \partial_{\mu} P = 0, \tag{4.79}$$

if one wants the physical source to vanish — both of which involve a single condition on the components of $\mathbf{C}$, so locally one is guaranteed to find several families of solutions to either equation.

Incidentally, the reason Killing's equations (4.2) do not always admit solutions is because there are more equations (ten) than degrees of freedom in $\mathbf{C}$ (four). It goes without saying that a solution will exist only in very special circumstances (i.e., whenever the necessary symmetries are present). Conditions (4.78) and (4.79), on the other hand, are single scalar equations with four degrees of freedom in the choice of $\mathbf{C}$.

Since the physical source represents the net 4-force density as measured by an observer in the frame in which the state variables are measured, condition (4.79) will automatically be satisfied by all three momentum equations whenever the fluid is in equilibrium. But via expression (4.79) it should be possible to identify a set of source-free conservative variables even when the fluid is not in equilibrium. For example, for a neutron star experiencing small radial oscillations, one could locally define a frame that everywhere experiences a radial acceleration equal to the net force density divided by the mass density. These radial accelerations would produce a radial inertial force that should counterbalance the net radial force experienced by the fluid. (This is equivalent to a Lagrangian treatment of the fluid.) In practice, however, it likely would not be trivial to globally determine the needed acceleration for the frame in which the radial variable is measured.

Most professionals in the field have an averse reaction to my suggesting that it is possible for the source to vanish without a Killing vector. I imagine that this is because they understand that Killing vectors give rise to conserved quantities, but in their experience they do not have any reason to believe that conserved quantities can exist without the symmetry that a Killing vector indicates. Nevertheless, the L.H.S. of Eq. (4.78) is a scalar quantity resulting from contracting two second-order tensors together. This is perfectly analogous to a dot product between two vectors. Of course, the standard source term above is contracted

over twice, whereas the dot product involves a single contraction $A^i B_i$, but the idea is the same. There are three ways to make a dot product $(\mathbf{A} \cdot \mathbf{B})$ be zero.

1. You can make all the components of one vector **A** be zero (so that **A** is the zero vector),

2. You can make all the components of the other vector **B** be zero (so that **B** is the zero vector), or

3. You can just choose **A** and **B** to be perpendicular to one another (in which case neither **A** nor **B** needs to be the zero vector).

The first alternative requires **A** to be zero, but places no condition whatsoever on **B**. The second alternative requires **B** to be zero, but places no condition whatsoever on **A**. The final alternative requires neither **A** nor **B** to be zero, but imposes a condition that – if it is to be satisfied – depends on both vectors **A** and **B**.

Similarly, whenever the stress-energy tensor is zero, condition (4.78) is satisfied without regard to the choice of characteristic vector; whenever the characteristic vector is a Killing vector, condition (4.78) is satisfied without regard to the stress-energy tensor; and even when the stress-energy tensor is not zero and the characteristic vector is not a Killing vector, it is still possible for condition (4.78) to be satisfied, but it will require information about both the stress-energy tensor and the characteristic vector.

Though the condition for eliminating the physical source is not quite as neat as the condition for eliminating the standard source, these ideas should carry over seamlessly, and it should always be possible to identify conservative variables that are locally (and globally) conserved.

Given that the physical source can be thought of as the net force per unit volume along the direction of the characteristic vector **C**, one can conclude that (4.79) describes **a vector field that is everywhere orthogonal to the net force as measured in the chosen state variable frame**. This explanation also appears to be consistent with my claim that there is not a unique choice for **C** that will cause the physical source to vanish. Choosing a **C** with any orientation inside the 3-dimensional hypersurface that is orthogonal to the net force will suffice. Moreover, the magnitude of **C** is immaterial. This implies that there

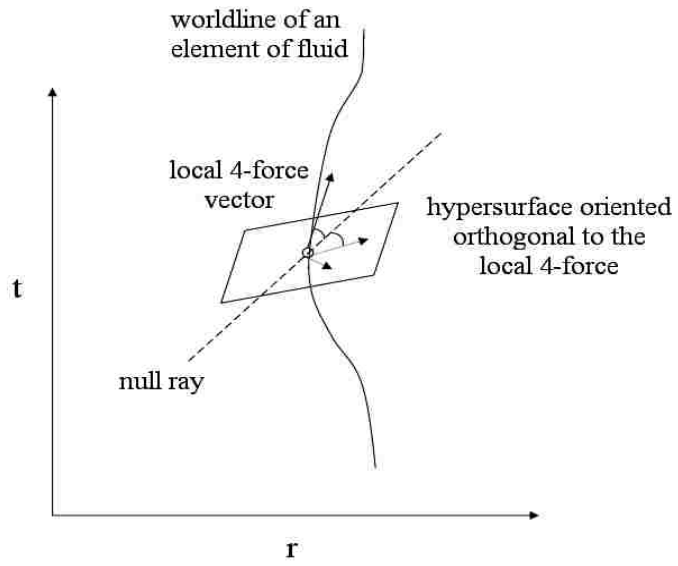

Figure 4.1: Three source-eliminating (and locally-conserved-variable-identifying) vector fields. Any vector **C** will produce a source term that equals a generalized 4-force (as measured in the state variable frame) along **C**. Clearly, then, any vector living in a three-dimensional hypersurface which is orthogonal to the 4-force vector (like the two above) must produce a physical source term that is zero.

is indeed a three-parameter family of possible solutions to (4.79) — an implication that is consistent with the number of degrees of freedom in (4.79).

While it may be difficult to find a vector field that globally satisfies Eq. (4.79), in practice it may not be necessary. In fact, it may be possible to design a code that "chooses" conservative state variables locally according to a set of solutions to Eq. (4.79). The code could then recover the set of primitive variables from the set of conservatives at each grid cell, and the process could begin again in the next time step.

4.5 Flow-Complementing Vectors

Another useful approach may be to base the choice of **C** on what one may know *a priori* about the fluid flow, rather than about the underlying geometry of the manifold. For example, if the direction of fluid flow is already known everywhere, then one or two of the characteristic vectors can be chosen to be orthogonal to the flow direction. The corresponding advection variable(s), $\rho h u_i C^i{}_{(\eta)}$, must then be zero, so there is nothing to advect.

Moreover, that means the source will not include contributions that are meant to cancel with the divergence term (as will be shown near the end of this section). In cases where only the principal part of the fluid flow is known, it may still be beneficial to use this approach to minimize the amount of material that needs to be advected in a particular direction.

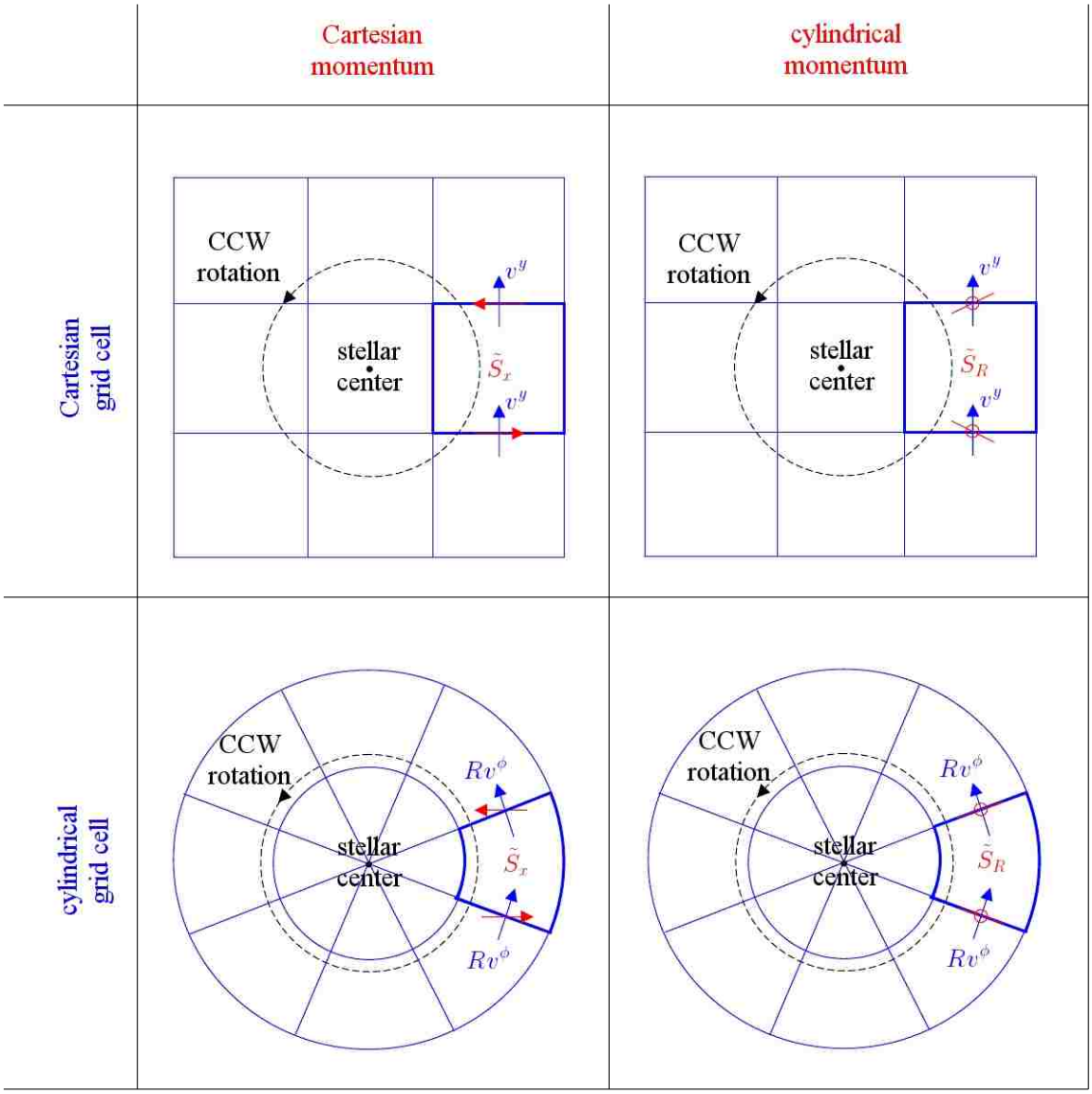

Figure 4.2: Comparison of various approaches to advection of a near-equilibrium system. Schematic diagrams illustrating the role that advection plays in a grid cell centered on the $+x$ axis for four distinct treatments of fluid executing purely circular motion, such as in the equatorial plane of an equilibrium, rotating neutron star. Upper-left diagram: Cartesian momenta advected on a Cartesian grid; bottom-left diagram: Cartesian momenta advected on a cylindrical grid; top-right diagram: cylindrical momenta advected on a Cartesian grid; and bottom-right diagram: cylindrical momenta advected on a cylindrical grid.

Now consider developing a numerical algorithm that is designed to evolve a uniformly rotating, axisymmetric neutron star in steady-state equilibrium. We will examine only two-dimensional transport in the equatorial plane of the star, but we will consider four approaches to handling the problem: advection of Cartesian momenta on a Cartesian grid; cylindrical momenta on a cylindrical grid; Cartesian momenta on a cylindrical grid; and cylindrical momenta on a Cartesian grid. A schematic diagram of each approach is illustrated in the various panels of Figure 4.2. Each diagram outlines one particular circular streamline of an axisymmetric star that is rotating counter-clockwise on some grid structure, and one cell located off-center along the $+x$ axis is highlighted. Various features are color-coded to emphasize their dependence on either the choice of coordinates (blue) or the choice of state variables (red).

In each case, there are two relevant components of velocity: one that will be advected, and one that acts as the advecting mechanism. We will call the first the *state variable velocity* because it is part of the conservative state variable being advected. And the second we will call the *transport velocity* because it is used to transport the other across the cell interface. The transport velocity is always perpendicular to the cell face, whereas the state variable velocity may point in any direction (relative to the grid cells). Consequently, in each case, a pair a vectors (one blue and one red) is shown at each of the relevant transport faces of the highlighted cell. The blue vector indicates the direction of transport across the cell interface, while the red vector indicates the orientation of the component of the 3-velocity associated with the chosen momentum state variable. No attempt is made to illustrate the magnitude of these vectors, but only their orientation. (In cases where a particular vector is zero, a headless arrow hooped by a small circle, representing '0', is used to indicate the relevant orientation.) We will examine the role of both the flux (transport) term and the source term on the evolution of the fluid's momentum in the highlighted cell. Because the star is presumed to be in steady-state, each integration time step should leave the value of the momentum density unchanged. This means that, ideally after numerical evaluation, the flux term and the source term should have the same value so that the net "time_update" is zero. Because they are generally evaluated in very different ways, precise cancelation of the

flux and source terms is unlikely to be achieved. But if the selected approach leads to an algorithm in which the two terms are inherently small – better yet, zero – the steady-state configuration can be better preserved throughout an evolution.

Because in our example problem the fluid is moving along circular trajectories, there is no motion along the x-axis. Hence, in all four illustrated approaches the transport velocity perpendicular to the right- and left-hand faces of the highlighted grid cell must be zero and, as a result, contributions to the flux term will arise only from advection through the upper and lower faces of that cell. Let us consider how a time_update of one of the components of the momentum density (we will call it $\psi_{(1)}$) is calculated in each case.

- **Advection of Cartesian momenta on a Cartesian grid ($\mathbf{C}_{(1)} = \mathbf{e}_x$), as illustrated in the top-left panel of Figure 4.2:** In this case, the relevant transport velocity (perpendicular to the upper and lower faces of the cell) is $\pm v^y$ (a "blue" variable, which depends on the choice of coordinates) and $\psi_{(1)}$ (a "red" variable, which depends on the choice of conservative variables) is constructed from the v^x component of the velocity. For any numerical transport algorithm in which cell-centered state variables are interpolated to the cell faces, positive x-momentum will be carried into the cell from below, and negative x-momentum will be carried out to the cell above. Hence, advection alone will tend to cause a net increase in the value of $\psi_{(1)}$ (and consequently also of $\hat{S}_x$) in our highlighted cell. (In other words, the divergence of x-momentum is negative for this cell.) The physical source term is provided by the R.H.S. of Eq. (3.19b); in this case the relevant expression inside the curly brackets is

$$\{\text{R.H.S.}\} = \Big\{ \rho h u^\mu u^\beta \left(\partial_\mu g_{x\beta} - \Gamma^\delta_{\mu\beta} g_{\delta x} \right) - \partial_x P \Big\}, \tag{4.80}$$

  provided that this expression is evaluated in Cartesian-like coordinates, and would further reduce to

$$\{\text{R.H.S.}\} = \Big\{ -\rho h \; \partial_x \Phi - \partial_x P \Big\} \tag{4.81}$$

  in a Newtonian approximation (where Φ is the gravitational potential). For the highlighted cell, this term must also be negative and must have the same magnitude as

the net divergence if a steady-state is to be maintained. The source term will indeed be negative for our equilibrium configuration because the gravitational acceleration (obtained through the Christoffel symbols and derivatives of the metric due to the inherent relativistic curvature of the metric) overpowers the pressure gradient, providing a net centripetal force that holds the fluid in circular orbit. (At least this is an inertial observer's description of what happens.)

- **Advection of cylindrical momenta on a cylindrical grid ($\mathbf{C}_{(1)} = \mathbf{e}_R$), as illustrated in the bottom-right panel of Figure 4.2:** In this case, the relevant transport velocity (perpendicular to the upper and lower faces of the cell) is $\pm Rv^\phi$ (a blue quantity) while $\psi_{(1)}$ (a red quantity) is constructed from the v^R component of the velocity. Since there is no R-momentum anywhere, none will be carried into the cell from below and none will be carried out to the cell above. Hence, advection alone will not contribute to a net change in the value of $\psi_{(1)}$ (nor to $\hat{S}_R$) in our highlighted cell. (In other words, the divergence of R-momentum is zero for this cell.) The physical source term is provided by the R.H.S. of Eq. (3.19b); in this case the relevant expression inside the curly brackets is

$$\{\text{R.H.S.}\} = \Big\{\rho h u^\mu u^\beta \left(\partial_\mu g_{R\beta} - \Gamma^\delta_{\mu\beta} g_{\delta R}\right) - \partial_R P\Big\}, \tag{4.82}$$

provided this expression is evaluated in cylindrical coordinates, and would further reduce to

$$\{\text{R.H.S.}\} = \Big\{\rho h \left(R u^\phi u^\phi - \partial_R \Phi\right) - \partial_R P\Big\} \tag{4.83}$$

in a Newtonian approximation. For the highlighted cell, this term must also be zero if a steady-state is to be maintained. The source term will indeed be zero for our equilibrium configuration because, in addition to a gravitational acceleration, the Christoffel symbols and derivatives of the metric now produce a new geometry term (somewhat similar to the centrifugal pseudoforce) that will supplement the pressure gradient in providing an exact counterbalance to the gravitational acceleration. In this case, there is no net source term to alter the value of the R-coordinate of the fluid.

- **Advection of Cartesian momenta on a cylindrical grid ($\mathbf{C}_{(1)} = \mathbf{e}_x = (Rx\,\mathbf{e}_R - y\mathbf{e}_\phi\,)/R^2$), as illustrated in the bottom-left panel of Figure 4.2:** In this case, the relevant transport velocity (perpendicular to the upper and lower faces of the cell) is again $\pm Rv^\phi$ (a blue quantity), but $\psi_{(1)}$ (a red quantity) is constructed from the v^x component of the velocity. As happened in the "Cartesian-Cartesian" case associated with the upper-left panel of Figure 4.2, positive x-momentum will be carried into the cell from below, and negative x-momentum will be carried out to the cell above. Hence, advection alone will tend to cause a net increase in the value of $\psi_{(1)}$ (and $\hat{S}_x$) in our highlighted cell. (In other words, the divergence of x-momentum is again negative for this cell.) Since the source term is a scalar quantity, it cannot depend upon the choice of coordinates, but only on the choice of $\mathbf{C}$ (and, accordingly, on the choice of advection variable). Consequently, in this case, the physical source term will be the same as it was in the "Cartesian-Cartesian" case. Written in terms of the chosen grid coordinates (*i.e.*, cylindrical coordinates) the bracketed term on the R.H.S. of Eq. (3.19b) becomes,

$$\begin{aligned}\{\text{R.H.S.}\} \;=\; & \Big\{\rho h u^\mu u^\beta [g_{\beta R}\partial_\mu(x/R) + g_{\beta\phi}\partial_\mu y + (\partial_\mu g_{R\beta} - \Gamma^\delta_{\mu\beta} g_{\delta R})(x/R) + (\partial_\mu g_{\phi\beta} - \Gamma^\delta_{\mu\beta} g_{\delta\phi}) y] \\ & -[(x/R)\partial_R - (y/R^2)\partial_\phi]P\Big\}, \end{aligned} \tag{4.84}$$

where $x \equiv R\cos\phi$ and $y \equiv R\sin\phi$, and would further reduce to

$$\{\text{R.H.S.}\} = \Big\{ -\rho h\; [(x/R)\partial_R - (y/R^2)\partial_\phi]\Phi - [(x/R)\partial_R - (y/R^2)\partial_\phi]P\Big\} \tag{4.85}$$

in a Newtonian approximation. For the highlighted cell, the net divergence and source term are, once again, both negative and equal in magnitude, despite the fact that the evolution is carried out on a cylindrical grid.

- **Advection of cylindrical momenta on a Cartesian grid ($\mathbf{C}_{(1)} = \mathbf{e}_R = (x\,\mathbf{e}_x + y\,\mathbf{e}_y\,)/R$), as illustrated in the top-right panel of Figure 4.2:** In this case, the relevant transport velocity (perpendicular to the upper and lower faces of the cell) is $\pm v^y$ (a blue quantity) and $\psi_{(1)}$ (a red quantity) is constructed from the v^R component of the velocity. As happened in the "cylindrical-cylindrical" case associated with the

lower-right panel of Figure 4.2, since there is no R-momentum anywhere, none will be carried into the cell from below and none will be carried out to the cell above. Hence, advection alone will not contribute to a net change in the value of $\psi_{(1)}$ (nor of $\hat{S}_R$) in our highlighted cell. The physical source term is also as it was in the "cylindrical-cylindrical" case, that is, zero. Written in terms of the chosen grid coordinates (this time, Cartesian coordinates) the bracketed term on the R.H.S. of Eq. (3.19b) becomes,

$$\begin{aligned}\{\text{R.H.S.}\} \;=\; & \Big\{\rho h u^\mu u^\beta [g_{\beta x}\partial_\mu(x/R) + g_{\beta y}\partial_\mu(y/R) + (\partial_\mu g_{x\beta} - \Gamma^\delta_{\mu\beta} g_{\delta x})(x/R) \\ & + (\partial_\mu g_{y\beta} - \Gamma^\delta_{\mu\beta} g_{\delta y})(y/R)] - (1/R)(x\partial_x + y\partial_y)P\Big\}, \end{aligned} \tag{4.86}$$

where $R \equiv (x^2 + y^2)^{1/2}$, and would further reduce to

$$\{\text{R.H.S.}\} = \left\{\rho h \left(-yu^x + xu^u\right)^2 / R^3 - (\rho h/R)\left(x\partial_x + y\partial_y\right)\Phi - (1/R)\left(x\partial_x + y\partial_y\right)P\right\} \tag{4.87}$$

in a Newtonian approximation. Both the advection term and the source term are again identically zero, despite the fact that the evolution is carried out on a Cartesian grid.

Even though the advection and source terms cancel analytically in each of the four cases, it would be surprising if a numerical evaluation of the source terms arising from the two approaches involving the linear momenta as state variables produces values that exactly cancel the corresponding flux contributions. In the two approaches involving the cylindrical momenta as state variables, on the other hand, both the advection terms and the source terms are identically zero, so nothing special needs to happen in order for them to exactly cancel numerically.

From this analysis, we suspect that the choice of state variables is likely to be more important than the choice of coordinates whenever one's primary goal is to avoid the detrimental effects of an imperfect numerical balance between the source term and the advection term. We also conclude that the choice of coordinates can be made independently of the choice of state variables and, even if the basis vectors of the chosen coordinates are not identified with the definition of the state variables, the balance between the source term and the advection term is not adversely affected. But whatever the choice of state variables (and

coordinates), Eq. (3.5c) gives the appropriate physical formulation of the Euler equations. With a description in hand for constructing and evolving generalized state variables, we will focus our attention in the next subsection on the application of these ideas to a specific physical problem.

5. Additional Examples

As a simple example of the usefulness of the generalized Euler equations, consider a simple Newtonian problem involving an incompressible dust (i.e., pressure is neglected and the total time derivative of the density as measured in the comoving frame is zero) as viewed in cylindrical coordinates. The metric is

$$g_{\mu\nu} = \begin{pmatrix} -c^2 & 0 & 0 & 0 \\ 0 & 1 & 0 & 0 \\ 0 & 0 & R^2 & 0 \\ 0 & 0 & 0 & 1 \end{pmatrix}. \tag{5.1}$$

Consequently, the line element, $\mathrm{d}s^2 \equiv g_{\mu\nu}\ \mathrm{d}x^\mu\ \mathrm{d}x^\nu$, can be written

$$\mathrm{d}s^2 = -c^2\ \mathrm{d}t^2 + \mathrm{d}R^2 + R^2\ \mathrm{d}\phi^2 + \mathrm{d}z^2. \tag{5.2}$$

Additionally, assume that $h = 1$ and that motion is restricted to two dimensions – planes of constant z – so that $u^t = 1$, $u^R = \dot{R}$, $u^\phi = \dot{\phi}$, and $u^z = 0$. Then the stress energy tensor becomes,

$$T^{\mu\nu} = \rho u^\mu u^\nu = \begin{pmatrix} \rho & \rho\dot{R} & \rho\dot{\phi} & 0 \\ \rho\dot{R} & \rho\dot{R}^2 & \rho\dot{R}\dot{\phi} & 0 \\ \rho\dot{\phi} & \rho\dot{R}\dot{\phi} & \rho\dot{\phi}^2 & 0 \\ 0 & 0 & 0 & 0 \end{pmatrix}. \tag{5.3}$$

If the flow is further assumed to be nearly stationary, such that it can be thought of as rotating with constant angular velocity Ω, then one ideal choice for a characteristic vector is the helical quasi-Killing vector field $\mathbf{C} = \mathbf{e}_t + \omega\ \mathbf{e}_\phi$, where $\omega = \Omega$ is the angular velocity of the frame in which we want to measure angular momentum. Despite the fact that the two angular velocities are equal in this example, we will keep the symbol ω for use in our characteristic vector in order to emphasize that it, by definition, identifies the frame rotation rate.

5.1 Identification of a New Coordinate That Advances along the Chosen Characteristic Vector

It can be desirable to find a new coordinate (which we will denote using primes) such that t' advances along the vector field $\mathbf{C}$ and such that the induced metric (i.e., the spatial 3-metric)

does not change with time; in other words, we wish to require that the coordinate t' follow integral curves of the vector field $\mathbf{C}$, and that the functional dependence of the induced metric on the new spatial coordinates be identical to its dependence on the old spatial coordinates. Beginning with the requirement on t', we have

$$\mathbf{C} = \mathbf{e}_t + \omega\ \mathbf{e}_\phi = \mathbf{e}_{t'} = \frac{\partial t}{\partial t'}\ \mathbf{e}_t + \frac{\partial R}{\partial t'}\ \mathbf{e}_R + \frac{\partial \phi}{\partial t'}\ \mathbf{e}_\phi + \frac{\partial z}{\partial t'}\ \mathbf{e}_z. \tag{5.4}$$

Picking coefficients off of the unprimed basis vectors, we obtain four PDE's (written in terms of the primed coordinates) which need to be solved for the unprimed coordinates:

$$\frac{\partial t}{\partial t'} = 1 \tag{5.5a}$$
$$\frac{\partial R}{\partial t'} = 0 \tag{5.5b}$$
$$\frac{\partial \phi}{\partial t'} = \omega \tag{5.5c}$$
$$\frac{\partial z}{\partial t'} = 0. \tag{5.5d}$$

Fortunately, in this case the PDE's are simple and the following coordinate transformation can quickly be seen to satisfy all four PDE's.

$$t = t' \tag{5.6a}$$
$$R = R' \tag{5.6b}$$
$$\phi = \phi' + \omega t' \tag{5.6c}$$
$$z = z'. \tag{5.6d}$$

Of course, we know that this solution is correct because it identifies the set of cylindrical coordinates associated with the rotating frame. The important thing to recognize is that we were able to derive this coordinate transformation directly from the characteristic vector field $\mathbf{C}$.

Having found the appropriate transformation between the inertial-frame coordinates and the rotating-frame coordinates, it is possible to calculate the line element in the primed coordinates and pick off its coefficients to identify the new metric elements. Beginning with the differential coordinate transformations (e.g., $\mathrm{d}\phi = \mathrm{d}\phi' + \omega\ \mathrm{d}t'$) and substituting them

into the line element produces,

$$ds^2 = -c^2\ \mathrm{d}t'^2 + \mathrm{d}R'^2 + R'^2\left(\mathrm{d}\phi' + \omega\ \mathrm{d}t'\right)^2 + \mathrm{d}z'^2$$

and the corresponding metric is

$$g_{\mu\nu} = \begin{pmatrix} -c^2 + R^2\omega^2 & 0 & R^2\omega & 0 \\ 0 & 1 & 0 & 0 \\ R^2\omega & 0 & R^2 & 0 \\ 0 & 0 & 0 & 1 \end{pmatrix}, \tag{5.7}$$

where the primes have been left off R since it remains unchanged by the transformation, and the off-diagonal elements have appeared because of the cross term in $\mathrm{d}\phi^2$. As required, this metric will reduce to the inertial-frame metric in the limit as $\omega \to 0$. Next, the collection of covariant metric components can be inverted to obtain the set of contravariant metric components (i.e., the inverse metric),

$$g^{\mu\nu} = \begin{pmatrix} -1/c^2 & 0 & \omega/c^2 & 0 \\ 0 & 1 & 0 & 0 \\ \omega/c^2 & 0 & \frac{1}{R^2} - \frac{\omega^2}{c^2} & 0 \\ 0 & 0 & 0 & 1 \end{pmatrix}. \tag{5.8}$$

Comparing each of these to the ADM-decomposed metric (as defined in Subsection 7.1.2),

$$g_{\mu\nu} = \begin{pmatrix} -c^2\alpha^2 + \beta^2 & \beta_j \\ \beta_i & \gamma_{ij} \end{pmatrix}, \quad \text{or equivalently,} \quad g^{\mu\nu} = \begin{pmatrix} -\frac{1}{c^2\alpha^2} & \frac{\beta^j}{c^2\alpha^2} \\ \frac{\beta^i}{c^2\alpha^2} & \gamma^{ij} - \frac{\beta^i\beta^j}{c^2\alpha^2} \end{pmatrix}, \tag{5.9}$$

it is evident that the characteristic vector field $\mathbf{C}$ gives rise to the lapse function $\alpha = 1$, and the shift vector $\beta = R^2\omega\ \mathbf{e}^\phi = \omega\ \mathbf{e}_\phi$, expressed in terms of the inertial-frame coordinates.

5.2 Expression of the Field Equations in Terms of the New Coordinate

The Euler equations,

$$\frac{1}{\sqrt{-g}}\ \partial_\mu\left(\sqrt{-g}\ T^{\mu\nu}\right) = -T^{\mu\alpha}\Gamma^\nu_{\mu\alpha}, \tag{5.10}$$

can now be expressed in terms of the corotating coordinates. The factor of $\sqrt{-g} = cR$ in the corotating cylindrical coordinates, just as it does in inertial-frame cylindrical coordinates. With a little work, it can be shown that the only nonzero Christoffel symbols in the corotating

coordinates turn out to be

$$\Gamma^R_{tt} = -R\omega^2 \tag{5.11a}$$

$$\Gamma^R_{t\phi} = \Gamma^R_{\phi t} = -R\omega \tag{5.11b}$$

$$\Gamma^R_{\phi\phi} = -R \tag{5.11c}$$

$$\Gamma^\phi_{tR} = \Gamma^\phi_{Rt} = \omega/R \tag{5.11d}$$

$$\Gamma^\phi_{R\phi} = \Gamma^\phi_{\phi R} = 1/R. \tag{5.11e}$$

With each of the Christoffel symbols, writing out each of the terms appearing in the Euler equations is straightforward. Recalling that all the primed coordinates except ϕ' are interchangeable with the unprimed coordinates, the field equation associated with each of the corotating coordinates becomes

$$t: \quad \partial_{t'}\left(cR\rho\right) + \partial_R\left(cR\rho\dot{R}\right) + \partial_\phi\left(cR\rho\dot{\phi}'\right) = 0 \tag{5.12a}$$

$$R: \quad \partial_{t'}\left(cR\rho\dot{R}\right) + \partial_R\left(cR\rho\dot{R}^2\right) + \partial_\phi\left(cR\rho\dot{R}\dot{\phi}'\right) = R\omega^2\left(cR\rho\right) + 2R\omega\left(cR\rho\dot{\phi}'\right) + R\left(cR\rho\dot{\phi}'^2\right) \tag{5.12b}$$

$$\phi': \quad \partial_{t'}\left(cR\rho\dot{\phi}'\right) + \partial_R\left(cR\rho\dot{R}\dot{\phi}'\right) + \partial_\phi\left(cR\rho\dot{\phi}'^2\right) = -\frac{2\omega}{R}\left(cR\rho\dot{R}\right) - \frac{2}{R}\left(cR\rho\dot{R}\dot{\phi}'\right) \tag{5.12c}$$

$$z: \quad 0 = 0, \tag{5.12d}$$

where primes have additionally been left off of the partials ∂_R and ∂_ϕ because $\partial_{R'} = \partial_R$ and

$$\partial_{\phi'} = \frac{\partial t}{\partial \phi'}\,\partial_t + \frac{\partial \phi}{\partial \phi'}\,\partial_\phi = \partial_\phi,$$

but

$$\partial_{t'} = \partial_t + \omega\,\partial_\phi \neq \partial_t. \tag{5.13}$$

A little simplification allows us to write

$$t: \quad \partial_{t'}\left(R\rho\right) + \partial_R\left(R\rho\dot{R}\right) + \partial_\phi\left(R\rho\dot{\phi}'\right) = 0 \tag{5.14a}$$

$$R: \quad \partial_{t'}\left(R\rho\dot{R}\right) + \partial_R\left(R\rho\dot{R}^2\right) + \partial_\phi\left(R\rho\dot{R}\dot{\phi}'\right) = \rho R^2\left(\omega + \dot{\phi}'\right)^2 \tag{5.14b}$$

$$\phi': \quad \partial_{t'}\left(R\rho\dot{\phi}'\right) + \partial_R\left(R\rho\dot{R}\dot{\phi}'\right) + \partial_\phi\left(R\rho\dot{\phi}'^2\right) = -2\rho\dot{R}\left(\omega + \dot{\phi}'\right). \tag{5.14c}$$

With the Euler equations in this simplified form it is possible to start talking about a physical interpretation for the source terms. Using the product rule on the remaining partials gives

$$\begin{aligned}
t: \qquad & R\,\partial_{t'}\rho + \rho\dot{R} + R\dot{R}\,\partial_R\rho + \rho R\,\partial_R\dot{R} && (5.15a)\\
& \quad + R\dot{\phi}'\,\partial_\phi\rho + \rho R\,\partial_\phi\dot{\phi}' = 0 && (5.15b)\\
R: \qquad & R\,\partial_{t'}\left(\rho\dot{R}\right) + \rho\dot{R}^2 + R\dot{R}\,\partial_R\left(\rho\dot{R}\right) + \rho R\dot{R}\,\partial_R\dot{R} \\
& \quad + R\dot{\phi}'\,\partial_\phi\left(\rho\dot{R}\right) + \rho R\dot{R}\,\partial_\phi\dot{\phi}' = \rho R^2\left(\omega+\dot{\phi}'\right)^2 && (5.15c)\\
\phi': \qquad & R\,\partial_{t'}\left(\rho\dot{\phi}'\right) + \rho\dot{R}\dot{\phi}' + R\dot{R}\,\partial_R\left(\rho\dot{\phi}'\right) + \rho R\dot{\phi}'\,\partial_R\dot{R} \\
& \quad + R\dot{\phi}'\,\partial_\phi\left(\rho\dot{\phi}'\right) + \rho R\dot{\phi}'\,\partial_\phi\dot{\phi}' = -2\rho\dot{R}\left(\omega+\dot{\phi}'\right), && (5.15d)
\end{aligned}$$

while the chain rule implies that,

$$\begin{aligned}
\mathrm{d}_{t'}\rho &= \partial_{t'}\rho + \dot{R}\,\partial_R\rho + \dot{\phi}'\,\partial_\phi\rho = 0 \text{ (incompressible)} && (5.16a)\\
\mathrm{d}_{t'}\left(\rho\dot{R}\right) &= \partial_{t'}\left(\rho\dot{R}\right) + \dot{R}\,\partial_R\left(\rho\dot{R}\right) + \dot{\phi}'\,\partial_\phi\left(\rho\dot{R}\right) && (5.16b)\\
R\,\mathrm{d}_{t'}\left(\rho\dot{\phi}'\right) &= R\,\partial_{t'}\left(\rho\dot{\phi}'\right) + R\dot{R}\,\partial_R\left(\rho\dot{\phi}'\right) + R\dot{\phi}'\,\partial_\phi\left(\rho\dot{\phi}'\right), && (5.16c)
\end{aligned}$$

where $\mathrm{d}_{t'}$ denotes a total derivative with respect to t'. Substituting these values into the momentum field equations produces

$$\begin{aligned}
t: \qquad & \rho\left(\dot{R} + R\,\partial_R\dot{R} + R\,\partial_\phi\dot{\phi}'\right) = 0 && (5.17a)\\
R: \qquad & R\,\mathrm{d}_{t'}\left(\rho\dot{R}\right) + \rho\left(\dot{R}^2 + R\dot{R}\,\partial_R\dot{R} + R\dot{R}\,\partial_\phi\dot{\phi}'\right) = R^2\left(\omega+\dot{\phi}'\right)^2 && (5.17b)\\
\phi': \qquad & R\,\mathrm{d}_{t'}\left(\rho\dot{\phi}'\right) + \rho\left(\dot{R}\dot{\phi}' + R\dot{\phi}'\,\partial_R\dot{R} + R\dot{\phi}'\,\partial_\phi\dot{\phi}'\right) = -2\dot{R}\left(\omega+\dot{\phi}'\right). && (5.17c)
\end{aligned}$$

Furthermore, substituting the energy equation (5.17a) into the L.H.S. of each of the momentum equations eliminates all but the first term on the L.H.S. Cancelling a factor of R from the R-equation, we have now arrived at a more useful form of the Euler equations,

$$\begin{aligned}
R: \qquad & \mathrm{d}_{t'}\left(\rho\dot{R}\right) = R\left(\omega+\dot{\phi}'\right)^2 && (5.18a)\\
\phi': \qquad & R\,\mathrm{d}_{t'}\left(\rho\dot{\phi}'\right) = -2\dot{R}\left(\omega+\dot{\phi}'\right). && (5.18b)
\end{aligned}$$

In this simplified form, it will now be very straightforward to interpret each of the terms appearing in the momentum equations.

5.3 Interpretation of the Field Equations

Now, since a dust has no pressure and a flat metric implies no gravity, the acceleration of the dust as measured in the corotating frame should be given by the centrifugal acceleration plus the Coriolis acceleration. Let us verify that this is indeed the case. The centrifugal acceleration is

$$\mathbf{a}_{cent} = -\omega \times (\omega \times \mathbf{R}) = -\omega\ \hat{z} \times \left(\omega\ \hat{z} \times R\ \hat{R}\right) = \omega^2 R\ \hat{R}, \tag{5.19}$$

while the Coriolis acceleration is

$$\mathbf{a}_{cor} = -2\omega \times \mathbf{v} = -2\omega\ \hat{z} \times \left(\dot{R}\ \hat{R} + R\dot{\phi}'\ \hat{\phi}\right) = -2\omega \left(\dot{R}\ \hat{\phi} - R\dot{\phi}'\ \hat{R}\right). \tag{5.20}$$

Meanwhile, expanding out the source terms appearing in the momentum equations for the sake of comparison, we find that

$$R: \qquad \mathrm{d}_{t'}\left(\rho\dot{R}\right) \;=\; \rho R\omega^2 + 2\rho R\omega\dot{\phi}' + \rho R\dot{\phi}'^2 \tag{5.21a}$$

$$\phi': \qquad R\ \mathrm{d}_{t'}\left(\rho\dot{\phi}'\right) \;=\; -2\rho\dot{R}\omega - 2\rho\dot{R}\dot{\phi}'. \tag{5.21b}$$

The first source term in the R-equation is the centrifugal force density. The second term is the R-component of the Coriolis force density. Meanwhile, the first source term in the ϕ'-equation is the ϕ'-component of the Coriolis force density. Thus, moving the remaining source terms over to the L.H.S., we can write,

$$R: \qquad \mathrm{d}_{t'}\left(\rho\dot{R}\right) - \rho R\dot{\phi}'^2 \;=\; F_{cent} + F_{cor,R} \tag{5.22}$$

$$\phi': \qquad R\ \mathrm{d}_{t'}\left(\rho\dot{\phi}'\right) + 2\rho\dot{R}\dot{\phi}' \;=\; F_{cor,\phi'}. \tag{5.23}$$

The only task remaining is to show that each L.H.S. represents a physicalforce density (or more precisely, a time-rate-of-change of momentum density) as measured in the corotating coordinate system. We will do this by writing out the time-rate-of-change of momentum vector in Cartesian coordinates. Then we will transform it into corotating coordinates. In Cartesian coordinates we know that the time-rate-of-change of momentum along the x-direction is $\mathrm{d}_t\left(\rho\dot{x}\right) = 0$ and along the y-direction it is $\mathrm{d}_t\left(\rho\dot{y}\right) = 0$. Now the total inertial-

frame time derivative can be written

$$\begin{aligned}\partial_t + \dot{R}\,\partial_R + \dot{\phi}\,\partial_\phi &= \partial_t + \dot{x}\,\partial_x + \dot{y}\,\partial_y \\ &= \partial_t + \dot{x}\left(\cos\phi\,\partial_R - \frac{\dot{x}\sin\phi}{R}\,\partial_\phi\right) + \dot{y}\left(\sin\phi\,\partial_R + \frac{\cos\phi}{R}\,\partial_\phi\right) \\ &= \partial_t + (\dot{x}\cos\phi + \dot{y}\sin\phi)\,\partial_R + \frac{1}{R}\left(-\dot{x}\sin\phi + \dot{y}\cos\phi\right)\partial_\phi. \qquad (5.24)\end{aligned}$$

This allows us to identify

$$\dot{R} = \dot{x}\cos\phi + \dot{y}\sin\phi \qquad (5.25a)$$

$$R\dot{\phi} = -\dot{x}\sin\phi + \dot{y}\cos\phi, \qquad (5.25b)$$

Consequently,

$$\begin{aligned}\mathrm{d}_t\left(\rho\dot{R}\right) = \dot{\rho}\dot{R} + \rho\ddot{R} &= \dot{\rho}\left(\dot{x}\cos\phi + \dot{y}\sin\phi\right) + \rho\left(\ddot{x}\cos\phi - \dot{x}\dot{\phi}\sin\phi + \ddot{y}\sin\phi + \dot{y}\dot{\phi}\cos\phi\right) \\ &= (\dot{\rho}\dot{x} + \rho\ddot{x})\cos\phi + (\dot{\rho}\dot{y} + \rho\ddot{y})\sin\phi - \rho\dot{x}\dot{\phi}\sin\phi + \rho\dot{y}\dot{\phi}\cos\phi \\ &= \rho\dot{\phi}\left(-\dot{x}\sin\phi + \dot{y}\cos\phi\right) \\ &= \rho R\dot{\phi}^2 \qquad (5.26a)\end{aligned}$$

$$\begin{aligned}\mathrm{d}_t\left(\rho R\dot{\phi}\right) = \dot{\rho}R\dot{\phi} + \rho R\ddot{\phi} + \rho\dot{R}\dot{\phi} &= \dot{\rho}\left(-\dot{x}\sin\phi + \dot{y}\cos\phi\right) + \rho\left(-\ddot{x}\sin\phi - \dot{x}\dot{\phi}\cos\phi + \ddot{y}\cos\phi - \dot{y}\dot{\phi}\sin\phi\right) \\ &= -\left(\dot{\rho}\dot{x} + \rho\ddot{x}\right)\sin\phi + \left(\dot{\rho}\dot{y} + \rho\ddot{y}\right)\cos\phi + \rho\left(-\dot{x}\dot{\phi}\cos\phi - \dot{y}\dot{\phi}\sin\phi\right) \\ &= -\rho\dot{\phi}\left(\dot{x}\cos\phi + \dot{y}\sin\phi\right) \\ &= -\rho\dot{R}\dot{\phi} \\ \implies \dot{\rho}R\dot{\phi} + \rho R\ddot{\phi} &= -2\rho\dot{R}\dot{\phi}. \qquad (5.26b)\end{aligned}$$

Then $\ddot{R} - R\dot{\phi}^2 = 0$ and $R\ddot{\phi} + 2\dot{R}\dot{\phi} = 0$. After some thought, it becomes clear that this implies $a_R = \ddot{R} - R\dot{\phi}^2$ and $a_\phi = R\ddot{\phi} + 2\dot{R}\dot{\phi}$ in cylindrical coordinates. Then, in corotating coordinates the appropriate accelerations are

$$a_R = \ddot{R} - R\dot{\phi'}^2 \qquad (5.27a)$$

$$a_{\phi'} = R\ddot{\phi'} + 2\dot{R}\dot{\phi'}, \qquad (5.27b)$$

just what we expected them to be. Thus the field equations do, indeed, read

$$R: \quad F_R = F_{cent} + F_{cor,R} \qquad (5.28a)$$

$$\phi': \quad F_{\phi'} = F_{cor,\phi'} \qquad (5.28b)$$

in corotating (or helical) coordinates.

5.4 Use the Characteristic Vector to Make a Weighted Linear Combination of the Field Equations Such That the Source Vanishes

As given by Eq. (3.2), the field equations can be written,

$$\frac{1}{\sqrt{-g}}\partial_\mu\left(\sqrt{-g}\;T^{\mu\nu}C_{\nu(\eta)}\right) = T^{\mu\nu}\nabla_\mu C_{\nu(\eta)}$$

so that if $\mathbf{C}_{(\eta)}$ is a Killing vector field, the R.H.S. vanishes. In our scenario, one Killing vector (the helical Killing vector) is $\mathbf{C} = \mathbf{e}_t + \omega\ \mathbf{e}_\phi = \mathbf{e}_{t'}$. This is expressed in terms of contravariant components and covariant basis vectors. We need to write it in terms of covariant components and contravariant basis vectors since the indices on $\mathbf{C}$ in equation (3.2) are down. It is,

$$\mathbf{C} = -c^2\ \mathbf{e}^t + R^2\omega\ \mathbf{e}^\phi = \left(-c^2 + R^2\omega^2\right)\mathbf{e}^{t'} + R^2\omega\ \mathbf{e}^{\phi'}.$$

This is telling us that instead of using the t, R, ϕ', and z equations as they are (5.12a-5.12d), we might want to consider taking $(-c^2 + R^2\omega^2)$ times the t-equation, plus $R^2\omega$ times the ϕ'-equation. Doing so produces the following:

$$\begin{aligned}\left(-c^2 + R^2\omega^2\right)&\left[\partial_{t'}\left(cR\rho\right) + \partial_R\left(cR\rho\dot{R}\right) + \partial_\phi\left(cR\rho\dot{\phi}'\right)\right] \\ &+\ R^2\omega\left[\partial_{t'}\left(cR\rho\dot{\phi}'\right) + \partial_R\left(cR\rho\dot{R}\dot{\phi}'\right) + \partial_\phi\left(cR\rho\dot{\phi}'^2\right)\right] \\ &= R^2\omega\left[-\frac{2\omega}{R}\left(cR\rho\dot{R}\right) - \frac{2}{R}\left(cR\rho\dot{R}\dot{\phi}'\right)\right]. \end{aligned} \tag{5.29}$$

Now, in order for the source to vanish, we need to move the weighting factors inside the partials by applying the product rule in reverse. When we do this, we find that

$$
\begin{aligned}
&\partial_{t'}\left(cR\left(-c^2+R^2\omega^2\right)\rho\right)-cR\rho\frac{\partial}{\partial t'}\left(-c^2+R^2\omega^2\right)\\
&+\partial_R\left(cR\left(-c^2+R^2\omega^2\right)\rho\dot{R}\right)-cR\rho\dot{R}\frac{\partial}{\partial R}\left(-c^2+R^2\omega^2\right)\\
&+\partial_\phi\left(cR\left(-c^2+R^2\omega^2\right)\rho\dot{\phi}'\right)-cR\rho\dot{\phi}'\frac{\partial}{\partial\phi}\left(-c^2+R^2\omega^2\right)\\
&+\partial_{t'}\left(cR\left(R^2\omega\right)\rho\dot{\phi}'\right)-cR\rho\dot{\phi}'\frac{\partial}{\partial t'}\left(R^2\omega\right)\\
&+\partial_R\left(cR\left(R^2\omega\right)\rho\dot{R}\dot{\phi}'\right)-cR\rho\dot{R}\dot{\phi}'\frac{\partial}{\partial R}\left(R^2\omega\right)\\
&+\partial_\phi\left(cR\left(R^2\omega\right)\rho{\dot{\phi}'}^2\right)-cR\rho{\dot{\phi}'}^2\frac{\partial}{\partial\phi}\left(R^2\omega\right)\\
&=R^2\omega\left[-\frac{2\omega}{R}\left(cR\rho\dot{R}\right)-\frac{2}{R}\left(cR\rho\dot{R}\dot{\phi}'\right)\right].
\end{aligned}
\tag{5.30}
$$

The partial derivatives inside the new terms that have appeared (the ones with the minus signs out front) can be evaluated at this time. Many of them are zero. At the same time, the remaining terms can be organized and simplified by combining like partials:

$$
\begin{aligned}
&\partial_{t'}\left[cR\left(\left(-c^2+R^2\omega^2\right)\rho+R^2\omega\ \rho\dot{\phi}'\right)\right]\\
&+\partial_R\left[cR\left(\left(-c^2+R^2\omega^2\right)\rho\dot{R}+R^2\omega\ \rho\dot{R}\dot{\phi}'\right)\right]-cR\rho\dot{R}\left(2R\omega^2\right)-cR\rho\dot{R}\dot{\phi}'\left(2R\omega\right)\\
&+\partial_\phi\left[cR\left(\left(-c^2+R^2\omega^2\right)\rho\dot{\phi}'+R^2\omega\ \rho{\dot{\phi}'}^2\right)\right]\\
&=-2R\omega^2\left(cR\rho\dot{R}\right)-2R\omega\left(cR\rho\dot{R}\dot{\phi}'\right).
\end{aligned}
\tag{5.31}
$$

This is where the small miracle occurs. We see that the extra terms that have appeared on the L.H.S. turn out to be exactly what is needed to cancel with the R.H.S.! The field equations now read

$$
\begin{aligned}
&\partial_{t'}\left[cR\left(\left(-c^2+R^2\omega^2\right)\rho+R^2\omega\ \rho\dot{\phi}'\right)\right]\\
&+\partial_R\left[cR\left(\left(-c^2+R^2\omega^2\right)\rho\dot{R}+R^2\omega\ \rho\dot{R}\dot{\phi}'\right)\right]\\
&+\partial_\phi\left[cR\left(\left(-c^2+R^2\omega^2\right)\rho\dot{\phi}'+R^2\omega\ \rho{\dot{\phi}'}^2\right)\right]\ =\ 0.
\end{aligned}
\tag{5.32}
$$

This is how the helical equation would have read if we had started with equation (3.2) and chosen $\mathbf{C}$ to be our helical Killing vector. One can easily verify this by comparing the two.

5.5 Find Other Vector Fields That Identify Additional Weighted Linear Combinations That Eliminate the Source

I must warn the reader in advance that this section gets a bit messy. We are looking for solutions to { R.H.S. of (3.2) } = 0; that is,

$$T^{\mu\nu}\nabla_\mu C_\nu = 0. \tag{5.33}$$

Let us write out $\nabla_\mu C_\nu = \partial_\mu C_\nu - \Gamma^\alpha_{\mu\nu} C_\alpha$ component by component in corotating coordinates using the Christoffel symbols we introduced in equations (5.11a-5.11e).

$$\nabla_\mu C_\nu = \begin{pmatrix} \partial_{t'}C_{t'} + R\omega^2 C_R & \partial_{t'}C_R - \frac{\omega}{R}C_\phi & \partial_{t'}C_\phi + R\omega C_R & \partial_{t'}C_z \\ \partial_R C_{t'} - \frac{\omega}{R}C_\phi & \partial_R C_R & \partial_R C_\phi - \frac{1}{R}C_\phi & \partial_R C_z \\ \partial_\phi C_{t'} + R\omega C_R & \partial_\phi C_R - \frac{1}{R}C_\phi & \partial_\phi C_\phi + RC_R & \partial_\phi C_z \\ \partial_z C_{t'} & \partial_z C_R & \partial_z C_\phi & \partial_z C_z \end{pmatrix}, \tag{5.34}$$

where primes were kept only on the t-component of $\mathbf{C}$ for the same reason that they are kept only on partial derivatives with respect to t. Then in order for the R.H.S. of (3.2) to vanish, it must be true that

$$\begin{aligned} & \rho\left(\partial_{t'}C_{t'} + R\omega^2 C_R\right) + \rho\dot{R}\left(\partial_{t'}C_R - \frac{\omega}{R}C_\phi\right) + \rho\dot{\phi'}\left(\partial_{t'}C_\phi + R\omega C_R\right) \\ + \;& \rho\dot{R}\left(\partial_R C_{t'} - \frac{\omega}{R}C_\phi\right) + \rho\dot{R}^2\left(\partial_R C_R\right) + \rho\dot{R}\dot{\phi'}\left(\partial_R C_\phi - \frac{1}{R}C_\phi\right) \\ + \;& \rho\dot{\phi'}\left(\partial_\phi C_{t'} + R\omega C_R\right) + \rho\dot{R}\dot{\phi'}\left(\partial_\phi C_R - \frac{1}{R}C_\phi\right) + \rho\dot{\phi'}^2\left(\partial_\phi C_\phi + RC_R\right) = 0 \end{aligned} \tag{5.35}$$

Since this is the *only* constraint on $\mathbf{C}$, and $\mathbf{C}$ has four degrees of freedom (i.e., its four components), we are free to choose three of those components at will. But if we want to find a vector field that will pick a linear combination of the field equations that includes the R-equation, then the vector field must at least possess a nonzero R-component. The simplest choice that includes a nonzero R-component is $C_R = 1$, $C_\phi = 0$, $C_z = 0$. Eq. (5.35) is profoundly deflated. All we have left is

$$\partial_{t'}C_{t'} + \dot{R}\,\partial_R C_{t'} + \dot{\phi'}\,\partial_\phi C_{t'} + R\left(\omega + \dot{\phi'}\right)^2 = 0. \tag{5.36}$$

The first three terms are just a total time derivative, so

$$\mathrm{d}_{t'}C_{t'} = -R\left(\omega + \dot{\phi'}\right)^2 \tag{5.37}$$

is the appropriate condition on $C_{t'}$. Apparently $C_{t'}$ just needs to be the t'-integral of $-R\left(\omega+\dot{\phi}'\right)^2$. That is the good news. The bad news is that, while ω does not change with t', both R and $\dot{\phi}'$ *do* change with t'. And they do so in a somewhat complicated way — one that we must determine before we can integrate.

In order to determine how the R.H.S. of (5.37) depends on t', we are going to have to transform it back into Cartesian coordinates. (Remember, we know that both $\dot{x}$ and $\dot{y}$ are uniform and unchanging.) Before we do that, though, let us rewrite (5.37) in cylindrical coordinates. It becomes

$$\mathrm{d}_t C_t = -R\dot{\phi}^2. \tag{5.38}$$

And in Cartesian coordinates,

$$\mathrm{d}_t C_t = -\frac{\left(x\dot{y}-y\dot{x}\right)^2}{\left(x^2+y^2\right)^{3/2}}. \tag{5.39}$$

While $\dot{x}$ and $\dot{y}$ can be thought of as constants, x and y themselves depend on t as follows:

$$x(t) = \dot{x}t + x_0 \tag{5.40}$$

$$y(t) = \dot{y}t + y_0, \tag{5.41}$$

where x_0 and y_0 are the values of x and y at the moment in question. Then, x_0 and y_0 are constants. Finally, we can rewrite (5.37) with all the time dependence explicitly manifest. It is

$$\mathrm{d}_t C_t = -\frac{\left(x_0\dot{y}-y_0\dot{x}\right)^2}{\left[\left(\dot{x}t+x_0\right)^2+\left(\dot{y}t+y_0\right)^2\right]^{3/2}}; \tag{5.42}$$

the time dependence only appears in the denominator. Integrating over time, we find that

$$C_t = -\frac{\left(\dot{x}^2+\dot{y}^2\right)t + x_0\dot{x} + y_0\dot{y}}{\sqrt{\left(\dot{x}t+x_0\right)^2+\left(\dot{y}t+y_0\right)^2}}. \tag{5.43}$$

And once this integration has been performed, we can simplify our result by substituting (5.40) and (5.41) back in (since we no longer need to know the explicit time dependence).

$$C_t = -\frac{\left(\dot{x}^2+\dot{y}^2\right)t + x_0\dot{x} + y_0\dot{y}}{\sqrt{x^2+y^2}}. \tag{5.44}$$

Finally, we must convert back to helical coordinates. When we do, we obtain, first,

$$C_t = -\frac{1}{R}\left[\left(\dot{R}^2 + {R_0}^2\dot{\phi}^2\right)t + R_0\dot{R}\right] \tag{5.45}$$

in cylindrical coordinates, then

$$C_{t'} = -\frac{1}{R}\left[\left(\dot{R}^2 + {R_0}^2\left(\omega + \dot{\phi}'\right)^2\right)t + R_0\dot{R}\right] \tag{5.46}$$

in corotating coordinates. This is a bit of a mess, but now we know that if we take $C_{t'}$ times the t-equation (5.12a), plus 1 times the R-equation (5.12b), and use the product rule in reverse to move the coefficients inside the partials on the L.H.S, then the additional terms that appear on the left will cancel with the terms on the right. In other words, we have found a second equation — an "R-equation" — with zero source term that will supplement (and be independent from) the helical equation (5.32).

Our next objective will be to check that

$$\mathbf{C} = -\frac{1}{R}\left[\left(\dot{R}^2 + {R_0}^2\left(\omega + \dot{\phi}'\right)^2\right)t + R_0\dot{R}\right]\ \mathbf{e}^t + \mathbf{e}^R \tag{5.47}$$

really does eliminate the source term on (5.12b) as promised. Alas, a step-by-step presentation of the procedure will be dreadfully long and messy, so we will begin with a somewhat hand-wavey outline. The reader who does not wish to see the calculation carried out in painful detail can then skip to the next section.

After taking the appropriate linear combination of equations and moving the coefficient $C_{t'}$ inside the partials, we will be left with two kinds of partials on the L.H.S. The first set of partials will be of the form $\partial_\mu\left(\sqrt{-g}\ T^{\mu\nu}C_\nu\right)$, whereas the second set will be of the form $-\sqrt{-g}\ T^{\mu\nu}\partial_\mu C_\nu$. The latter, once evaluated, are the partials that will cancel with the sources on the R.H.S. An examination of these partials shows that they (when taken with their appropriate coefficients) add up to a total time derivative of $C_{t'}$. But we intentionally chose $C_{t'}$ so that $\mathrm{d}_{t'}C_{t'}$ would specifically equal $-R\left(\omega + \dot{\phi}'\right)^2$, which is the source term on the R.H.S. Thus we can be assured that they will cancel and our sketchy outline is complete.

We now proceed to give the more detailed presentation of the procedure. The appropriate linear combination of equations (5.12a-5.12d) is

$$\begin{aligned}
-\frac{1}{R}\left[\left(\dot{R}^2 + {R_0}^2\left(\omega + \dot{\phi}'\right)^2\right)t + R_0\dot{R}\right]&\left[\partial_{t'}\left(cR\rho\right) + \partial_R\left(cR\rho\dot{R}\right) + \partial_\phi\left(cR\rho\dot{\phi}'\right)\right] \\
&+\ \left[\partial_{t'}\left(cR\rho\dot{R}\right) + \partial_R\left(cR\rho\dot{R}^2\right) + \partial_\phi\left(cR\rho\dot{R}\dot{\phi}'\right)\right] \\
&= R\omega^2\left(cR\rho\right) + 2R\omega\left(cR\rho\dot{\phi}'\right) + R\left(cR\rho{\dot{\phi}'}^2\right).
\end{aligned} \tag{5.48}$$

We next move the coefficient inside the partials on the L.H.S. (via the product rule in reverse) to obtain

$$
\begin{aligned}
& \partial_{t'}\left[cR\left(-\frac{\left(\dot{R}^2+{R_0}^2\left(\omega+\dot{\phi}'\right)^2\right)t+R_0\dot{R}}{R}\rho+\rho\dot{R}\right)\right] \\
- \quad & cR\rho\,\partial_{t'}\left[-\frac{\left(\dot{R}^2+{R_0}^2\left(\omega+\dot{\phi}'\right)^2\right)t+R_0\dot{R}}{R}\right] \\
+ \quad & \partial_R\left[cR\left(-\frac{\left(\dot{R}^2+{R_0}^2\left(\omega+\dot{\phi}'\right)^2\right)t+R_0\dot{R}}{R}\rho\dot{R}+\rho\dot{R}^2\right)\right] \\
- \quad & cR\rho\dot{R}\,\partial_R\left[-\frac{\left(\dot{R}^2+{R_0}^2\left(\omega+\dot{\phi}'\right)^2\right)t+R_0\dot{R}}{R}\right] \\
+ \quad & \partial_\phi\left[cR\left(-\frac{\left(\dot{R}^2+{R_0}^2\left(\omega+\dot{\phi}'\right)^2\right)t+R_0\dot{R}}{R}\rho\dot{\phi}'+\rho\dot{R}\dot{\phi}'\right)\right] \\
- \quad & cR\rho\dot{\phi}'\,\partial_\phi\left[-\frac{\left(\dot{R}^2+{R_0}^2\left(\omega+\dot{\phi}'\right)^2\right)t+R_0\dot{R}}{R}\right] \\
= \quad & R\omega^2\left(cR\rho\right)+2R\omega\left(cR\rho\dot{\phi}'\right)+R\left(cR\rho{\dot{\phi}'}^2\right). \qquad (5.49)
\end{aligned}
$$

From the chain rule, we can see that the second, fourth, and sixth terms on the L.H.S. add together to give a total time derivative. Recognizing this allows us to rewrite the equation as

$$
\begin{aligned}
& \partial_{t'}\left[cR\left(-\frac{\left(\dot{R}^2+{R_0}^2\left(\omega+\dot{\phi}'\right)^2\right)t+R_0\dot{R}}{R}\rho+\rho\dot{R}\right)\right] \\
+ \quad & \partial_R\left[cR\left(-\frac{\left(\dot{R}^2+{R_0}^2\left(\omega+\dot{\phi}'\right)^2\right)t+R_0\dot{R}}{R}\rho\dot{R}+\rho\dot{R}^2\right)\right] \\
+ \quad & \partial_\phi\left[cR\left(-\frac{\left(\dot{R}^2+{R_0}^2\left(\omega+\dot{\phi}'\right)^2\right)t+R_0\dot{R}}{R}\rho\dot{\phi}'+\rho\dot{R}\dot{\phi}'\right)\right] \\
- \quad & cR\rho\ \mathrm{d}_{t'}\left[-\frac{\left(\dot{R}^2+{R_0}^2\left(\omega+\dot{\phi}'\right)^2\right)t+R_0\dot{R}}{R}\right] \\
= \quad & cR\rho\left(R\left(\omega+\dot{\phi}'\right)^2\right). \qquad (5.50)
\end{aligned}
$$

Since the term with the total time derivative on the left equals the source on the right (see equations 5.37 to 5.46), the two will cancel, leaving us with

$$
\begin{aligned}
& \partial_{t'}\left[cR\left(\frac{\left(\dot{R}^2+{R_0}^2\left(\omega+\dot{\phi}'\right)^2\right)t+R_0\dot{R}}{R}\rho+\rho\dot{R}\right)\right] \\
+ \ & \partial_R\left[cR\left(\frac{\left(\dot{R}^2+{R_0}^2\left(\omega+\dot{\phi}'\right)^2\right)t+R_0\dot{R}}{R}\rho\dot{R}+\rho\dot{R}^2\right)\right] \\
+ \ & \partial_\phi\left[cR\left(\frac{\left(\dot{R}^2+{R_0}^2\left(\omega+\dot{\phi}'\right)^2\right)t+R_0\dot{R}}{R}\rho\dot{\phi}'+\rho\dot{R}\dot{\phi}'\right)\right] \quad = \quad 0. \qquad (5.51)
\end{aligned}
$$

for the R-equation.

5.6 Generalize the Procedure for Any ADM-Decomposed Metric at a Particular Timestep

Our goal in this section will be to reproduce the results of §5.1 using the most generalized ADM-decomposed metric, given in equation (5.9). The resulting coordinate transformation will tell us how to choose the lapse function and the shift vector at time slice $n+1$, using

the lapse function, the shift vector, the induced metric, and the chosen characteristic vector field $\mathbf{C}$ at time slice n.

We begin with the characteristic vector field $\mathbf{C} = \partial_t + C^i\ \partial_i$, where, as a reminder, summation is implied. The vector is chosen so that the t-component is intentionally one. (This can always be accomplished by means of a scaling factor since it is only the direction of $\mathbf{C}$, and not its magnitude, that concerns us.) Analogous to equation (5.4), $\mathbf{C}$ is expressed in some primed coordinate system (which now varies only infinitesimally from the unprimed coordinate system) such that

$$\mathbf{C} = \partial_t + C^i\ \partial_i = \partial_{t'} = \frac{\partial t}{\partial t'}\ \partial_t + \frac{\partial x^i}{\partial t'}\ \partial_i. \tag{5.52}$$

Picking off coefficients as before,

$$\frac{\partial t}{\partial t'} = 1 \tag{5.53}$$

$$\frac{\partial x^i}{\partial t'} = C^i. \tag{5.54}$$

These relations imply the coordinate transformation,

$$t = t' \tag{5.55}$$

$$x^i = x'^i + C^i t'. \tag{5.56}$$

The ADM line element associated with (5.9) is

$$\mathrm{d}s^2 = \left(-c^2\alpha^2 + \beta^2\right)\mathrm{d}t^2 + 2\beta_i\ \mathrm{d}t\ \mathrm{d}x^i + \gamma_{ij}\ \mathrm{d}x^i\mathrm{d}x^j.$$

Plugging the differential coordinate transformations,

$$\mathrm{d}t = \mathrm{d}t' \quad \text{and} \quad \mathrm{d}x^i = \mathrm{d}x'^i + C^i\ \mathrm{d}t',$$

into the line element produces (after some work)

$$\begin{aligned}\mathrm{d}s^2 &= \left[\left(-c^2\alpha^2 + \beta^2\right) + 2\beta_i C^i + \gamma_{ij}C^iC^j\right]\mathrm{d}t'^2 + 2\left(\beta_i + \gamma_{ij}C^j\right)\mathrm{d}t'\mathrm{d}x'^i + \gamma_{ij}\ \mathrm{d}x'^i\mathrm{d}x'^j \\ &= \left(-c^2\alpha'^2 + \beta'^2\right)\mathrm{d}t'^2 + 2\beta'_i\ \mathrm{d}t'\mathrm{d}x'^i + \gamma_{ij}\ \mathrm{d}x'^i\mathrm{d}x'^j. \end{aligned}\tag{5.57}$$

Notice that this *still* has the form of an ADM-metric, as it should. The new shift vector can then be picked off. It is

$$\beta'_i = \beta_i + \gamma_{ij}C^j = \beta_i + C_i. \tag{5.58}$$

Of course, these are the covariant components of the new shift vector. What we really want are the contravariant components,

$$\beta'^{i} = \gamma^{ik}\beta'_{k} = \gamma^{ik}\left(\beta_k + \gamma_{kj}C^j\right) = \beta^i + \delta^i{}_j C^j = \beta^i + C^i. \tag{5.59}$$

It turns out that the change in shift vectors at a particular time step is just the spatial part of the characteristic vector, $\beta' - \beta = \mathbf{C}_{\text{sp}}$!

We are now in a position to calculate the squared magnitude of the new shift vector,

$$\beta'^2 = \left(\beta^i + C^i\right)\left(\beta_i + C_i\right) = \beta^2 + 2\beta_i C^i + \gamma_{ij}C^i C^j. \tag{5.60}$$

Comparing this to equation (5.57), evidently the lapse function is unaffected by our characteristic vector field,

$$\alpha'^2 = \alpha^2. \tag{5.61}$$

Only the shift vector is influenced by $\mathbf{C}$. This is because we chose a characteristic vector with a timelike component that is always equal to $+1$.

6. Application

Because it involves so many subtle details, in practice it can be more confusing than one might guess to set up and interpret the equations of motion when the type of momentum one chooses to advect does not agree with the coordinates used to discretize the grid. It is worth taking some time to explore the richness of this formalism by considering its application to just such a problem.

Up to this point we have focused on a three-dimensional subset of the full four-dimensional generalized Valencia formulation. Now we briefly identify a few additional features that emerge from the broader four-dimensional generalization which, as mentioned earlier in §3.2, provides for a mixing of the momentum and energy equations. As an example application, we will again consider modeling an axisymmetric neutron star that is rotating uniformly with angular velocity Ω. But we could just as well consider a synchronously rotating binary star system in circular orbit whose orbital angular velocity is Ω.

Tables 6.1 and 6.2 are designed to support and catalog the ideas discussed here. The mathematical expressions that appear in each major row of both tables define, in the Newtonian limit, key elements of the particular Euler equation that corresponds to a particular choice of the state variable. More specifically, the 3$^{\text{rd}}$ column of both tables identifies the vector $\mathbf{C}_{(\eta)}$ required to construct a particular state variable, while the last column of Table 6.1 shows the corresponding functional form of $\psi_{(\eta)}$ and the last column of Table 6.2 shows the corresponding functional form of the principal element of $\mathcal{S}_{(\eta)}$. Fully generalized relativistic expressions for these functions can be obtained from Eq. (3.19b) when dealing strictly with momentum state variables; expressions from Appendix B will need to be used when generalizing expressions that incorporate a nonzero contribution from the energy equation.

6.1 Choosing a Collection of Generalized Advection Variables

6.1.1 Rest Mass State Variable Never Changes

For any physical problem we may wish to consider, the conservative advection variable associated with the continuity equation is rest-mass density,

$$\psi_{(1)} = \rho.$$

6.1.2 Momentum State Variables Defined by Cylindrical Geometry

Because the axisymmetric, uniformly rotating neutron star in our example problem is in quasi-equilibrium, the principal part of the motion will be in the azimuthal direction (about the center of mass), and it will be extremely important to conserve angular momentum for this problem. It is, therefore, natural to choose angular momentum as one of our generalized advection variables. (Use method two in §2.6.2.)

$$\mathbf{C}_{(2)} = \mathbf{e}_\phi = -y\mathbf{e}_x + x\mathbf{e}_y \qquad \rightarrow \qquad \psi_{(2)} = \rho h u_\phi = \rho h \left(-y u_x + x u_y\right).$$

We also know that there will be very little motion in the radial direction, so radial momentum is a good choice for an additional generalized advection variable. (Use method three in §2.6.2.)

$$\mathbf{C}_{(3)} = \mathbf{e}_R = \frac{x\mathbf{e}_x + y\mathbf{e}_y}{R} \qquad \rightarrow \qquad \psi_{(3)} = \rho h u_R = \rho h \frac{x u_y + y u_x}{R}. \tag{6.1}$$

For the same reason, vertical momentum is also a good candidate for our third generalized advection variable. (Again use method three in §2.6.2.)

$$\mathbf{C}_{(4)} = \mathbf{e}_z \qquad \rightarrow \qquad \psi_{(4)} = \rho h u_z. \tag{6.2}$$

Consequently, based on our §4 discussion, we will focus here on strategies that utilize cylindrical components of the momentum to define the three state variables identified by Euler equation indices $\eta = 2, 3$ and 4. It is clear from the §4 discussion that the vectors $\mathbf{C}_{(\eta)}$ chosen to accomplish this can be expressed in terms of the basis vectors associated with any

number of different grid geometries, including the two considered in Figure 4.2. For example, if the grid is defined by cylindrical coordinates, then the $\mathbf{C}$ vectors should be expressed in the form $\mathbf{C}_{(2)} = \mathbf{e}_R$, $\mathbf{C}_{(3)} = \mathbf{e}_\phi$, and $\mathbf{C}_{(4)} = \mathbf{e}_z$, as indicated by the mathematical expressions labeled "Case B" in each of the first three major rows of Tables 6.1 and 6.2. If, however, the grid is defined by Cartesian coordinates, the $\mathbf{C}$ vectors should be expressed in the form $\mathbf{C}_{(2)} = (x\mathbf{e}_x + y\mathbf{e}_y)/R$, $\mathbf{C}_{(3)} = -y\mathbf{e}_x + x\mathbf{e}_y$, and $\mathbf{C}_{(4)} = \mathbf{e}_z$, as indicated by the mathematical expressions labeled "Case A" in each of the first three major rows of Tables 6.1 and 6.2.

Similarly, although the form of the expression for each of the generalized advection variables $\psi_{(\eta)}$ will differ according to the choice of coordinates, they will be functionally identical to one another. For example, as shown in the last column of Table 6.1, when expressed in terms of cylindrical coordinates (Case B), $\psi_{(3)} = \rho h R^2 u^\phi$; and when expressed in terms of Cartesian coordinates (Case A), $\psi_{(3)} = \rho h(-yu^x + xu^y)$. But these are functionally the same; that is, $\rho h R^2 u^\phi = \rho h(-yu^x + xu^y)$. The same goes for the source functions. As shown in the last column of Table 6.2, for example, the expression used to specify $\mathcal{S}_{(3)}$ takes a different form depending on whether it is written out in Cartesian coordinates (Case A) or in cylindrical coordinates (Case B), but the function itself is the same. That is,

$$\mathcal{S}_{(3)} = (y\partial_x - x\partial_y)P + \rho h(y\partial_x - x\partial_y)\Phi = -\partial_\phi P - \rho h\ \partial_\phi \Phi,$$

and this source function should approach zero in steady state.

6.1.3 Energy State Variable Defined by Helical Killing Vector

Due to the stationary nature of this situation, a timelike Killing vector exists, which can be used to construct our final generalized advection variable. (Use method two in §2.6.2.)

$$\mathbf{C}_{(5)} = \mathbf{e}_t + \omega\mathbf{e}_\phi \qquad \rightarrow \qquad \psi_{(5)} = \rho h\,(u_t + \omega u_\phi)\,. \tag{6.3}$$

Because $\mathbf{C}_{(5)}$ is a quasi-Killing vector, $\psi_{(5)}$ — which is total energy density minus rotational kinetic energy density — is a globally conserved quantity. The actual state variable to be evolved, τ — total energy density minus rest-mass energy density minus rotational kinetic energy density — is also globally conserved.

Table 6.1

η	Case[a]	$\mathbf{C}_{(\eta)}$	$\psi_{(\eta)}$
2	A	$(x\mathbf{e}_x + y\mathbf{e}_y)/R$	$\rho h\,(xu^x + yu^y)/R$
	B	$\mathbf{e}_R$	$\rho h u^R$
	C	$\mathbf{e}_R$	$\rho h u^R$
	D	$(x'\mathbf{e}_{x'} + y'\mathbf{e}_{y'})/R$	$\rho h(x'u^{x'} + y'u^{y'})/R$
3	A	$-y\mathbf{e}_x + x\mathbf{e}_y$	$\rho h\,(-yu^x + xu^y)$
	B	$\mathbf{e}_\phi$	$\rho h R^2 u^\phi$
	C	$\mathbf{e}_{\phi'}$	$\rho h R^2(u^{\phi'} + \omega u^{t'})$
	D	$-y'\mathbf{e}_{x'} + x'\mathbf{e}_{y'}$	$\rho h(-y'u^{x'} + x'u^{y'} + R^2\omega u^{t'})$
4	A,B,C,D	$\mathbf{e}_z$	$\rho h u^z$
3′	A	$-y\mathbf{e}_x + x\mathbf{e}_y + (R^2\bar{\omega}/c^2)\mathbf{e}_t$	$\rho h(-yu^x + xu^y - R^2\bar{\omega}u^t)$
	B	$\mathbf{e}_\phi + (R^2\bar{\omega}/c^2)\,\mathbf{e}_t$	$\rho h R^2\left(u^\phi - \bar{\omega}u^t\right)$
	C	$(1 - R^2\bar{\omega}\omega/c^2)\mathbf{e}_{\phi'} + (R^2\bar{\omega}/c^2)\mathbf{e}_{t'}$	$\rho h R^2[u^{\phi'} + (\omega - \bar{\omega})u^{t'}]$
	D	$(1 - R^2\bar{\omega}\omega/c^2)(-y'\mathbf{e}_{x'} + x'\mathbf{e}_{y'}) + (R^2\bar{\omega}/c^2)\mathbf{e}_{t'}$	$\rho h[-y'u^{x'} + x'u^{y'} + R^2(\omega - \bar{\omega})u^{t'}]$
5	A	$-\mathbf{e}_t + \bar{\omega}(y\mathbf{e}_x - x\mathbf{e}_y)$	$\rho h[c^2u^t + \bar{\omega}(yu^x - xu^y)]$
	B	$-\left(\mathbf{e}_t + \bar{\omega}\mathbf{e}_\phi\right)$	$\rho h\left(c^2u^t - R^2\bar{\omega}u^\phi\right)$
	C	$-\mathbf{e}_{t'}$	$\rho h[(c^2 - R^2\omega^2)u^{t'} - R^2\omega u^{\phi'}]$
	D	$-\mathbf{e}_{t'}$	$\rho h[(c^2 - R^2\omega^2)u^{t'} + \omega(y'u^{x'} - x'u^{y'})]$

[a]Case A: Expressions given in inertial-frame Cartesian coordinates;
Case B: Expressions given in inertial-frame cylindrical coordinates;
Case C: Expressions given in rotating-frame cylindrical coordinates;
Case D: Expressions given in rotating-frame Cartesian coordinates.

Table 6.2

η	Case[a]	$\mathbf{C}_{(\eta)}$	$\mathcal{S}_{(\eta)}$
2	A	$(x\mathbf{e}_x + y\mathbf{e}_y)/R$	$\rho h\left(-yu^x + xu^y\right)^2/R^3 - (1/R)\left(x\partial_x + y\partial_y\right)P - (\rho h/R)\left(x\partial_x + y\partial_y\right)\Phi$
	B	$\mathbf{e}_R$	$\rho h R u^\phi u^\phi - \partial_R P - \rho h \partial_R \Phi$
	C	$\mathbf{e}_R$	$\rho h R(u^{\phi'} + \omega u^{t'})^2 - \partial_R P - \rho h \partial_R \Phi$
	D	$(x'\mathbf{e}_{x'} + y'\mathbf{e}_{y'})/R$	$\rho h(-y'u^{x'} + x'u^{y'} + R^2\omega u^{t'})^2/R^3 - (1/R)(x'\partial_{x'} + y'\partial_{y'})P - (\rho h/R)(x'\partial_{x'} + y'\partial_{y'})\Phi$
3	A	$-y\mathbf{e}_x + x\mathbf{e}_y$	$\left(y\partial_x - x\partial_y\right)P + \rho h\left(y\partial_x - x\partial_y\right)\Phi$
	B	$\mathbf{e}_\phi$	$-\partial_\phi P - \rho h \partial_\phi \Phi$
	C	$\mathbf{e}_{\phi'}$	$-\partial_{\phi'} P - \rho h \partial_{\phi'} \Phi$
	D	$-y'\mathbf{e}_{x'} + x'\mathbf{e}_{y'}$	$(y'\partial_{x'} - x'\partial_{y'})P + \rho h(y'\partial_{x'} - x'\partial_{y'})\Phi$
4	A,B,C,D	$\mathbf{e}_z$	$-\partial_z P - \rho h \partial_z \Phi$
3′	A	$-y\mathbf{e}_x + x\mathbf{e}_y + (R^2\bar{\omega}/c^2)\mathbf{e}_t$	$-2\rho h(xu^x + yu^y)u^t\bar{\omega} + (y\partial_x - x\partial_y)P + \rho h(y\partial_x - x\partial_y)\Phi$
	B	$\mathbf{e}_\phi + (R^2\bar{\omega}/c^2)\,\mathbf{e}_t$	$-2\rho h R u^R u^t \bar{\omega} - \partial_\phi P - \rho h \partial_\phi \Phi$
	C	$(1 - R^2\bar{\omega}\omega/c^2)\mathbf{e}_{\phi'} + (R^2\bar{\omega}/c^2)\mathbf{e}_{t'}$	$-2\rho h R u^R u^{t'}\bar{\omega} - (1 - R^2\bar{\omega}\omega/c^2)\partial_{\phi'} P - \rho h \partial_{\phi'} \Phi$
	D	$(1 - R^2\bar{\omega}\omega/c^2)(-y'\mathbf{e}_{x'} + x'\mathbf{e}_{y'}) + (R^2\bar{\omega}/c^2)\mathbf{e}_{t'}$	$-2\rho h(x'u^{x'} + y'u^{y'})u^{t'}\bar{\omega} - (1 - R^2\bar{\omega}\omega/c^2)(y'\partial_{x'} - x'\partial_{y'})P - \rho h(y'\partial_{x'} - x'\partial_{y'})\Phi$
5	A	$-\mathbf{e}_t + \bar{\omega}(y\mathbf{e}_x - x\mathbf{e}_y)$	$[-\rho h(xu^x + yu^y)(-yu^x + xu^y)/R^2 + (y\partial_x - x\partial_y)P]\bar{\omega}$
	B	$-\left(\mathbf{e}_t + \bar{\omega}\mathbf{e}_\phi\right)$	$(-\rho h R u^R u^\phi + \partial_\phi P)\bar{\omega}$
	C	$-\mathbf{e}_{t'}$	$-\rho h R u^R(u^{\phi'} + \omega u^{t'})\bar{\omega}$
	D	$-\mathbf{e}_{t'}$	$-\rho h(x'u^{x'} + y'u^{y'})(-y'u^{x'} + x'u^{y'} + R^2\omega u^{t'})\bar{\omega}/R^2$

[a]Case A: Expressions given in inertial-frame Cartesian coordinates;
Case B: Expressions given in inertial-frame cylindrical coordinates;
Case C: Expressions given in rotating-frame cylindrical coordinates;
Case D: Expressions given in rotating-frame Cartesian coordinates.

For a uniformly rotating, axisymmetric neutron star in static equilibrium, the steady-state configuration can be associated with a helical, timelike Killing vector, namely $\mathbf{e}_{t'}$, the timelike basis vector in the corotating coordinate frame. By identifying $\mathbf{C}_{(5)}$ as the negative of that Killing vector, it is possible to construct a generalized energy state variable, which in steady-state also produces no source. As shown in the row of expressions marked $\eta = 5$ in Tables 6.1 and 6.2, in terms of inertial-frame cylindrical coordinates (Case B), $\mathbf{C}_{(5)} = -(\mathbf{e}_t + \bar{\omega}\mathbf{e}_\phi)$, where again $\bar{\omega}$ is the angular velocity of the frame in which the state variables are measured. The corresponding advection variable is $\psi_{(5)} = \rho h \left(c^2 u^t - R^2 \bar{\omega} u^\phi\right)$, total energy density minus rotational kinetic energy density (or just total energy density as measured in the corotating frame). Within the context of classical mechanics, this is known as the Jacobi energy density (or the Jacobi integral; see [38], [13]) in rotating cylindrical coordinates. The Jacobi energy associated with a generalized coordinate system is given by

$$\text{Jacobi energy} \equiv \dot{q}_j \frac{\partial L}{\partial \dot{q}_j} - L, \tag{6.4}$$

where $L \equiv T - V$ is the Lagrangian, T is the kinetic energy, V is the potential energy, and the $\dot{q}_j$ are the generalized velocities associated with the generalized coordinates q_j.

The actual state variable to be evolved, $\hat{\tau}$ — total energy density minus rest-mass energy density minus rotational kinetic energy density — is also globally conserved.

6.2 Choosing a Grid Geometry

6.2.1 Generalized Procedure

Now that we have five advection variables in hand, we must choose a grid geometry. It may be possible to prescribe a set of coordinates that correspond to the chosen collection of advection variables. This is done by requiring that one generalized coordinate, call it x'^η, increase in the direction of $\mathbf{C}_{(\eta)}$, and simultaneously that $\mathbf{C}_{(\eta)}$ always lie tangent to surfaces of constant x'^ν, where $\nu \neq \eta$. This requirement can be written

$$\partial_\eta x'^\alpha = C^\alpha{}_{(\eta)}. \tag{6.5}$$

As a simple example, consider the case where the four $\mathbf{C}_{(\eta)}$'s are chosen to be the four basis vectors $\mathbf{e}_{(\eta)}$ in a particular coordinate system. Then the R.H.S. of (6.5) is $\delta^\alpha{}_\eta$. The L.H.S.

will also be ${\delta^\alpha}_\eta$ if and only if each of the *generalized* coordinates x'^α is the corresponding coordinate from the *particular* coordinate system. In other words, by using basis vectors as your $\mathbf{C}$'s, you have actually chosen $\mathbf{C}$'s that correspond to the particular coordinate system that those basis vectors represent.

As a slightly less trivial example, suppose we want to find the coordinates that correspond to the following collection of $\mathbf{C}$'s (expressed in flat-space Cartesian coordinates),

$$\begin{aligned}
\mathbf{C}_{(2)} &\equiv \frac{x\ \mathbf{e}_x + y\ \mathbf{e}_y}{R}, \\
\mathbf{C}_{(3)} &\equiv -y\ \mathbf{e}_x + x\ \mathbf{e}_y, \\
\mathbf{C}_{(4)} &\equiv \mathbf{e}_z, \\
\mathbf{C}_{(5)} &\equiv \mathbf{e}_t.
\end{aligned}$$

Eq. (6.5) produces the following requirements on the generalized coordinates,

$$\begin{array}{cccc}
\partial_2 x = \dfrac{x}{R} & \partial_2 y = \dfrac{y}{R} & \partial_2 z = 0 & \partial_2 t = 0 \\
\partial_3 x = -y & \partial_3 y = x & \partial_3 z = 0 & \partial_3 t = 0 \\
\partial_4 x = 0 & \partial_4 y = 0 & \partial_4 z = 1 & \partial_4 t = 0 \\
\partial_5 x = 0 & \partial_5 y = 0 & \partial_5 z = 0 & \partial_5 t = 1
\end{array}$$

It should be immediately obvious that $x^4 = z$ and $x^5 = t$. This leaves us with just the four conditions in the upper left-hand quadrant. Taking the partial with respect to x'^3 of both sides of the third condition, and then plugging the fourth condition into the R.H.S. produces

$${\partial_3}^2 x = -x.$$

Similarly,

$${\partial_3}^2 y = -y.$$

The general solution is

$$\begin{aligned}
x &= A(x'^2)\cos\left(x'^3 + B(x'^2)\right), \\
y &= A(x'^2)\sin\left(x'^3 + B(x'^2)\right),
\end{aligned}$$

where $A(x'^2)$ and $B(x'^2)$ are free parameters. Of course, A and B still have to be chosen so that the first two conditions are satisfied. The simplest thing is to try $B = 0$. Then the first two conditions give

$$\begin{aligned} A'(x'^2)\cos\left(x'^3\right) &= x/R, \\ A'(x'^2)\sin\left(x'^3\right) &= y/R. \end{aligned}$$

These conditions are satisfied if and only if $A(x'^2) = x'^2$. Then,

$$\begin{aligned} x &= x'^2\cos x'^3 = R\cos\phi \\ y &= x'^2\sin x'^3 = R\sin\phi \end{aligned}$$

So $x'^2 = R$ and $x'^3 = \phi$, as expected.

In general, if the $\mathbf{C}$'s are not chosen to be basis vectors, then finding a corresponding coordinate system amounts to solving a set of n^2 coupled partial differential equations, and is certainly nontrivial.

While it is possible to choose a grid geometry that reflects the symmetries of the advection variables (cylindrical in this case), it is not necessary. One could advect the cylindrical quantities listed above on a Cartesian grid with no trouble if there were a good reason to do so. (For instance, it is more straightforward to use a Cartesian grid to implement adaptive mesh refinement.) Just the same, we will adopt a cylindrical grid geometry for our present example. But in order to reduce numerical diffusion, the grid will be corotating. The coordinates become

$$x^\mu \equiv \begin{pmatrix} t' = t \\ R \\ \phi' = \phi - \omega t \\ z \end{pmatrix}, \tag{6.6}$$

where primes denote rotating coordinates.

6.2.2 Adopting a Rotating Coordinate System and/or Rotating-Frame State Variables

In order to reduce the effects of numerical diffusion that inevitably arise when fluid is transported across a grid, it can be useful to adopt a non-stationary grid that generally moves

with the fluid [14, 52, 74, 51, 75]. In particular, when modeling a rotating neutron star or a binary system, it can be useful to adopt a cylindrical grid that is rotating with an angular velocity ω that is similar, if not equal, to the angular velocity Ω of the fluid. In this case the appropriate coordinates are

$$\begin{pmatrix} t' = t \\ R \\ \phi' = \phi - \omega t \\ z \end{pmatrix},$$

where we have used primes to distinguish rotating coordinates from their nonrotating counterparts. For each major row of Tables 6.1 and 6.2, "Case C" details the expressions for $\mathbf{C}_{(\eta)}$, $\psi_{(\eta)}$, and $\mathcal{S}_{(\eta)}$ as viewed from this rotating cylindrical frame of reference.

We note that, when expressed in terms of the basis vectors that define this rotating-frame cylindrical coordinate system (Case C), the expression for $\psi_{(3)}$ reflects the shift in frames, that is,

$$\rho h R^2 u^\phi \rightarrow \rho h R^2 (u^{\phi'} + \omega u^{t'}),$$

while the expressions for $\psi_{(2)}$ and $\psi_{(4)}$ remain unchanged from their inertial-frame counterparts (Case B). Among the source terms that have already been discussed — namely those associated in Tables 6.1 and 6.2 with $\eta = 2, 3$, and 4 — only $\mathcal{S}_{(2)}$ explicitly reflects the shift in frames,

$$\rho h R u^\phi u^\phi \rightarrow \rho h R (u^{\phi'} + \omega u^{t'})^2 \ ,$$

through the appearance of two additional terms, one describing a perceived Coriolis acceleration ($2\rho h R \omega u^{\phi'} u^{t'}$) and another describing a centrifugal acceleration ($\rho h R \omega^2 u^{t'} u^{t'}$). But in no way do any of these new terms alter the actual numerical value of either $\psi_{(3)}$ or $\mathcal{S}_{(2)}$ since they are buried within the u^ϕ inside the original expressions.

It is important to emphasize that the "Case C" expressions just discussed all represent hybrid schemes in the following sense. The vector fields $\mathbf{C}_{(2)}$, $\mathbf{C}_{(3)}$, and $\mathbf{C}_{(4)}$ and their associated generalized advection variables $\psi_{(2)}$, $\psi_{(3)}$, and $\psi_{(4)}$ are all identified with the basis vectors that correspond to an inertial-frame cylindrical coordinate system whereas the basis vectors of the adopted grid are all identified with a rotating-frame cylindrical coordinate system. This is not the conventional approach. Historically in the astrophysics community

when a rotating grid has been adopted [52, 51, 75], the advection/state variables also have been constructed from the rotating-frame cylindrical basis vectors. To accomplish this using our generalized formalism, the vector field used to construct a state variable associated with the angular momentum density of the fluid must be changed from $\mathbf{C}_{(3)}$ to $\mathbf{C}_{(3')}$, as defined in Tables 6.1 and 6.2, where $\bar{\omega}$ is defined as the angular velocity of the rotating frame in which the angular momentum is measured (not to be confused with ω, the angular velocity of the rotating grid, nor with Ω, the actual angular velocity of the fluid — although, ideally, the three will all be similar to one another, if not equal). For example, when written in terms of the adopted rotating-frame coordinates (Case C),

$$\mathbf{C}_{(3')} = \mathbf{e}_{\phi'} + (R^2\bar{\omega}/c^2)(\mathbf{e}_{t'} - \omega\mathbf{e}_{\phi'}).$$

The generalized advection variable $\psi_{(3')}$ and source function $\mathcal{S}_{(3')}$ that arise as a result are detailed for "Case A", "Case B" and "Case C" grid coordinates in the major row of Tables 6.1 and 6.2 that is labeled $\eta = 3'$.

As can be seen from earlier work [52, 51, 75], we notice that an additional Coriolis term ($-2\rho h R\bar{\omega}u^R u^{t'}$) appears in the source function of the angular momentum conservation equation when the $\mathbf{C}_{(3')}$ vector field is specified. Unlike the Coriolis term that previously appeared in the radial equation (as a consequence of expressing it in a rotating coordinate frame), this Coriolis term actually *does* alter the numerical value of the source, (i.e., $\mathcal{S}_{(3')} \neq \mathcal{S}_{(3)}$). This is a significant (if subtle) distinction because only one of the two Coriolis terms can actually spoil the delicate balance between the source term and the flux term. In this sense, the Coriolis term that appears in the azimuthal equation as a result of evolving rotating-frame angular momentum is more substantive than the one that appears in the radial equation upon the selection of a rotating grid.

It is somewhat surprising that the two terms describing a Coriolis acceleration (typically written in vector form as $-2\rho h\ \omega \times \mathbf{v}'$, where $\mathbf{v}'$ is the rotating-frame 3-velocity) appear for such distinctly different reasons. Strictly speaking, then, these terms really should be written

$$\text{Coriolis force density} = -2\rho h \left(\omega \times v^{\phi'}\mathbf{e}_{\phi'} + \bar{\omega} \times v^R \mathbf{e}_R\right) \tag{6.7}$$

to reflect the fact that they are actually produced for different reasons and by two independent angular velocities, ω and $\bar{\omega}$.

7. Numerical Evidence

7.1 Implementation

7.1.1 Finite Volume Approach

Finite volume codes focus on quantities that need to be updated in one particular grid cell from one time step to the next. The basic approach follows a logic very similar to the thought process that was outlined in Chapter 2. First, the set of meaningful (observable) quantities — called the primitives — at the center of a given cell need to be converted to a set of conservative variables; that is, a set of variables ${\mathcal{F}^0}_{(\eta)}$ that are described by field equations that each take the form of Eq. (2.28). Since there are only two ways that the amount of a conservative quantity within a grid cell can change —

1. By a nonzero net flux out of (or into) the cell during the appropriate interval of time, or

2. By the spontaneous creation (or destruction) of that quantity within the cell during the appropriate interval of time due to a nonzero source,

— the amount of the conservative quantity in a cell after the time step will be equal to the amount that was there before the time step minus the net amount that was advected out of the cell during the time step plus the amount that was spontaneously created within the cell during the time step.

$$\text{New Value} = \text{Old Value} - \text{Flux} + \text{Source}. \tag{7.1}$$

Consequently, finite volume codes can generally be broken up into four distinct modules.

1. A **setup module**, which defines the grid and reads in the initial data,

2. A **flux module**, which reconstructs at cell faces variables which are known at cell centers in order to compute how much net of each quantity is advected out of the cell during the given time step,

3. A **source module**, which computes updates due to any nonzero source terms that may be present, and

4. A **driver module**, which uses all the previous information to update the conservative variables at each time step and recover the corresponding primitives that are needed for the subsequent time step.

7.1.2 The Setup Module

A specific coordinate system must be chosen in order for the grid to be defined by the setup module. The first step in choosing a set of coordinates involves slicing up the four-dimensional spacetime into a foliation of spacelike hypersurfaces, which are threaded together by a congruence (a bundle) of timelike curves. This is accomplished using the ADM formalism (see [10], [24], [63], [73]), first published in 1962 by Arnowitt, Deser, and Misner. It involves decomposing the 4-metric into

1. An induced 3-metric on a given hypersurface γ_{ij},

2. A shift 3-vector β, which is everywhere tangent to the hypersurfaces and describes the movement of the coordinate system from one hypersurface to the next, and

3. A lapse function α, which parameterizes the timelike curves.

The mathematical relationships among the components of the 4-metric and each of the decomposed quantities can be summarized as follows.

$$g_{00} = -\left(\alpha^2 - \gamma_{ij}\beta^i\beta^j\right) = -\left(\alpha^2 - \beta^2\right) \tag{7.2}$$

$$g_{0i} = \gamma_{ij}\beta^j = \beta_i \tag{7.3}$$

$$g_{ij} = \gamma_{ij}. \tag{7.4}$$

The inverse metric, then, becomes

$$g^{00} = -\frac{1}{\alpha^2} \tag{7.5}$$

$$g^{0i} = \frac{\beta^i}{\alpha^2} \tag{7.6}$$

$$g^{ij} = \gamma^{ij} - \frac{\beta^i\beta^j}{\alpha^2}. \tag{7.7}$$

Inverting the equations yields the following definitions for the ADM variables:

$$\alpha = \frac{1}{\sqrt{-g^{00}}} = \sqrt{\beta^2 - g_{00}} \tag{7.8}$$

$$\beta_i = g_{0i}, \quad \beta^i = \alpha^2 g^{0i} \tag{7.9}$$

$$\gamma_{ij} = g_{ij}, \quad \gamma^{ij} = g^{ij} + \frac{\beta^i \beta^j}{\alpha^2}. \tag{7.10}$$

Another useful relation is

$$g = -\alpha^2 \gamma, \tag{7.11}$$

where g and γ are determinants of the 4-metric and 3-metric, respectively. It should also be noted that the line element can be written in the form

$$ds^2 = -\alpha^2 dx^0 dx^0 + \gamma_{ij} \left(dx^i + \beta^i dx^0\right) \left(dx^j + \beta^j dx^0\right). \tag{7.12}$$

Incidentally, the physical components of the 3-velocity of the coordinates (as measured by an Eulerian observer) are

$$v(i)_{\text{coords}} = \frac{\sqrt{\gamma}}{\sqrt{\gamma\{i\}}} \frac{c\beta^i}{\alpha}, \tag{7.13}$$

and the 4-velocity of the coordinates is

$$\mathbf{u}_{\text{coords}} = \frac{c\ \mathbf{e}_0}{\sqrt{g_{00}}} = c \left(\sqrt{-g_{00}}\ \mathbf{e}^0 + \frac{g_{0i}}{\sqrt{-g_{00}}}\ \mathbf{e}^i \right). \tag{7.14}$$

Once a satisfactory coordinate map has been chosen for the hypersurfaces (i.e., once the three desired spacelike coordinates have been chosen), the grid structure can be constructed numerically. At each grid cell, the initial data is then read into the primitive variables from some preconstructed initial data model. Primitive variables must be used for the initial data (as opposed to the conservative variables) because the primitives are the quantities that live on the initial hypersurface — they are the quantities that can be measured by a coordinate observer.

7.1.3 The Flux Module

The flux module is where updates to the conservative variables arising from the flux terms are computed. First, a one-dimensional line of data is loaded by the module. Then, an appropriate flux reconstruction scheme (like Kurganov-Tadmor) is employed to reconstruct

fluxes at each of the cell faces. Next, the fluxes through two adjacent faces are subtracted to obtain the net change in the corresponding conservative variable due to advection through the cell faces. This net change is calculated for each cell on the grid, one line of data at a time. The process is then repeated in each of the other two directions, and these contributions are added to those from the difference fluxes in the first direction. The total net difference flux from all three directions becomes the flux part of the update that will be used to update the corresponding conservative variable.

7.1.4 The Source Module

The source module is more straightforward than the flux piece. It finds the appropriate update to the conservative variables due to the source terms. This is accomplished by first defining the components of the stress-energy tensor from the current primitive fluid variables. Then spacelike partial derivatives of the metric components are found using a multi-point stencil to compute finite differences. The source term is then constructed in terms of the stress-energy tensor components (with both indices up), and partial derivatives of the metric (with all indices down).

7.1.5 The Driver Module

The initial data for each cell is called from the setup module (or, for subsequent time steps, the data from the last time step is used) and conservative variables are constructed on the initial hypersurface from the primitive variables. A Runge-Kutta (RK) scheme is then used to update the conservative variables according to the structure of equation (7.1). The RK scheme breaks the time step up into substeps and, with the help of the flux and source modules, produces updates to the appropriate conservative quantity for a given substep. Then it converts the conservative variables back into the corresponding primitives in order that the appropriate fluxes can be constructed at the next time substep. This variable conversion is done at each RK substep, using a conservative-to-primitive variable solver and is, in fact, one of the costliest pieces of the code, but it is necessary. Subsequently, conservative variables are constructed for the next substep. After the final substep has been

performed, the primitive variables are found and take the place of the initial data for the next timestep.

7.2 Proposed Additions and Alterations

We suggest modifying a finite volume code so that, rather than following an approach which can be outlined by Eq. (2.61a),

$$\overbrace{\frac{1}{\sqrt{-g}}\,\partial_0\left(\sqrt{-g}\;\rho h u_i\;u^0\right)}^{\substack{\text{time-rate-of-change of}\\ \text{state variable}}} \;+\; \overbrace{\frac{1}{\sqrt{-g}}\,\partial_j\left(\sqrt{-g}\;\rho h u_i\;u^j\right)}^{\substack{\text{traditional flux of}\\ \text{state variable}}} = \underbrace{\rho h u^\mu u_\alpha \Gamma^\alpha_{\mu i}}_{\substack{\text{gravity ``force''}\\ \text{impacting}\\ \text{state variable}}} \underbrace{-\partial_i P}_{\substack{\text{pressure ``force''}\\ \text{impacting}\\ \text{state variable}}} ,$$

it will follow an approach which can be outlined by Eq. (3.6),

$$\overbrace{\frac{1}{\sqrt{-g}}\,\partial_0\left(\sqrt{-g}\;\rho h u_\nu C^\nu{}_{(\eta)}\;u^0\right)}^{\substack{\text{time-rate-of-change of}\\ \text{generalized state variable}}} \;+\; \overbrace{\frac{1}{\sqrt{-g}}\,\partial_j\left(\sqrt{-g}\;\rho h u_\nu C^\nu{}_{(\eta)}\;u^j\right)}^{\substack{\text{traditional flux of}\\ \text{generalized state variable}}} = \underbrace{\rho h u^\mu u_\nu\;\nabla_\mu C^\nu{}_{(\eta)}}_{\substack{\text{gravity ``force''}\\ \text{impacting generalized}\\ \text{state variable}}} \underbrace{-C^\mu{}_{(\eta)}\;\partial_\mu P}_{\substack{\text{pressure ``force''}\\ \text{impacting generalized}\\ \text{state variable}}} .$$

7.2.1 The Setup Module

For an evolution in a static background, this is a good place to define the characteristic vector fields $\mathbf{C}_{(\eta)}$ that one wants to use. For more dynamic models, a separate module would likely be needed for computing the most ideal characteristic vectors on the fly.

7.2.2 The Flux Module

The conservative variables that appear in the flux module must be replaced with new conservative variables—linear combinations of the old ones, weighted by each of the chosen characteristic vectors $\mathbf{C}_{(\eta)}$—before flux updates can be constructed. The four characteristic vectors compose the rows of a transformation matrix, which takes the collection of old

conservative four-momentum variables to the new conservative four-momentum variables.

$$\begin{pmatrix} \mathcal{F}^{0\prime}{}_{(0)} \\ \mathcal{F}^{0\prime}{}_{(1)} \\ \mathcal{F}^{0\prime}{}_{(2)} \\ \mathcal{F}^{0\prime}{}_{(3)} \end{pmatrix} = \begin{pmatrix} C^t{}_{(0)} & C^x{}_{(0)} & C^y{}_{(0)} & C^z{}_{(0)} \\ C^t{}_{(1)} & C^x{}_{(1)} & C^y{}_{(1)} & C^z{}_{(1)} \\ C^t{}_{(2)} & C^x{}_{(2)} & C^y{}_{(2)} & C^z{}_{(2)} \\ C^t{}_{(3)} & C^x{}_{(3)} & C^y{}_{(3)} & C^z{}_{(3)} \end{pmatrix} \begin{pmatrix} \mathcal{F}^0{}_{(t)} \\ \mathcal{F}^0{}_{(x)} \\ \mathcal{F}^0{}_{(y)} \\ \mathcal{F}^0{}_{(z)} \end{pmatrix} \tag{7.15}$$

7.2.3 The Source Module

As can be seen by comparing Eq. (3.6) with Eq. (2.61a), the source module cannot be treated like the flux module since the new sources are not just linear combinations of the old sources, weighted by the characteristic vector. The source updates must be entirely reconstructed from the primitive variables, though the structure of the source module is not otherwise changed.

This new source can be written most succinctly in terms of the stress energy tensor.

$$\mathcal{S}_{(\eta)} \equiv T^{\mu\nu}\nabla_\mu C_{\nu\ (\eta)} \tag{7.16}$$

In what follows, underlined terms are identical and can be combined.

$$\begin{aligned}
\mathcal{S}_{(\eta)} \equiv\ & g_{\gamma\nu}T^{\mu\gamma}\left[\partial_\mu C^\nu{}_{(\eta)} + \tfrac{1}{2}g^{\beta\nu}\left(\partial_\mu g_{\alpha\beta} + \partial_\alpha g_{\beta\mu} - \partial_\beta g_{\mu\alpha}\right)C^\alpha{}_{(\eta)}\right] \\
=\ & T^{\mu\gamma}\left[\tfrac{1}{2}C^\alpha{}_{(\eta)}\left(\partial_\mu g_{\alpha\gamma} + \partial_\alpha g_{\gamma\mu} - \partial_\gamma g_{\mu\alpha}\right) + g_{\gamma\alpha}\partial_\mu C^\alpha{}_{(\eta)}\right] \\
=\ & T^{00}\left[\tfrac{1}{2}C^0{}_{(\eta)}\left(\partial_0 g_{00} + \cancel{\partial_0 g_{00}} - \cancel{\partial_0 g_{00}}\right) + g_{00}\partial_0 C^0{}_{(\eta)}\right. \\
& \qquad \left. + \tfrac{1}{2}C^i{}_{(\eta)}\left(\cancel{\partial_0 g_{i0}} + \partial_i g_{00} - \cancel{\partial_0 g_{0i}}\right) + g_{0i}\partial_0 C^i{}_{(\eta)}\right] \\
& + T^{0j}\left[\tfrac{1}{2}C^0{}_{(\eta)}\left(\underline{\partial_0 g_{0j}} + \underline{\partial_0 g_{j0}} - \cancel{\partial_j g_{00}}\right) + g_{j0}\partial_0 C^0{}_{(\eta)}\right. \\
& \qquad \left. + \tfrac{1}{2}C^i{}_{(\eta)}\left(\cancel{\partial_0 g_{ij}} + \underline{\underline{\partial_i g_{j0}}} - \cancel{\partial_j g_{0i}}\right) + g_{ji}\partial_0 C^i{}_{(\eta)}\right] \\
& + T^{k0}\left[\tfrac{1}{2}C^0{}_{(\eta)}\left(\cancel{\partial_k g_{00}} + \cancel{\partial_0 g_{0k}} - \cancel{\partial_0 g_{k0}}\right) + g_{00}\partial_k C^0{}_{(\eta)}\right. \\
& \qquad \left. + \tfrac{1}{2}C^i{}_{(\eta)}\left(\cancel{\partial_k g_{i0}} + \underline{\underline{\partial_i g_{0k}}} - \cancel{\partial_0 g_{ki}}\right) + g_{0i}\partial_k C^i{}_{(\eta)}\right] \\
& + T^{kj}\left[\tfrac{1}{2}C^0{}_{(\eta)}\left(\cancel{\partial_k g_{0j}} + \partial_0 g_{jk} - \cancel{\partial_j g_{k0}}\right) + g_{j0}\partial_k C^0{}_{(\eta)}\right. \\
& \qquad \left. + \tfrac{1}{2}C^i{}_{(\eta)}\left(\cancel{\partial_k g_{ij}} + \partial_i g_{jk} - \cancel{\partial_j g_{ki}}\right) + g_{ji}\partial_k C^i{}_{(\eta)}\right]
\end{aligned}$$

$$\begin{aligned}
\Longrightarrow \mathcal{S}_{(\eta)} =\ & T^{00}\left[\tfrac{1}{2}C^0{}_{(\eta)}\partial_0 g_{00} + \tfrac{1}{2}C^i{}_{(\eta)}\partial_i g_{00} + g_{00}\partial_0 C^0{}_{(\eta)} + g_{0i}\partial_0 C^i{}_{(\eta)}\right] \\
& + T^{0i}\left[C^0{}_{(\eta)}\partial_0 g_{0i} + C^j{}_{(\eta)}\partial_j g_{0i} + g_{00}\partial_i C^0{}_{(\eta)} + g_{0j}\partial_i C^j{}_{(\eta)} + g_{0i}\partial_0 C^0{}_{(\eta)} + g_{ij}\partial_0 C^j{}_{(\eta)}\right] \\
& + T^{ij}\left[\tfrac{1}{2}C^0{}_{(\eta)}\partial_0 g_{ij} + \tfrac{1}{2}C^k{}_{(\eta)}\partial_k g_{ij} + g_{0j}\partial_i C^0{}_{(\eta)} + g_{jk}\partial_i C^k{}_{(\eta)}\right]
\end{aligned}$$

For an explicit term-by-term expansion of this new source, see Appendix F.

7.2.4 The Driver Module

The driver module can be treated in a way that is similar to the way the flux module is handled. Weighted linear combinations of the conservative variables must be taken in order to get the generalized conservative variables before the flux and source updates can be added (since they are updates to the generalized conservative variables). After the generalized conservative variables have been updated, they must be transformed back into the original conservative variables before the conservative-to-primitive solver can be called (since the solver needs the original conservative variables). This is done by inverting the matrix of vectors $\mathbf{C}_{(\eta)}$.

$$\begin{pmatrix} \mathcal{F}^0{}_{(0)} \\ \mathcal{F}^0{}_{(1)} \\ \mathcal{F}^0{}_{(2)} \\ \mathcal{F}^0{}_{(3)} \end{pmatrix} = \begin{pmatrix} C^t{}_{(0)} & C^x{}_{(0)} & C^y{}_{(0)} & C^z{}_{(0)} \\ C^t{}_{(1)} & C^x{}_{(1)} & C^y{}_{(1)} & C^z{}_{(1)} \\ C^t{}_{(2)} & C^x{}_{(2)} & C^y{}_{(2)} & C^z{}_{(2)} \\ C^t{}_{(3)} & C^x{}_{(3)} & C^y{}_{(3)} & C^z{}_{(3)} \end{pmatrix}^{-1} \begin{pmatrix} \mathcal{F}^{0\prime}{}_{(0)} \\ \mathcal{F}^{0\prime}{}_{(1)} \\ \mathcal{F}^{0\prime}{}_{(2)} \\ \mathcal{F}^{0\prime}{}_{(3)} \end{pmatrix} \tag{7.17}$$

So, to recap, at each substep of the RK scheme, the primitives must be converted to conservative variables, and the conservative variables must be transformed into the generalized conservative variables before the updates can come in. Then they must be transformed back into the original conservative variables and, finally, the primitives must be recovered so that appropriate updates can be calculated for the next substep.

7.3 Toy Model

In order to test some of the ideas presented in this dissertation research, I have developed a simple toy model — a two-dimensional Newtonian code for integrating the Euler equations describing the motion of an ideal gas. This toy model is organized on a Cartesian grid, but it is capable of evolving the set of traditional Cartesian state variables or a set of generalized state variables as described here in Chapter 3. It is also capable of explicitly removing (or keeping) the naked pressure terms that appear on either side of the field equations when updating state variables.

Using this toy code, I evolved an axisymmetric star in full body rotation on a Cartesian grid: first, keeping naked pressure terms and evolving Cartesian state variables; second, removing naked pressure terms and evolving the same Cartesian state variables; and third, removing naked pressure terms and evolving cylindrical state variables. The results are summarized in Figure 7.1 and appear to support the ideas presented in this disseration — that quantities which should be naturally conserved (like angular momentum, in this case) are better conserved numerically when the naked pressure terms are removed and generalized state variables are chosen to accommodate symmetries inherent to the problem.

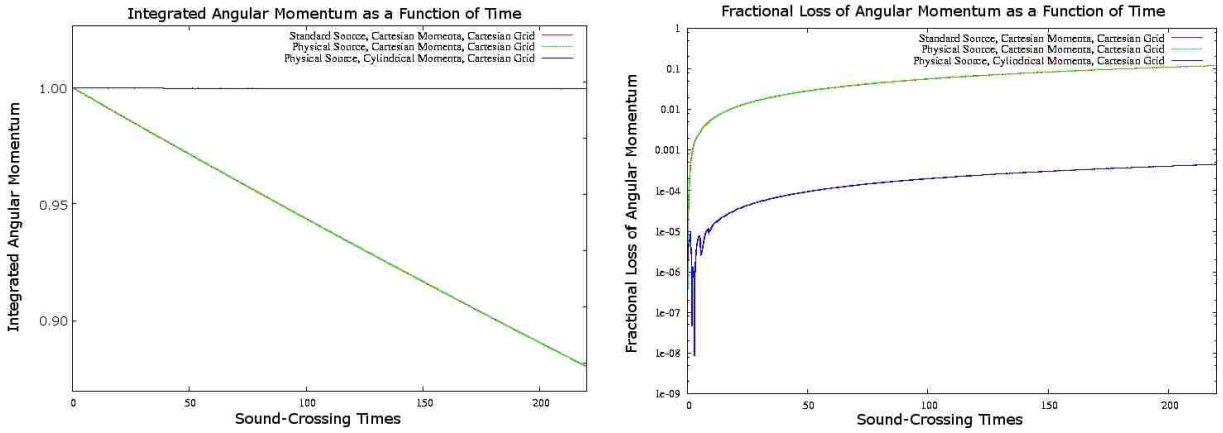

Figure 7.1: Conservation of angular momentum: comparison of results using a toy model for three distinct numerical approaches. *Left panel:* The total angular momentum integrated over the neutron star is shown as a function of time for three distinct models. The first model (shown in red) incorporates Cartesian state variables, as does the second model (green). Unlike the first model, the second model has had all naked pressure terms explicitly removed. But because both simulations are Newtonian and are carried out on a Cartesian grid, the naked pressure terms are zero (or, at least, are very small). So the performance of these two models is nearly identical — that is, angular momentum is artificially lost at a rate of about 5% per hundred sound-crossing times for each model. The third model (blue), on the other hand, employs cylindrical state variables. This appears to have a profound effect on performance, as the resulting rate of angular momentum loss is now negligible. *Right panel:* The fractional loss of integrated angular momentum for the three models illustrated in the left panel is shown on a logarithmic scale, again as a function of time. Here it is apparent that the use of cylindrical state variables reduces the artificial numerical rate of angular momentum loss by a factor of about a thousand for this particular Newtonian model, which is evolved on a Cartesian grid.

7.4 Flower Code

In order to test some of the ideas presented in this dissertation using a more sophisticated, preexisting code, I spent over a year familiarizing myself with the Flower code written some years ago by Patrick Motl here at LSU. I focused on a set of initial conditions for an axisymmetric neutron star in full-body rotation on a Schwarzschild background. Each fluid element within the spherically symmetric star was also given a small radial kick so that it would undergo small-amplitude radial oscillations throughout the evolution.

The plan was to compare code performance for this set of initial conditions using a variety of approaches: keeping naked pressure terms vs. explicitly removing them, evolving Cartesian state variables vs. evolving cylindrical state variables, and evolving on a Cartesian mesh vs. evolving on a cylindrical mesh. All together this led to a grand total of 2^3 versions of the code I planned to test and compare. These eight versions of the code are summarized in the table below. (And four of them were represented visually back in Figure 4.2.) I was able to get the four versions of the Flower code that were carried out on a Cartesian mesh to a point where I believe they were properly functioning as they were designed to function. I was never able to work all the bugs out of the four versions of the code that were to be carried out on a cylindrical mesh.

Table 7.1

Eight Versions of the Flower Code I Tried to Compare

Version	Naked Pressure Terms	Advected Variables	Discretization	Status
1	included	Cartesian	Cartesian	working
2	removed	Cartesian	Cartesian	working, better conservation achieved
3	included	cylindrical	Cartesian	unstable, naked pressure terms blow up
4	removed	cylindrical	Cartesian	working, conservation improved further
5	included	Cartesian	cylindrical	bugs
6	removed	Cartesian	cylindrical	bugs
7	included	cylindrical	cylindrical	bugs
8	removed	cylindrical	cylindrical	bugs

While the four versions that were designed for evolution on a cylindrical mesh never worked properly, a comparison of the results from the four versions that do appear to be

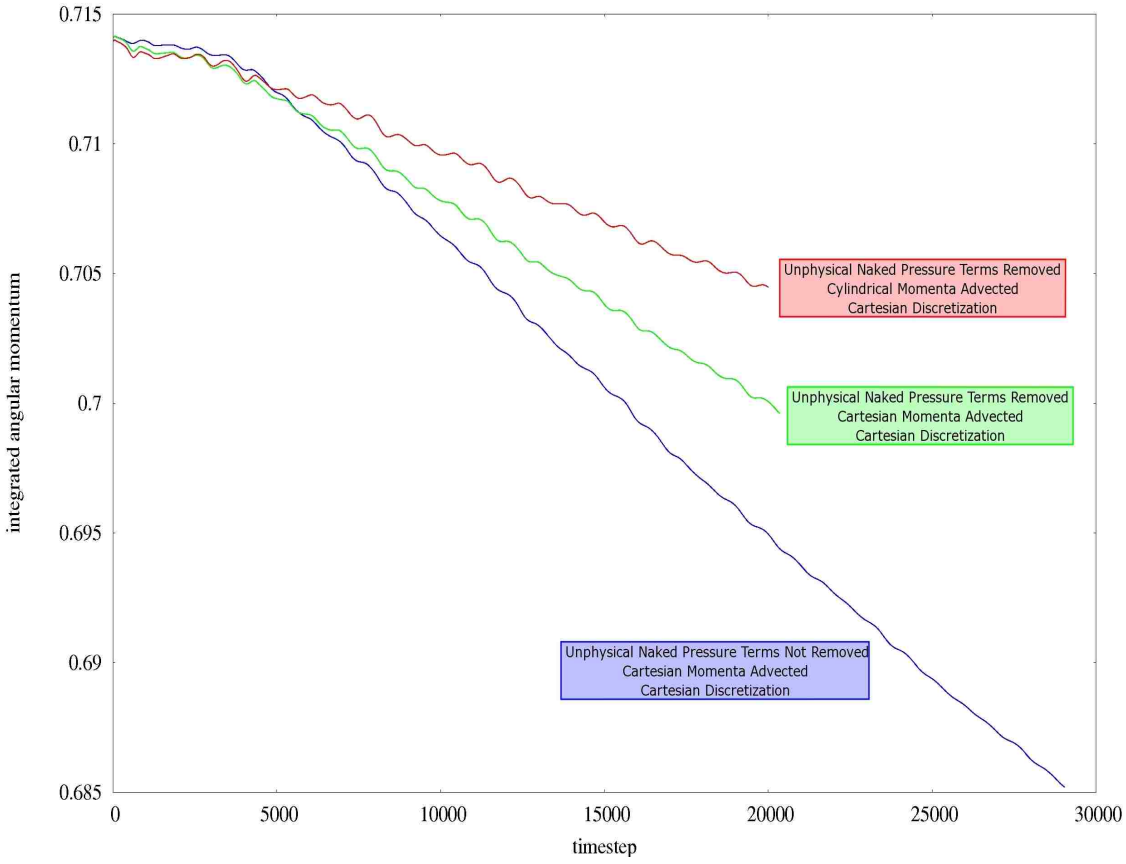

Figure 7.2: Conservation of angular momentum: comparison of results using the Flower code for three distinct numerical approaches. The curve from each of the first two code modifications shows an improvement in the conservation of integrated angular momentum over the previous model. The magnitude of the slope of each curve represents the rate at which global angular momentum is lost. The slope of the green curve is 71% the slope of the blue curve, and the slope of the red curve is a mere 48% the slope of the blue curve. The tiny oscillations give an idea of the time scale since they correspond to tiny radial pulsations.

working properly is most relevant to the code modifications we are proposing as a result of this dissertation research. We were particularly interested in the ability of each version of the code to conserve angular momentum since in a time-independent axisymmetric potential angular momentum must be exactly conserved in nature. Figure 7.2 shows the integrated angular momentum of the simulated neutron star as a function of time for versions of the code labelled 1, 2, and 4 in Table 7.1. Each successive version of the code that is plotted in Figure 7.2 shows a level of improvement over the preceding curve in the sense that the rate of numerical angular momentum loss has decreased, and consequently represents an improvement in code performance due to a code modification we are recommending.

The small oscillations that are visible in each curve come from the tiny radial pulsations in the neutron star and indicate the period of pulsation. The interesting feature is that after about 5000 (equally spaced) timesteps, all three curves become almost linear. The magnitude of the slope represents the rate at which angular momentum is being lost from the model, so a gentler slope corresponds to better angular momentum conservation.

The blue curve, which comes from a run with no code modifications, approaches a slope of about 11.2×10^{-7} (in code units). The green curve, which benefits from the removal of unphysical terms, approaches a slope of about 8.0×10^{-7} (in code units), or 71% of the slope of the blue curve. The red curve, which benefits from both the removal of unphysical terms and the advection of cylindrical momenta, approaches a slope of about 5.3×10^{-7} (also in code units), or 48% the slope of the blue curve.

So, at least for this model, the application of our recommended code modifications appears to reduce the rate of global angular momentum loss to half. One might speculate that the rate of angular momentum loss would be decreased further still if the simulation were to be carried out on a cylindrical grid.

8. Conclusions

When developing a numerical algorithm to perform a time-integration of the set of hyperbolic equations that govern compressible fluid flows — in nonrelativistic as well as relativistic environments — it has become customary to write each equation in a form that, broadly speaking, displays the following three terms:

$$\text{time\_update} \quad + \quad \text{flux} \quad = \quad \text{source}. \tag{8.1}$$

The Valencia formulation of the relativistic fluid equations has become popular in the numerical relativity community because, even in its analytic continuum representation, the so-called conservative equations display this structure. Starting from the Valencia formulation, it is relatively straightforward to map the partial differential equations into finite-difference or finite-volume expressions that are suitable for numerical integration. Based on ideas originally introduced by Papadopoulos and Font [58], we have developed a generalization of the Valencia formulation that preserves this form and, in addition, offers some flexibility in choosing which elements of the physics are incorporated into the flux term and which are incorporated into the source term. This is accomplished through the definition of a set of four characteristic vector fields $\mathbf{C}_{(\eta)}$, each of which generates an independent linear combination of the standard equations. As we have argued, a judicious choice of these vector fields should lead to a more accurate numerical treatment of fluid flows in a variety of situations.

The advantages of our generalized Valencia formulation can be illustrated most readily in the context of steady-state or nearly steady-state flows. In steady-state flows, the time_update should be zero, so the flux term should equal the source term; and in models that are intended to represent *nearly* steady-state flows, the flux term should *nearly* equal the source term. However, in most computational fluid algorithms, the segment of the numerical code that is designed to evaluate the flux term is very different from the segment that is designed to evaluate the source. Hence, differences between the flux term and the source term can arise that are principally of numerical origin and, as a result, it may be difficult for the numerical algorithm to properly preserve a steady-state or nearly steady-state flow.

In this regard the standard Valencia formulation promotes one particular practice that we consider ill-advised: In the three components of the momentum conservation equation, the pressure gradient appears on the L.H.S. inside the flux term. As a result, an unphysical "naked" pressure term appears on both sides of the equation. This term is weighted by connection coefficients – which are large in regions where the basis vectors change rapidly from one point to the next – so its appearance is inconsequential on a flat metric in Cartesian coodinates. But on non-Cartesian grids (particularly near the coordinate poles) or on any grid in general relativistic flows – this naked pressure term can be large and cancelation of its effects between the two sides of the equation is required in order to properly represent a steady-state flow. Because the flux and source terms usually are evaluated by distinctly different segments of the numerical algorithm, of course, cancelation can be difficult to achieve.

In fact, as we have presented in §2.7, we constructed a highly accurate one-dimensional model of a spherically symmetric TOV star using Mathematica (and thousands of radial zones), and showed that in a moderately relativisitic environment the naked pressure term can easily be comparable in size to the physical pressure gradient itself. When this occurs, the (nontraditional) pressure flux that codes are currently computing consists of nearly equal contributions of pressure gradient and unphysical mathematical artifact (from the failure of naked pressure terms to cancel numerically).

Furthermore, by implementing a PPM flux reconstruction scheme (after the manner it would be performed on a Cartesian grid), we were able to produce the artificial numerical remainder from the naked pressure terms. In many models (particularly those approaching the Newtonian regime), this remainder was orders of magnitude smaller than the inevitable numerical error that arises from imperfect cancellation between numerical evaluations of gravity and pressure. But for other models (those in the relativistic regime), the numerical remainder from the naked pressure terms rivaled the other error term (particularly near the center of the star). The greatest concern over this unnecessary error arises when one is trying to resolve any minute non-equilibrium behavior in a near equilibrium flow.

Our first recommendation, therefore, is to move the pressure gradient from the L.H.S.

(flux) to the R.H.S. (source) so that the naked pressure term never arises. In doing this, care should certainly be taken to ensure that pressure is still numerically reconstructed at cell faces in a way that satisfies the Rankin-Jouinot conditions[1] and preserves the total-variation-diminishing[2] (TVD) nature of the reconstruction scheme.

It appears as though additional improvements in numerical algorithm design can be achieved by forming a weighted linear combination of all the equations of motion, and then moving additional pieces of the standard flux term to the R.H.S. and treating them as part of the source. This can be accomplished through the definition of a characteristic vector field that will specify the weighting factors for each of the Euler equations. As we have discussed in Chapters 4-5, precisely which pieces should be moved is a matter of choice and will likely depend on the problem. Whenever possible, choosing a characteristic vector that satisfies Killing's equations will generally eliminate the source. But when no such vector exists, one possible alternative involves finding the characteristic vector that most nearly satisfies Killings equations. This can be accomplished by minimizing the modulus of $\nabla_\mu C_\nu + \nabla_\nu C_\mu$ – the L.H.S. of Killing's equations – by using the calculus of variations. As we have shown in §4.3, this results in a first-order system of equations (4.49) constraining the characteristic vector,

$$\nabla_\mu \left(\nabla^\mu C^\nu + \nabla^\nu C^\mu \right) = 0^\nu .$$

If one knows *a priori* about the underlying symmetries of a problem, it probably will not be necessary to solve this set of equations because the ideal characteristic vectors can still be chosen to reflect the underlying symmetry. For highly dynamic flows, on the other hand, these "quasi-Killing" equations may prove more useful in attempting to minimize the source.

In many situations, though, it can be advantageous to adopt a strategy wherein the physical source is designed to be zero in steady state. Then the flux term also will naturally be zero in steady state. For example, because orbital motion or rotation can play an important

[1] The Rankin-Jouinot conditions are designed to ensure the long-term stability of fluid simulations by watching for shocks in the fluid quantities, and reducing the flux reconstruction scheme to first-order throughout the vicinity of the shocks in order to prevent the appearance of Gibbs-type phenomenae in their reconstruction.

[2] "Total variation diminishing" is a term that describes any flux reconstruction scheme that cannot allow the appearance of new extrema in the fluid quantities near shock discontinuities.

role in defining an equilibrium or near equilibrium configuration in many astrophysical fluid problems, it can be advantageous to advect radial momentum rather than the x and y components of linear momentum. The standard Valencia formulation does not immediately accommodate such a switch in the principal state variable without also adopting cylindrical coordinates (and, consequently, a cylindrical grid). But by setting one of the characteristic vectors to $\mathbf{e}_R$ in our generalized Valencia formulation, radial momentum becomes one of the state variables and, in the associated (radial) component of the momentum equation, the source term assumes the desired form namely, it vanishes for steady-state. (Incidentally, this is only possible after moving the gradient of the pressure out of the flux term and into the source – thereby constructing what we refer to as a *physical source*.) Similarly, by setting a separate characteristic vector to $\mathbf{e}_\phi$, angular momentum (as viewed from an inertial frame of reference) becomes one of the state variables and the source term can be minimized in a second momentum equation. This is because $\mathbf{e}_\phi$ is a Killing vector and trivially causes both the flux and source terms to be zero. Furthermore, as discussed in Chapter 5, in certain problems it may also be useful to identify another of the characteristic vectors as the helical Killing vector.

It becomes clear through our generalized Valencia formalism that the components of the momentum vector that are chosen to serve as state variables do not have to correspond with the components of the momentum vector that are used to define the transport velocity. For example, radial and angular momentum might be selected as principal state variables and these state variables can be transported across a Cartesian-like grid using Cartesian-like components of the momentum vector to define the transport velocity. We suspect that this type of hybrid scheme will offer multiple advantages: Cartesian-like coordinates can be used to define the grid on which the metric and its derivatives are specified (via a solution of the Einstein equations) and the identical Cartesian-like grid structure can be used during an evaluation of the flux term to define, without interpolation, area elements on the boundary of each grid cell as well as the transport velocity. At the same time, the components of the momentum vector that define the state variables can be specified using a different coordinate base in such a way that the source terms are minimized.

An additional advantage may arise in the context of fluid flow simulations that benefit from the incorporation of adaptive mesh refinement (AMR). Effective AMR techniques are challenging to implement in any context so it is not surprising that in the relativity community the most successful implementations of AMR, to date, have been on numerical grids with the simplest structure — *i.e.*, Cartesian-like grids. Generally speaking, the advantages that might be gained by moving to a curvilinear or multi-block grid are far outweighed by the challenges that must be overcome in order to implement an effective AMR technique in a non-Cartesian grid environment. Our proposed hybrid scheme may allow the numerical relativity community to realize many of the benefits that would normally be attributed to the adoption of, say, a cylindrical grid – namely, the conservative transport of angular momentum rather than linear momentum, and minimizing the source term in nearly steady-state configurations that are dominated by rotation – while sticking with a Cartesian-like grid on which AMR can be straightforwardly incorporated.

We draw attention to one interesting and rather surprising construction that can be drawn from our generalized formalism. It is customary to expect that if a simulation is carried out on a cylindrical grid that is rotating uniformly with an angular frequency ω, the source term associated with the transport of angular momentum will include a Coriolis term whose magnitude is proportional to ω. However, our work makes it clear that, strictly speaking, only part of the Coriolis term ($-2\rho h\omega \times v^{\phi'}\mathbf{e}_{\phi'}$) originates from the adoption of a rotating grid. The other part ($-2\rho h\bar{\omega} \times v^{R}\mathbf{e}_{R}$) arises from the adoption of a state variable that defines the angular momentum density in a rotating frame of reference. (Consequently, in terms of our nomenclature, the Coriolis term will depend on both the angular velocity of the coordinates ω and the angular velocity of the rotating frame in which angular momentum is measured $\bar{\omega}$.) Through our new formalism, one can envision performing a simulation on a rotating grid while adopting a state variable that tracks the angular momentum density as measured in the inertial frame; in this case, the relevant source term will not include a contribution from the Coriolis acceleration. Hence, when modeling a near steady-state rotational flow, the source term can be minimized (no Coriolis term) while simultaneously

minimizing the effects of numerical diffusion because the transport velocity in the azimuthal direction will be small.

Combining all of these ideas, we suggest that the preferred approach to modeling near steady-state flows in astrophysical environments where rotation plays an important role (such as rotating neutron stars or binary systems containing neutron stars) will involve the adoption of *inertial-frame, cylindrical* momenta as state variables while performing the evolution on a *rotating, Cartesian* coordinate grid. In this context, for completeness, we have added "Case D" to each of the major rows in Tables 1 and 2. This case details the functional form of $\mathbf{C}_{(\eta)}$, $\psi_{(\eta)}$ and $\mathcal{S}_{(\eta)}$ when cylindrical momenta and the Jacobi energy are transported across a rotating, Cartesian grid, that is, a grid defined by,

$$\begin{pmatrix} t' = t \\ x' = x\cos\omega t + y\sin\omega t \\ y' = -x\sin\omega t + y\cos\omega t \end{pmatrix}, \tag{8.2}$$

resulting in the metric,

$$\mathbf{g} = \begin{pmatrix} R^2\omega^2 - c^2 & -y'\omega & x'\omega & 0 \\ -y'\omega & 1 & 0 & 0 \\ x'\omega & 0 & 1 & 0 \\ 0 & 0 & 0 & 1 \end{pmatrix}. \tag{8.3}$$

The use of inertial-frame cylindrical momenta as state variables (in particular, $\eta = 3$ instead of $\eta = 3'$ in Tables 1 and 2) should result in relatively small flux and source terms, better ensuring a conservative treatment of the key state variables; the adoption of a Cartesian grid should facilitate a straightfoward implementation of AMR and may provide an interpolation-free interface with a companion code that solves the Einstein equations to determine values of the metric across the grid; and the adoption of a rotating grid should minimize the effects of numerical diffusion. A hybrid scheme such as this promises to offer the best of several different worlds.

It may even be possible to choose locally a set of state variables in such a way that the source term vanishes altogether – even when no Killing vectors exist. As was discussed in Chapter 4, this could potentially be accomplished by reconstructing a different set of state variables in each cell at each timestep using an independent set of four characteristic vectors each satisfying Eq. (4.79),

$$\rho h u^\mu u_\nu \nabla_\mu C^\nu - C^\mu \, \partial_\mu P = 0,$$

and using these on-the-fly conservative variables to recover the primitive variables in each cell. Though one may initially suspect that it is not possible to find four independent solutions of (4.79) for problems not possessing any special symmetries, an analysis of the degrees of freedom in the problem indicates that, at least locally, there are many families of solutions to (4.79). In Chapter 4 we have provided two such examples in cases when a corresponding Killing vector does not exist. The first was a perfect TOV star. Though the spherical symmetry gives rise to both an azimuthal Killing vector and a timelike Killing vector, no such radial Killing vector exists. Nevertheless, by moving the pressure gradient to the R.H.S. and including it as part of the source, radial momentum is conserved, just as one would expect in an equilibrium situation. The second example involved imprinting a rotation onto the TOV star and rearranging its mass distribution so that it once again is in equilibrium. The radial source can again be made to vanish by adopting as our generalized state variable the radial momentum as measured in the corotating frame. This introduces a centrifugal term into the source that now helps the weakened pressure force[3] to balance gravity. From a mathematical standpoint, it is the new characteristic vector that gives rise to the centrifugal term.

Each of the new ideas laid out in this formal presentation clearly begs some detailed numerical testing. To that end, members of our collaborative research group have started projects of their own that implement one or more of the code improvements that we have recommended. Dominic Marcello is already having success working on a code to model mass transferring binary stars that evolves angular momentum as measured in the inertial frame, but on a rotating-frame cylindrical grid. Zach Byerly is developing a code that will also evolve inertial-frame angular momentum, but on a rotating-frame Cartesian grid. We hope that in addition to all the benefits Dominic reaps, Zach will also benefit significantly from the inclusion of AMR in his code. Over time, we hope that rigorous numerical tests will be made of other ideas that have arisen from our formal analysis of a generalized formulation of the conservative fluid equations.

[3]The pressure gradient decreases as a result of the rearrangement of the star's mass distribution.

Bibliography

[1] P. Ajith, 2008, *Class. Quant. Grav.* **25**, 114033. (arXiv:gr-1c/0712.0343)

[2] M. Anderson, *et al.*, 2008, *Phys. Rev. D* **77**, 024006. (arXiv:gr-qc/0708.2720)

[3] M. Anderson, E.W. Hirschmann, L. Lehner, S.L. Liebling, P.M. Motl, D. Neilsen, C. Palenzuela & J.E. Tohline, 2008, *Phys. Rev. D* **77**, 024006.

[4] M. Anderson, E.W. Hirschmann, L. Lehner, S.L. Liebling, P.M. Motl, D. Neilsen, C. Palenzuela & J.E. Tohline, 2008, *Phys. Rev. Lett.* **100**, 191101.

[5] M. Anderson, E.W. Hirschmann, S.L. Liebling & D. Neilsen, 2006, *Class. Quant. Grav.* **23**, 6503.

[6] L. Antón, O. Zanotti, J.A. Miralles, J.M. Martí, J.M. Ibáñez, J.A. Font & J.A. Pons, 2006, *Ap. J.*, **637**, 296.

[7] R. Arnowitt, S. Deser & C.W. Misner, 1962, *The Dynamics of General Relativity, Gravitation: An Introduction to Current Research* (L. Witten, Wiley).

[8] B. Aylott, *et al.*, 2009, *Class. Quant. Grav* **26**, 114008. (arXiv:gr-qc/0905.4227)

[9] L. Baiotti, B. Giacomazzo & L. Rezzolla, 2009, *Class. Quant. Grav.* **26**, 114005.

[10] F. Banyuls, J.A. Font, J.M. Ibáñez, J.M. Martí & J.A. Miralles, 1997, *Ap. J.* **476**, 221.

[11] T.W. Baumgarte & S.L. Shapiro, 2003, *Phys. Rept.* **376**, 41.

[12] C. Beetle, B. Bromley & R.H. Price, 2006, *Phys. Rev. D* **74**, 024013.

[13] J. Binney & S. Tremaine, 1987, *Galactic Dynamics* (Princeton University Press, Princeton).

[14] D.C. Black & P. Bodenheimer, 1975, *Ap.J.* **199**, 619.

[15] C. Bona, J. Carot & C. Palenzuela-Luque, 2005, *Phys. Rev. D* **72**, 124010.

[16] B. Bruegmann, J.A. Gonzalez, M. Hannam, S. Husa & U. Sperhake, 2008, *Phys. Rev. D* **77**, 124047. (arXiv:gr-qc/0707.0135)

[17] A. Buonanno, G. B. Cook & F. Pretorius, 2007, *Phys. Rev. D* **75**, 124018. (arXiv:gr-qc/0610122)

[18] M. Campanelli, C.O. Lousto, P. Marronetti & Y. Zlochower, 2005, *Phys. Rev. Lett.* **96**, 111101. (arXiv:gr-qc/0511048v2)

[19] M. Campanelli, C.O. Lousto & Y. Zlochower, 2006, *Phys. Rev. D* **73**, 061501. (arXiv:gr-qc/0601091v1)

[20] M. Campanelli, C.O. Lousto & Y. Zlochower, 2006, *Phys. Rev. D* **74**, 041501. (arXiv:gr-qc/0604012v2)

[21] M. Campanelli, C.O. Lousto & Y. Zlochower, 2006, *Phys. Rev. D* **74**, 084023. (arXiv:astro-ph/0608275v4)

[22] M. Campanelli, C.O. Lousto, Y. Zlochower, B. Krishnan & D. Merritt, 2007, *Phys. Rev. D* **75**, 064030. (arXiv:gr-qc/0612076v4)

[23] P. Colella & P.R. Woodward, 1984, *J. Comput. Phys.* **54**, 174.

[24] G.B. Cook, 2000, *Living Rev. Rel.* **3**, 5.

[25] R. d'Inverno, 1992, *Introducing Einstein's Relativity* (Oxford University Press, Oxford).

[26] M.C.R. d'Souza, P.M. Motl, J.E. Tohline & J. Frank, 2006, *Ap. J* **643**, 381. (arXiv:astro-ph/0512137v1)

[27] M.D. Duez, T.W. Baumgarte, S.L. Shapiro, M. Shibata & K. Uryū, 2002, *Phys. Rev. D* **65**, 024016.

[28] M.D. Duez, F. Foucart, L.E. Kidder, H.P. Pfeiffer, M.A. Scheel & S.A. Teukolsky, 2008, *Phys. Rev. D* **78**, 104015.

[29] M.D. Duez, F. Foucart, L.E. Kidder, C.D. Ott & S.A. Teukolsky, 2010, *Class. Quant. Grav.* **27**, 114106. (arXiv:astro-ph/0912.3528)

[30] Z.B. Etienne, Y.T. Liu, S.L. Shapiro & T.W. Baumgarte, 2009, *Phys. Rev. D* **79**, 044024.

[31] J.A. Faber, T.W. Baumgarte, S.L. Shapiro & K. Taniguchi, 2006, *Ap. J.* **641**, L93.

[32] J.A. Font, 2000, *Living Rev. Rel.* **3**, 2.

[33] J.A. Font, 2003, *Living Rev. Rel.* **6**, 4.

[34] J.A. Font, 2008, *Living Rev. Rel.* **11**, 7.

[35] P.C. Fragile, C.C. Lindner, P. Anninos & J.D. Salmonson, 2009, *Ap. J* **691**, 482.

[36] D. Garfinkle & C. Gundlach, 1999, *Class. Quant. Grav.* **16**, 4111.

[37] D.J. Griffiths, 1999, *Introduction to Electrodynamics*, 3rd Ed. (Prentice Hall, Upper Saddle River).

[38] H. Goldstein, C. Poole & J. Safko, 2002, *Classical Mechanics*, 3rd Ed. (Addison Wesley, San Francisco).

[39] M. Hannam, *et al.*, 2009, *Phys. Rev. D* **79**, 084025.

[40] B.v.L.A. Harten & P.D. Lax, 1983, *SIAM Rev.* **25**, 35.

[41] B.J. Kelly, J.G. Baker, W.D. Boggs J.M. Centrella, J.R. Van Meter, & S.T. McWilliams, 2009, *J. Phys. Conf. Ser.* **154**, 012050.

[42] X.-D. Liu & S. Osher, 1994, *J. Comput. Phys.* **115**, 213.

[43] X.-D. Liu & S. Osher, 1998, *J. Comput. Phys.* **142**, 304.

[44] Y.T. Liu, S.L. Shapiro, Z.B. Etienne & K. Taniguchi, 2008, *Phys. Rev. D* **78**, 024012. (arXiv:astro-ph/0803.4193)

[45] R. Matzner, 1968, *J. Math. Phys.* **1063**, 1657.

[46] C.W. Misner, K. Thorne & J.A. Wheeler, 1973, *Gravitation* (W.H. Freeman & Company, New York).

[47] P.J. Montero, J.A. Font & M. Shibata, 2008, *Phys. Rev. D* **78**, 064037. (arXiv:gr-qc/0805.3099v2)

[48] P.M. Motl, J. Frank., J.E. Tohline & M.C.R. d'Souza, 2007, *Ap. J.*, **670**, 1314. (arXiv:astro-ph/0702388)

[49] D. Neilsen & M.W. Choptuik, 2000, *Class. Quant. Grav.* **17**, 733.

[50] D. Neilsen, E.W. Hirschmann & R.S. Millward, 2006, *Class. Quant. Grav.* **23**, S505.

[51] K.C.B. New & J.E. Tohline, 1997, *Ap.J.* **490**, 311.

[52] M.L. Norman & J.R. Wilson, 1978, *Ap.J.* **224**, 497.

[53] J.R. Oppenheimer & G.M. Volkoff, 1939, *Phys. Rev.* **55**, 374.

[54] T. Padmanabhan, 2000, *Theoretical Astrophysics, Volume I: Astrophysical Processes* (Cambridge University Press, New York).

[55] T. Padmanabhan, 2001, *Theoretical Astrophysics, Volume II: Stars and Stellar Systems* (Cambridge University Press, New York).

[56] C. Palenzuela, M. Anderson, L. Lehner, S.L. Liebling & D. Neilsen, 2009, *Phys. Rev. Lett.* **103**, 081101.

[57] Y. Pan, A. Buonanno, L.T. Buchman, T. Chu, L.E. Kidder, H.P. Pfeiffer & M.A. Scheel, 2009, arXiv:gr-qc/0912.3466.

[58] P. Papadopoulos & J.A. Font, 1999, arXiv:gr-qc/9912054v1.

[59] H.P. Pfeiffer, L.E. Kidder, M.A. Scheel & S.A. Teukolsky, 2003, *Comput. Phys. Commun.* **152**, 253.

[60] F. Pretorius, 2006, *Class. Quant. Grav.* **23**, S529.

[61] D. Pollney, *et al.*, 2007, *Phys. Rev. D*, **76**, 124002. (arXiv:gr-qc/0707.2559)

[62] D. Pollney, C. Reisswig, E. Schnetter, N. Dorband & P. Diener, 2009, arXiv:gr-qc/0910.3803.

[63] O. Reula, 1998, *Living Rev. Rel.* **1**, 3.

[64] L. Rezzolla, L. Baiotti, B. Giacomazzo, D. Link & J.A. Font, 2010, arXiv:gr-qc/1001.3074.

[65] M.M. Romanova, A.V. Koldoba, G.V. Ustyugova, A.K. Kulkarni, M. Long & R.V.E. Lovelace, 2009, arXiv:astro-ph/0901.4269v1.

[66] J.A. Rossmanith, D.S. Bale & R.J. LeVeque, 2004, *J. Comput. Phys.* **199**, 631.

[67] M. Shibata, K. Kyutoku, T. Yamamoto & K. Taniguchi, 2009, *Phys. Rev. D* **79**, 044030.

[68] M. Shibata & K. Taniguchi, 2006, *Phys. Rev. D* **73**, 064027.

[69] M. Shibata, K. Taniguchi & K. Uryū, 2003, *Phys. Rev. D* **68**, 084020.

[70] M. Shibata, K. Taniguchi & K. Uryū, 2005, *Phys. Rev. D* **71**, 084021.

[71] M. Shibata & K. Uryū, 2000, *Phys. Rev. D* **61**, 064001.

[72] M. Shibata & K. Uryū, 2002, *Progress of Theoretical Physics* **107**, 265.

[73] L. Smarr & J.W. York, 1978, *Phys. Rev. D* **17**, 2529.

[74] J.M. Stone & M.L. Norman, 1992, *Ap.J.S.* **80**, 753.

[75] F.D. Swesty, E.Y.M. Wang & A.C. Calder, 2000, *Ap.J.* **541**, 937.

[76] A. Tchekovskoy, J.C. McKinney & R. Narayan, 2007, *MNRAS* **379**, 469. (arXiv:astro-ph/0704.2608)

[77] J.I. Thorpe, S.T. McWilliams, B.J. Kelly, R.P. Fahey, K. Arnaud & J.G. Baker, 2009, *Class. Quant. Grav.* **26**, 09026. (arXiv:astro-ph/0811.0833)

[78] W. Tichy & P. Marronetti, 2008, *Phys. Rev. D* **78**, 081501.

[79] M. Tiglio, L. Lehner & D. Neilsen, 2004, *Phys. Rev. D* **70**, 104018.

[80] R.C. Tolman, 1939, *Phys. Rev.* **55**, 364.

[81] R.M. Wald, 1984, *General Relativity* (University of Chicago Press, Chicago).

[82] W. Zhang & A.I. MacFadyen, 2006, *Ap.J.S.* **164**, 255. (arXiv:astro-ph/0505481v2)

[83] B. Zink, E. Schnetter & M. Tiglio, 2008, *Phys. Rev. D* **77**, 103015.

Appendix A

Useful Relations Involving the Construction of Conservative Variables from the Primitives

We begin with physical definitions of the so-called primitive variables:

$$\rho \equiv \text{proper baryon number density of the fluid.} \tag{A.1}$$
$$\Gamma \equiv \text{adiabatic index of the fluid} \tag{A.2}$$
$$\epsilon \equiv P/\left[\rho c^2(\Gamma-1)\right] = \text{proper specific internal energy density of the fluid.} \tag{A.3}$$
$$h \equiv 1+\epsilon+P/\rho c^2 = 1+\Gamma\epsilon = \text{proper specific enthalpy of the fluid.} \tag{A.4}$$
$$P \equiv \text{proper isotropic pressure of the fluid.} \tag{A.5}$$
$$v_i \equiv \text{covariant components of the fluid's 3-velocity as measured in the coordinate frame.} \tag{A.6}$$

From these, the conservative variables (each measured in the coordinate frame) are constructed according to the following relations:

$$D \equiv \rho W = \text{baryon number density,} \tag{A.7}$$
$$S_j \equiv \rho h c W^2 v_j = \text{momentum density in the } j\text{-direction,} \tag{A.8}$$
$$E \equiv \rho h c^2 W^2 - P = \text{total energy density of the fluid,} \tag{A.9}$$
$$\tau \equiv \rho h c^2 W^2 - P - c^2 D = \text{total energy density minus baryon number density,} \tag{A.10}$$

where

$$W \equiv \alpha u^0/c = \left(1-v^2/c^2\right)^{-1/2} = \text{Lorentz factor.} \tag{A.11}$$
$$u^\mu \equiv W\left(c/\alpha\ ,\ v^i - c\beta^i/\alpha\right)^T = \text{contravariant components of the fluid's 4-velocity.} \tag{A.12}$$

This last relationship can also be written

$$u_\mu = W\left(\beta^j v_j - c\alpha\ ,\ v_i\right). \tag{A.13}$$
$$v^i = \frac{u^i}{W} + \frac{c\beta^i}{\alpha}. \tag{A.14}$$
$$v_i = u_i/W. \tag{A.15}$$

Appendix B

Derivation of the Generalized Valencia Formulation from the Fundamental Equations of Motion

B.1 The Continuity Equation (No Source)

Begin with Eq. (2.1).

$$\nabla_\mu J^\mu = 0.$$

$$\Longrightarrow \frac{1}{\sqrt{-g}}\,\partial_\mu\left(\sqrt{-g}\;J^\mu\right) = 0.$$

$$\Longrightarrow \frac{1}{\sqrt{-g}}\,\partial_\mu\left(\sqrt{-g}\;\rho u^\mu\right) = 0.$$

$$\Longrightarrow \frac{1}{\alpha\sqrt{\gamma}}\left(\partial_0\;\alpha\sqrt{\gamma}\;\rho u^0 + \partial_i\;\alpha\sqrt{\gamma}\;\rho u^i\right) = 0.$$

Use $W \equiv \alpha u^0/c$.

$$\frac{1}{\alpha\sqrt{\gamma}}\left(\partial_0\;\sqrt{\gamma}\;\rho c W + \partial_i\;\alpha\sqrt{\gamma}\;\rho c W\frac{u^i}{\alpha u^0}\right) = 0.$$

Divide through by c.

$$\frac{1}{\alpha\sqrt{\gamma}}\left(\partial_0\;\sqrt{\gamma}\;D + \partial_i\;\alpha\sqrt{\gamma}\;D\frac{u^i}{\alpha u^0}\right) = 0, \tag{B.1}$$

where

$$D \equiv \rho W. \tag{B.2}$$

This is the continuity equation as it appears in the original Valencia formulation, as presented in §2.5.

B.2 The Momentum Equations (Physical Source)

Begin with the spacelike components of Eq. (2.2).

$$\nabla_\mu T^\mu{}_i = 0_i.$$

$$\Longrightarrow \frac{1}{\sqrt{-g}}\,\partial_\mu\left(\sqrt{-g}\;T^\mu{}_i\right) = T^\mu{}_\alpha\Gamma^\alpha_{\mu i}.$$

$$\Longrightarrow \frac{1}{\sqrt{-g}}\,\partial_\mu\Big[\sqrt{-g}\,(\rho h u_i u^\mu + P\delta^\mu{}_i)\Big] = T^\mu{}_\alpha\Gamma^\alpha_{\mu i}.$$

$$\Longrightarrow \frac{1}{\alpha\sqrt{\gamma}}\Big[\partial_0\;\alpha\sqrt{\gamma}\,(\rho h u_i u^0) + \partial_j\;\alpha\sqrt{\gamma}\,(\rho h u_i u^j + P\delta^j{}_i)\Big] = T^{\mu\nu}g_{\nu\alpha}\Gamma^\alpha_{\mu i}.$$

Use $u_i = W v_i$.

$$\frac{1}{\alpha\sqrt{\gamma}}\Big[\partial_0\ \sqrt{\gamma}\left(\rho h \alpha W v_i u^0\right) + \partial_j\ \alpha\sqrt{\gamma}\left(\rho h W v_i u^j + P\delta^j{}_i\right)\Big] = T^{\mu\nu} g_{\nu\alpha}\cdot \tfrac{1}{2} g^{\alpha\beta}\left(\partial_\mu g_{i\beta} + \partial_i g_{\beta\mu} - \partial_\beta g_{\mu i}\right).$$

The metric and inverse metric on the right combine to form a Kroenecker delta $\delta^\beta{}_\nu$, which is then used to convert β's into ν's in the last term on the right. Also, use $W \equiv \alpha u^0/c$.

$$\frac{1}{\alpha\sqrt{\gamma}}\left[\partial_0\ \sqrt{\gamma}\left(\rho h c W^2 v_i\right) + \partial_j\ \alpha\sqrt{\gamma}\left(\rho h c W^2 v_i \frac{u^j}{\alpha u^0} + P\delta^j{}_i\right)\right] = \tfrac{1}{2} T^{\mu\nu}\left(\partial_\mu g_{i\nu} + \partial_i g_{\nu\mu} - \partial_\nu g_{\mu i}\right).$$

Divide through by c to obtain

$$\frac{1}{\alpha\sqrt{\gamma}}\left[\partial_0\ \sqrt{\gamma}\ S_i + \partial_j\ \alpha\sqrt{\gamma}\left(S_i\frac{u^j}{\alpha u^0} + \frac{P}{c}\delta^j{}_i\right)\right] = \mathcal{S}_{(i)}, \tag{B.3}$$

where

$$S_i \equiv \rho h W^2 v_i, \tag{B.4}$$

$$\mathcal{S}_{(i)} \equiv T^{\mu\nu}\left(\partial_\mu g_{\nu i} - \Gamma^\delta_{\mu\nu} g_{\delta i}\right)/c. \tag{B.5}$$

These are the momentum equations as they appear in the original Valencia formulation, as presented in §2.5.

Now contract both sides of the momentum equations with the components (in grid coordinates) of some 3-vector $C^i{}_{(k')}$. On the L.H.S., bring $C^i{}_{(k')}$ inside the partials. The penalty is the appearance of additional terms, which should be moved over to the R.H.S. and included as part of the source.

$$\frac{1}{\alpha\sqrt{\gamma}}\left[\partial_0\ \sqrt{\gamma}\ \tilde{S}_{(k')} + \partial_j\ \alpha\sqrt{\gamma}\left(\tilde{S}_{(k')}\frac{u^j}{\alpha u^0} + \frac{P}{c}C^j{}_{(k')}\right)\right] = \text{source},$$

where

$$\begin{aligned}
\tilde{S}_{(k')} &\equiv S_i C^i{}_{(k')} = \rho h W^2 v_i C^i{}_{(k')}, \\
\text{source} &\equiv T^{\mu\nu}\left(\partial_\mu g_{\nu i} - \Gamma^\delta_{\mu\nu} g_{\delta i}\right) C^i{}_{(k')}/c + \frac{S_i}{\alpha}\ \partial_0 C^i{}_{(k')} + S_i\frac{u^j}{\alpha u^0}\ \partial_j C^i{}_{(k')} + \frac{P}{c}\ \partial_i C^i{}_{(k')}.
\end{aligned}$$

Move the pressure piece from the L.H.S. to the R.H.S., and use the product rule to expand it into three terms. Meanwhile, substitute in expression (2.4) for the stress-energy tensor. The momentum equations now take the form

$$\frac{1}{\alpha\sqrt{\gamma}}\left(\partial_0\ \sqrt{\gamma}\ \tilde{S}_{(k')} + \partial_j\ \alpha\sqrt{\gamma}\ \tilde{S}_{(k')}\frac{u^j}{\alpha u^0}\right) = \tilde{\mathcal{S}}_{(k')},$$

where

$$\begin{aligned}
\tilde{\mathcal{S}}_{(k')} &\equiv \left(\rho h u^\mu u^\nu - P g^{\mu\nu}\right)\left(\partial_\mu g_{\nu i} - \Gamma^\delta_{\mu\nu} g_{\delta i}\right) C^i{}_{(k')}/c + \frac{S_i}{\alpha}\ \partial_0 C^i{}_{(k')} + S_i\frac{u^j}{\alpha u^0}\ \partial_j C^i{}_{(k')} + \cancel{\frac{P}{c}\ \partial_i C^i{}_{(k')}} \\
&- \frac{P}{c} C^j{}_{(k')}\frac{\partial_j\sqrt{-g}}{\sqrt{-g}} - \cancel{\frac{P}{c}\ \partial_j C^j{}_{(k')}} - C^j{}_{(k')}\ \partial_j P/c.
\end{aligned}$$

Use $\partial_\nu\sqrt{-g} = \Gamma^\mu_{\mu\nu}\sqrt{-g}$. Separate the pressure piece from the first term in the source and use the fact that $\partial_\mu g_{\nu i} - \Gamma^\delta_{\mu\nu} g_{\delta i} = g_{\nu\alpha}\Gamma^\alpha_{\mu i}$, as shown by following the source term from the fourth step of this subsection down to the seventh (see Eq. B.5). The source then becomes

$$\begin{aligned}
\tilde{\mathcal{S}}_{(k')} &\equiv \rho h u^\mu u^\nu \left(\partial_\mu g_{\nu i} - \Gamma^\delta_{\mu\nu} g_{\delta i}\right) C^i{}_{(k')}/c + \cancel{\frac{P}{c} \Gamma^\mu_{\mu i} C^i{}_{(k')}} + \frac{S_i}{\alpha}\, \partial_0 C^i{}_{(k')} + S_i \frac{u^j}{\alpha u^0}\, \partial_j C^i{}_{(k')} \\
&- \cancel{\frac{P}{c} C^j{}_{(k')} \Gamma^\mu_{\mu j}} - C^j{}_{(k')}\, \partial_j P/c \\
&= \rho h u^\mu u^\nu \left(\partial_\mu g_{\nu i} - \Gamma^\delta_{\mu\nu} g_{\delta i}\right) C^i{}_{(k')}/c + \frac{S_i}{\alpha}\, \partial_0 C^i{}_{(k')} + S_i \frac{u^j}{\alpha u^0}\, \partial_j C^i{}_{(k')} - C^j{}_{(k')}\, \partial_j P/c.
\end{aligned}$$

All together, then, we have

$$\frac{1}{\alpha\sqrt{\gamma}} \left(\partial_0\, \sqrt{\gamma}\, \tilde{S}_{(k')} + \partial_j\, \alpha\sqrt{\gamma}\, \tilde{S}_{(k')} \frac{u^j}{\alpha u^0} \right) = \tilde{\mathcal{S}}_{(k')}, \tag{B.6}$$

where

$$\tilde{S}_{(k')} \equiv \rho h W^2 v_i C^i{}_{(k')}, \tag{B.7}$$

$$\begin{aligned}
\tilde{\mathcal{S}}_{(k')} &\equiv \rho h u^\mu u^\nu \left(\partial_\mu g_{\nu i} - \Gamma^\delta_{\mu\nu} g_{\delta i}\right) C^i{}_{(k')}/c + \frac{S_i}{\alpha}\, \partial_0 C^i{}_{(k')} \\
&\quad + S_i \frac{u^j}{\alpha u^0}\, \partial_j C^i{}_{(k')} - C^j{}_{(k')}\, \partial_j P/c.
\end{aligned} \tag{B.8}$$

These are the momentum equations as they appear in our modified version of the Valencia formulation, as presented in §3.2.

B.3 The Energy Equation (Standard Source)

The energy equation is typically written in terms of the stress-energy tensor with both indices up, as opposed to the momentum equations, which were written in terms of the the stress-energy tensor with mixed indices. Begin by raising the ν index in Eq. (2.2), and select the $\nu = 0$ component.

$$\nabla_\mu T^{\mu 0} = 0.$$

$$\Longrightarrow \frac{1}{\sqrt{-g}}\, \partial_\mu \left(\sqrt{-g}\, T^{\mu 0}\right) = -T^{\mu\alpha}\Gamma^0_{\mu\alpha}.$$

$$\Longrightarrow \frac{1}{\sqrt{-g}}\, \partial_\mu \Big[\sqrt{-g}\, \left(\rho h u^0 u^\mu + P g^{\mu 0}\right)\Big] = -T^{\mu\alpha}\Gamma^0_{\mu\alpha}.$$

$$\Longrightarrow \frac{1}{\alpha\sqrt{\gamma}} \Big[\partial_0\, \alpha\sqrt{\gamma}\, \left(\rho h u^0 u^0 + P g^{00}\right) + \partial_j\, \alpha\sqrt{\gamma}\, \left(\rho h u^0 u^j + P g^{j0}\right)\Big] = -T^{\mu\alpha}\Gamma^0_{\mu\alpha}.$$

$$\Longrightarrow \frac{1}{\alpha\sqrt{\gamma}} \Big[\partial_0\, \sqrt{\gamma}\Big(\rho h \alpha u^0 u^0 + \alpha P\left(-1/c^2\right)\Big) + \partial_j\, \alpha\sqrt{\gamma}\Big(\rho h u^0 u^j + P\left(\beta^j/\alpha^2\right)\Big)\Big] = -T^{\mu\nu}\Gamma^0_{\mu\nu}.$$

Multiply both sides through by α. Use the product rule on the left to move α inside the partials. The penalty is an additional term involving the partials of α. Also use $W \equiv \alpha u^0/c$.

$$\begin{aligned}
\frac{1}{\alpha\sqrt{\gamma}} \left[\partial_0\, \sqrt{\gamma}\left(\rho h c^2 W^2 - P\right) + \partial_j\, \alpha\sqrt{\gamma}\left(\rho h c^2 W^2 \frac{u^j}{\alpha u^0} - P\frac{u^j}{\alpha u^0} + P\frac{v^j}{c}\right)\right] &- \cancel{\frac{1}{\sqrt{-g}}\sqrt{-g}}\, T^{\mu 0}\, \partial_\mu \alpha \\
&= -\alpha T^{\mu\nu}\Gamma^0_{\mu\nu}.
\end{aligned}$$

Subtract off c^2 times the continuity equation, and move the term involving partials of α over to the right-hand side to be included as part of the source.

$$\frac{1}{\alpha\sqrt{\gamma}}\left[\partial_0\ \sqrt{\gamma}\ \tau + \partial_j\ \alpha\sqrt{\gamma}\left(\tau\frac{u^j}{\alpha u^0} + \frac{P}{c}v^j\right)\right] = \mathcal{S}_{(5)}, \tag{B.9}$$

where

$$\begin{aligned} \tau &\equiv \rho h c^2 W^2 - P - c^2 D, & \text{(B.10)}\\ \mathcal{S}_{(5)} &\equiv \alpha\left(T^{\mu 0}\ \partial_\mu \ln\alpha - T^{\mu\nu}\Gamma^0_{\mu\nu}\right). & \text{(B.11)} \end{aligned}$$

This is the energy equation as it appears in the original Valencia formulation, as presented in §2.5.

Now scale both sides of the energy equation by $(c/\alpha)\,C^0{}_{(5)}$. Bring this quantity inside the partials on the L.H.S., and pay a penalty by adding additional terms to the source on the R.H.S.

$$\frac{1}{\alpha\sqrt{\gamma}}\left[\partial_0\ \sqrt{\gamma}\ \tilde{\tau} + \partial_j\ \alpha\sqrt{\gamma}\left(\tilde{\tau}\frac{u^j}{\alpha u^0} + \frac{P}{\alpha}v^j C^0{}_{(5)}\right)\right] = \tilde{\mathcal{S}}_{(5)}, \tag{B.12}$$

where

$$\begin{aligned} \tilde{\tau} &\equiv \frac{c\tau}{\alpha}C^0{}_{(5)} = \left(\rho h c^2 W^2 - P - c^2 D\right)(c/\alpha)\,C^0{}_{(5)}, & \text{(B.13)}\\ \tilde{\mathcal{S}}_{(5)} &\equiv c\left(T^{\mu 0}\ \partial_\mu \ln\alpha - T^{\mu\nu}\Gamma^0_{\mu\nu}\right)C^0{}_{(5)} + \frac{\tau}{\alpha}\Big[\,(c/\alpha)\,\partial_0 C^0{}_{(5)} + C^0{}_{(5)}\partial_0\,(c/\alpha)\,\Big] \\ &+ \left(\tau\frac{u^j}{\alpha u^0} + \frac{P}{c}v^j\right)\Big[\,(c/\alpha)\,\partial_j C^0{}_{(5)} + C^0{}_{(5)}\partial_j\,(c/\alpha)\,\Big]. & \text{(B.14)} \end{aligned}$$

B.4 Forming a Linear Combination of the Momentum and Energy Equations (Hybrid Physical+Standard Source)

We have derived generalized formulations for

- the momentum equations (with a *physical source* so that no artificial naked pressure terms appear and so that source terms and advection terms are each independently zero for steady-state problems),
- the energy equation (with a *standard source* so that no time derivatives of the pressure show up in the source term).

Now we will combine the two approaches by forming a linear combination of the momentum and energy equations, thus empowering us to mix momentum and energy equations while still reaping the benefits of each respective approach to the corresponding pressure terms.

For the momentum equations, proceed by allowing $\mathbf{C}_{(k')}$ to have a nonzero timelike component. Add $1/c$ times Eq. (B.12) (with $C^0{}_{(5)}$ replaced by $C^0{}_{(k')}$) to Eq. (B.6).

$$\frac{1}{\alpha\sqrt{\gamma}}\left[\partial_0\ \sqrt{\gamma}\ \hat{S}_{(k')} + \partial_j\ \alpha\sqrt{\gamma}\left(\hat{S}_{(k')}\frac{u^j}{\alpha u^0} + \frac{P}{c\alpha}v^j C^0{}_{(k')}\right)\right] = \hat{\mathcal{S}}_{(k')}, \tag{B.15}$$

where

$$\hat{S}_{(k')} \equiv \tilde{S}_{(k')} + \tau C^0{}_{(k')}/\alpha = \rho h W^2 v_i C^i{}_{(k')} + \left(\rho h c W^2 - \frac{P}{c} - cD\right)(c/\alpha)\, C^0{}_{(k')}, \tag{B.16}$$

$$\begin{aligned}\hat{\mathcal{S}}_{(k')} &\equiv \rho h u^\mu u^\nu \left(\partial_\mu g_{\nu i} - \Gamma^\delta_{\mu\nu} g_{\delta i}\right) C^i{}_{(k')}/c + \frac{S_i}{\alpha}\, \partial_0 C^i{}_{(k')} + S_i \frac{u^j}{\alpha u^0}\, \partial_j C^i{}_{(k')} - C^j{}_{(k')}\, \partial_j P/c \\ &+ \left(T^{\mu 0}\, \partial_\mu \ln\alpha - T^{\mu\nu}\Gamma^0_{\mu\nu}\right) C^0{}_{(k')} + \frac{\tau}{c\alpha}\Big[\,(c/\alpha)\,\partial_0 C^0{}_{(k')} + C^0{}_{(k')}\partial_0\,(c/\alpha)\,\Big] \\ &+ \left(\frac{\tau}{c}\frac{u^j}{\alpha u^0} + \frac{P}{c^2} v^j\right)\Big[\,(c/\alpha)\,\partial_j C^0{}_{(k')} + C^0{}_{(k')}\partial_j\,(c/\alpha)\,\Big].\end{aligned} \tag{B.17}$$

These are the momentum equations as they appear in the fully-generalized Valencia formulation. The modified momentum equation (as it appears in §3.2) can be immediately recovered by selecting $C^0{}_{(k')} = 0, C^i{}_{(k')} = \tilde{C}^i{}_{(k')}$. In order to recover the original momentum equation (as it appears in §2.5), one must further select $\tilde{C}^i{}_{(k')} = \delta^i{}_{(k')}$, and replace naked pressure terms.

Similarly, for the energy equation, proceed by allowing $\mathbf{C}_{(5)}$ to have nonzero spacelike components. Add c times Eq. (B.6) (with $C^i{}_{(k')}$ replaced by $C^i{}_{(5)}$) to Eq. (B.12).

$$\frac{1}{\alpha\sqrt{\gamma}}\left[\partial_0\, \sqrt{\gamma}\, \hat{\tau} + \partial_j\, \alpha\sqrt{\gamma}\left(\hat{\tau}\frac{u^j}{\alpha u^0} + \frac{P}{\alpha} v^j C^0{}_{(5)}\right)\right] = \hat{\mathcal{S}}_{(5)} \tag{B.18}$$

where

$$\hat{\tau} \equiv \tilde{\tau} + cS_i C^i{}_{(5)} = \left(\rho h c^2 W^2 - P - c^2 D\right)(c/\alpha)\, C^0{}_{(5)} + \rho h c W^2 v_i C^i{}_{(5)} \tag{B.19}$$

$$\begin{aligned}\hat{\mathcal{S}}_{(5)} &\equiv c\left(T^{\mu 0}\, \partial_\mu \ln\alpha - T^{\mu\nu}\Gamma^0_{\mu\nu}\right) C^0{}_{(5)} + \frac{\tau}{\alpha}\Big[\,(c/\alpha)\,\partial_0 C^0{}_{(5)} + C^0{}_{(5)}\partial_0\,(c/\alpha)\,\Big] \\ &+ \left(\tau\frac{u^j}{\alpha u^0} + \frac{P}{c} v^j\right)\Big[\,(c/\alpha)\,\partial_j C^0{}_{(5)} + C^0{}_{(5)}\partial_j\,(c/\alpha)\,\Big], \\ &+ \rho h u^\mu u^\nu \left(\partial_\mu g_{\nu i} - \Gamma^\delta_{\mu\nu} g_{\delta i}\right) C^i{}_{(k')} + \frac{cS_i}{\alpha}\, \partial_0 C^i{}_{(k')} \\ &+ cS_i \frac{u^j}{\alpha u^0}\, \partial_j C^i{}_{(k')} - C^j{}_{(k')}\, \partial_j P.\end{aligned} \tag{B.20}$$

This is the energy equation as it appears in the fully-generalized Valencia formulation. The original energy equation (as it appears in both §§2.5 & 3.2) can be immediately recovered by selecting $C^0{}_{(5)} = \alpha/c, C^i{}_{(5)} = 0$.

Appendix C

Term-by-Term Expansion of the Euler Equations

The divergence term involves a contraction over i, and is really three terms in one. Only one of the three terms will survive on each of the six faces. The state variable term, on the other hand, is nonzero only on the two hypersurfaces. Expanding (3.19*b*) into integrals over each of the two hypersurfaces and each of the six hyperfaces, we have

$$
\begin{aligned}
& \frac{1}{\sqrt{-g}} \int_{\partial\Omega_0^+} W\psi_{(\eta)} \left(\sqrt{\gamma}\ \mathrm{d}x^1\ \mathrm{d}x^2\ \mathrm{d}x^3\right) - \frac{1}{\sqrt{-g}} \int_{\partial\Omega_0^-} W\psi_{(\eta)} \left(\sqrt{\gamma}\ \mathrm{d}x^1\ \mathrm{d}x^2\ \mathrm{d}x^3\right) \\
+ & \frac{1}{\sqrt{-g}} \int_{\partial\Omega_1^+} W\psi_{(\eta)} \left[\frac{\sqrt{\gamma}}{\sqrt{\gamma\{1\}}} \left(v^1 - c\beta^1/\alpha\right)\right] \left(\sqrt{\gamma\{1\}}\ \mathrm{d}x^2\ \mathrm{d}x^3\right) \left(\alpha/c\ \mathrm{d}x^0\right) \\
- & \frac{1}{\sqrt{-g}} \int_{\partial\Omega_1^-} W\psi_{(\eta)} \left[\frac{\sqrt{\gamma}}{\sqrt{\gamma\{1\}}} \left(v^1 - c\beta^1/\alpha\right)\right] \left(\sqrt{\gamma\{1\}}\ \mathrm{d}x^2\ \mathrm{d}x^3\right) \left(\alpha/c\ \mathrm{d}x^0\right) \\
+ & \frac{1}{\sqrt{-g}} \int_{\partial\Omega_2^+} W\psi_{(\eta)} \left[\frac{\sqrt{\gamma}}{\sqrt{\gamma\{2\}}} \left(v^2 - c\beta^2/\alpha\right)\right] \left(\sqrt{\gamma\{2\}}\ \mathrm{d}x^1\ \mathrm{d}x^3\right) \left(\alpha/c\ \mathrm{d}x^0\right) \\
- & \frac{1}{\sqrt{-g}} \int_{\partial\Omega_2^-} W\psi_{(\eta)} \left[\frac{\sqrt{\gamma}}{\sqrt{\gamma\{2\}}} \left(v^2 - c\beta^2/\alpha\right)\right] \left(\sqrt{\gamma\{2\}}\ \mathrm{d}x^1\ \mathrm{d}x^3\right) \left(\alpha/c\ \mathrm{d}x^0\right) \\
+ & \frac{1}{\sqrt{-g}} \int_{\partial\Omega_3^+} W\psi_{(\eta)} \left[\frac{\sqrt{\gamma}}{\sqrt{\gamma\{3\}}} \left(v^3 - c\beta^3/\alpha\right)\right] \left(\sqrt{\gamma\{3\}}\ \mathrm{d}x^1\ \mathrm{d}x^2\right) \left(\alpha/c\ \mathrm{d}x^0\right) \\
- & \frac{1}{\sqrt{-g}} \int_{\partial\Omega_3^-} W\psi_{(\eta)} \left[\frac{\sqrt{\gamma}}{\sqrt{\gamma\{3\}}} \left(v^3 - c\beta^3/\alpha\right)\right] \left(\sqrt{\gamma\{3\}}\ \mathrm{d}x^1\ \mathrm{d}x^2\right) \left(\alpha/c\ \mathrm{d}x^0\right) \\
= & \frac{1}{\sqrt{-g}} \int_{\Omega} \mathcal{S}_{(\eta)} \left(\sqrt{\gamma}\ \mathrm{d}x^1\ \mathrm{d}x^2\ \mathrm{d}x^3\right) \left(\alpha/c\ \mathrm{d}x^0\right), \qquad \text{(C.1)}
\end{aligned}
$$

where $\partial\Omega_i^+$ refers to the i^+ boundary of the hypercell, and so forth. This equation is exact and can be discretized for numerical implementation by any scheme one chooses.

Keeping in mind that the six flux terms add to zero globally, one can see from Eq. (*C*.1) that whenever the source is zero, the volume integral of the advection variable measured by an Eulerian observer, $\int_\Omega W\psi_{(\eta)}\ \left(\sqrt{\gamma}\ \mathrm{d}^3x\right)$, is globally conserved.

Moreover, since the Eulerian observer is inertial, exact global conservation of $W\psi_{(\eta)}$ implies the exact global conservation of $\psi_{(\eta)}/W$, the advection variable as measured by another inertial observer — one that is instantaneously comoving with the fluid. In general, this is not the Lagrangian observer because the Lagrangian observer may not be inertial. This means that the fundamental quantity being conserved is the volume integral of the proper advection variable — that is, proper baryon number density, proper generalized momentum, or proper generalized energy. And the measurement of this quantity by any inertial observer will also be globally conserved.

Furthermore, with all the pressure terms included inside the source, there is nothing to spoil even local conservation. If the physical source can truly be eliminated, this implies that

the proper advection variable ψ is locally conserved everywhere. In general, though, it is very difficult to construct an everywhere-sourceless generalized momentum $\psi_{(j')} = \rho h u_\nu C^\nu{}_{(j')}$, and it may be impossible to construct an everywhere-sourceless generalized energy $\psi_{(0')} = \rho h u_\nu C^\nu{}_{(0')}$.

Appendix D

The Partial Derivative of $\sqrt{-g}$

We begin with the chain rule, which states that

$$\partial_\mu g = \frac{\partial g}{\partial x^\mu} = \frac{\partial g}{\partial g_{\alpha\beta}} \frac{\partial g_{\alpha\beta}}{\partial x^\mu} = g g^{\alpha\beta} \partial_\mu g_{\alpha\beta}.$$

Using the fact that covariant derivatives of the metric are zero,

$$\nabla_\mu g_{\alpha\beta} = \partial_\mu g_{\alpha\beta} - \Gamma^\nu_{\mu\alpha} g_{\nu\beta} - \Gamma^\nu_{\mu\beta} g_{\alpha\nu} = 0_{\mu\alpha\beta},$$

we have

$$\begin{aligned} \partial_\mu g_{\alpha\beta} &= \Gamma^\nu_{\mu\alpha} g_{\nu\beta} + \Gamma^\nu_{\mu\beta} g_{\alpha\nu} \\ \implies \partial_\mu g &= g g^{\alpha\beta} \left(\Gamma^\nu_{\mu\alpha} g_{\nu\beta} + \Gamma^\nu_{\mu\beta} g_{\alpha\nu} \right) \\ &= g\ \delta^\alpha_\nu \Gamma^\nu_{\mu\alpha} + g\ \delta^\beta_\nu \Gamma^\nu_{\mu\beta} \\ &= 2g \Gamma^\alpha_{\alpha\mu}. \end{aligned}$$

Meanwhile,

$$\partial_\mu \sqrt{-g} = \tfrac{1}{2} \frac{\partial_\mu (-g)}{\sqrt{-g}} = \frac{-g \Gamma^\nu_{\nu\mu}}{\sqrt{-g}} = \Gamma^\nu_{\nu\mu} \sqrt{-g},$$

as promised. See [25] for additional details.

Appendix E

Derivation of $\sigma_{(x)}$ throughout a TOV Star

A Tolman-Oppenheimer-Volkoff star has three distinguishing characteristics: one, it is spherically symmetric; two, it is in hydrostatic equilibrium; and three, it is generally at least mildly relativistic. In spherical coordinates, the metric for any TOV star can be written

$$g_{\mu\nu} = \begin{pmatrix} g_{tt}(r) & 0 & 0 & 0 \\ 0 & g_{rr}(r) & 0 & 0 \\ 0 & 0 & r^2 & 0 \\ 0 & 0 & 0 & r^2 \sin^2\theta \end{pmatrix}, \tag{E.1}$$

where $g_{tt}(r)$ and $g_{tt}(r)$ depend on the choice of central density, central pressure, and polytropic constant in the equation of state. The only nonzero Christoffel symbols resulting from the metric in spherical coordinates are

$$\begin{aligned}
\Gamma^t_{tr} = \Gamma^t_{rt} &= \frac{g'_{tt}(r)}{2\ g_{tt}(r)} \\
\Gamma^r_{tt} &= -\frac{g'_{tt}(r)}{2\ g_{rr}(r)} \\
\Gamma^r_{rr} &= \frac{g'_{rr}(r)}{2\ g_{rr}(r)} \\
\Gamma^r_{\theta\theta} &= -\frac{r}{g_{rr}(r)} \\
\Gamma^r_{\phi\phi} &= -\frac{r\sin^2\theta}{g_{rr}(r)} \\
\Gamma^\theta_{r\theta} = \Gamma^\theta_{\theta r} &= \frac{1}{r} \\
\Gamma^\theta_{\phi\phi} &= -\sin\theta\cos\theta \\
\Gamma^\phi_{r\phi} = \Gamma^\phi_{\phi r} &= \frac{1}{r} \\
\Gamma^\phi_{\theta\phi} = \Gamma^\phi_{\phi\theta} &= \cot\theta.
\end{aligned}$$

Now, if $\mathbf{C}$ is chosen to be one of the Cartesian unit vectors — say $\hat{x}$ — its spherical components are

$$\mathbf{C} \equiv \sin\theta\cos\phi\ \mathbf{e_r} + \frac{\cos\theta\cos\phi}{r}\ \mathbf{e}_\theta - \frac{\sin\phi}{r}\ \mathbf{e}_\phi.$$

Then the relevant naked pressure term $P\Gamma^\mu_{\mu r}$ – call it f – becomes

$$f = P\left[\tfrac{1}{2}\sin\theta\cos\phi\frac{\partial_r\left(g_{tt}g_{rr}\right)}{g_{tt}g_{rr}} + \frac{1-\sin\theta}{\sin\theta}\frac{\cos\phi}{r}\right]. \tag{E.2}$$

We can scale this artificial force to the physical forces in the problem by rewriting the radial momentum equation as

$$\frac{1}{\sqrt{-g}}\ \partial_\mu\left(\sqrt{-g}\ \rho h u^\mu u_\nu C^\nu\right) = \underbrace{\rho h u^\mu u_\nu \nabla_\mu C^\nu}_{\text{gravity}} - \underbrace{C^\mu \partial_\mu P}_{\text{pressure}}\ \left(1 + \underbrace{\epsilon_L - \epsilon_R}_{\substack{\text{relative}\\ \text{error}}}\right), \tag{E.3}$$

$$\text{where } \epsilon_L - \epsilon_R \equiv \frac{f_L - f_R}{\partial_x P} = \frac{f_L - f_R}{\left(\sin\theta\cos\phi\ \partial_r + \frac{\cos\theta\cos\phi}{r}\partial_\theta - \frac{\sin\phi}{r\sin\theta}\partial_\phi\right) P}.$$

In this form, the significance of the role played by the error term is apparent. Whenever $\epsilon_L - \epsilon_R \geq \sim 10^{-1}$, the artificial pressure gradient caused by subtrating the non-physical naked pressure terms begins to rival the true pressure gradient, and the simulation is significantly affected.

Since pressure varies only radially, both angular derivatives of P vanish, leaving

$$\epsilon_L - \epsilon_R = \frac{P}{\partial_r P}\left[\tfrac{1}{2}\frac{\partial_r\left(g_{tt}g_{rr}\right)}{g_{tt}g_{rr}} + \frac{1-\sin\theta}{r\sin^2\theta}\right]_{L-R}. \tag{E.4}$$

Moreover, analytic expressions for g_{tt} and g_{rr} in terms of P, ρ and $M(r) \equiv \int_0^r s^2\rho(s)\ ds$ are readily available (See e.g., [81]).

$$g_{tt} = -\exp\left(2\Phi\right) \quad \text{where } \partial_r\Phi = \frac{1}{r}\frac{\frac{GM(r)}{rc^2} + \frac{4\pi Gr^2P}{c^4}}{1 - \frac{2GM(r)}{rc^2}} \tag{E.5}$$

$$g_{rr} = \left(1 - \frac{2GM(r)}{rc^2}\right)^{-1} \tag{E.6}$$

From these relations, one finds that

$$\frac{\partial_r\left(g_{tt}g_{rr}\right)}{g_{tt}g_{rr}} = \frac{2}{r}\frac{\frac{Gr^2\rho}{c^2} + \frac{4\pi Gr^2P}{c^4}}{1 - \frac{2GM(r)}{rc^2}}. \tag{E.7}$$

Apparently, the naked pressure term f from the x-momentum equation is always positive. Finally, then, the error term can be written as

$$\epsilon_L - \epsilon_R = \frac{P}{r\partial_r P}\left[\frac{\frac{Gr^2\rho}{c^2} + \frac{4\pi Gr^2P}{c^4}}{1 - \frac{2GM(r)}{rc^2}} + \frac{1-\sin\theta}{\sin^2\theta}\right]_{L-R} \tag{E.8}$$

So if $P_L - P_R \to \frac{1}{72}\partial_x P$, then

$$\epsilon_L - \epsilon_R = \frac{1}{72\ r}\left(\frac{\frac{Gr^2\rho}{c^2} + \frac{4\pi Gr^2P}{c^4}}{1 - \frac{2GM(r)}{rc^2}} + \frac{1-\sin\theta}{\sin^2\theta}\right)\sin\theta\cos\phi \tag{E.9}$$

is the relative error that is made. This may look rather nasty at first glance, but everything here is distinctly non-negative. So I think it implies that in the +++ octant of the star, the error will always tend to augment the pressure force, thereby supporting a fraction of the star's weight artificially. Whereas, in the --- octant of the star, the error will always tend to augment the gravitational force. I think this will cause the star to migrate toward the +++ octant of the grid.

Appendix F

Term-by-Term Expansion of the Generalized Source

In §7.2.3, we showed that the generalized source can be written as

$$\begin{aligned}\mathcal{S}_{(\eta)} \;=\;& T^{00}\Big[\tfrac{1}{2}C^{0}{}_{(\eta)}\partial_0 g_{00} + \tfrac{1}{2}C^{i}{}_{(\eta)}\partial_i g_{00} + g_{00}\partial_0 C^{0}{}_{(\eta)} + g_{0i}\partial_0 C^{i}{}_{(\eta)}\Big] \\ &+ T^{0i}\Big[C^{0}{}_{(\eta)}\partial_0 g_{0i} + C^{j}{}_{(\eta)}\partial_j g_{0i} + g_{00}\partial_i C^{0}{}_{(\eta)} + g_{0j}\partial_i C^{j}{}_{(\eta)} + g_{0i}\partial_0 C^{0}{}_{(\eta)} + g_{ij}\partial_0 C^{j}{}_{(\eta)}\Big] \\ &+ T^{ij}\Big[\tfrac{1}{2}C^{0}{}_{(\eta)}\partial_0 g_{ij} + \tfrac{1}{2}C^{k}{}_{(\eta)}\partial_k g_{ij} + g_{0j}\partial_i C^{0}{}_{(\eta)} + g_{jk}\partial_i C^{k}{}_{(\eta)}\Big]\end{aligned}$$

Writing out all the components (time-dependent terms in gray) and omitting the (η) subscripts for conciseness, we find that

$$
\begin{aligned}
\mathcal{S} \;=\;& T^{tt}\left[\tfrac{1}{2}\left(C^t\partial_t g_{tt}+C^x\partial_x g_{tt}+C^y\partial_y g_{tt}+C^z\partial_z g_{tt}\right)\right.\\
&\left.\quad +g_{tt}\partial_t C^t+g_{tx}\partial_t C^x+g_{ty}\partial_t C^y+g_{tz}\partial_t C^z\right]\\
&+T^{tx}\left[C^t\partial_t g_{tx}+C^x\partial_x g_{tx}+C^y\partial_y g_{tx}+C^z\partial_z g_{tx}\right.\\
&\quad +g_{tt}\partial_x C^t+g_{tx}\partial_x C^x+g_{ty}\partial_x C^y+g_{tz}\partial_x C^z\\
&\left.\quad +g_{tx}\partial_t C^t+g_{xx}\partial_t C^x+g_{xy}\partial_t C^y+g_{xz}\partial_t C^z\right]\\
&+T^{ty}\left[C^t\partial_t g_{ty}+C^x\partial_x g_{ty}+C^y\partial_y g_{ty}+C^z\partial_z g_{ty}\right.\\
&\quad +g_{tt}\partial_y C^t+g_{tx}\partial_y C^x+g_{ty}\partial_y C^y+g_{tz}\partial_y C^z\\
&\left.\quad +g_{ty}\partial_t C^t+g_{xy}\partial_t C^x+g_{yy}\partial_t C^y+g_{yz}\partial_t C^z\right]\\
&+T^{tz}\left[C^t\partial_t g_{tz}+C^x\partial_x g_{tz}+C^y\partial_y g_{tz}+C^z\partial_z g_{tz}\right.\\
&\quad +g_{tt}\partial_z C^t+g_{tx}\partial_z C^x+g_{ty}\partial_z C^y+g_{tz}\partial_z C^z\\
&\left.\quad +g_{tz}\partial_t C^t+g_{xz}\partial_t C^x+g_{yz}\partial_t C^y+g_{zz}\partial_t C^z\right]\\
&+T^{xx}\left[\tfrac{1}{2}\left(C^t\partial_t g_{xx}+C^x\partial_x g_{xx}+C^y\partial_y g_{xx}+C^z\partial_z g_{xx}\right)\right.\\
&\left.\quad +g_{tx}\partial_x C^t+g_{xx}\partial_x C^x+g_{xy}\partial_x C^y+g_{xz}\partial_x C^z\right]\\
&+T^{yy}\left[\tfrac{1}{2}\left(C^t\partial_t g_{yy}+C^x\partial_x g_{yy}+C^y\partial_y g_{yy}+C^z\partial_z g_{yy}\right)\right.\\
&\left.\quad +g_{ty}\partial_y C^t+g_{xy}\partial_y C^x+g_{yy}\partial_y C^y+g_{yz}\partial_y C^z\right]\\
&+T^{zz}\left[\tfrac{1}{2}\left(C^t\partial_t g_{zz}+C^x\partial_x g_{zz}+C^y\partial_y g_{zz}+C^z\partial_z g_{zz}\right)\right.\\
&\left.\quad +g_{tz}\partial_z C^t+g_{xz}\partial_z C^x+g_{yz}\partial_z C^y+g_{zz}\partial_z C^z\right]\\
&+T^{xy}\left[C^t\partial_t g_{xy}+C^x\partial_x g_{xy}+C^y\partial_y g_{xy}+C^z\partial_z g_{xy}\right.\\
&\quad +g_{ty}\partial_x C^t+g_{xy}\partial_x C^x+g_{yy}\partial_x C^y+g_{yz}\partial_x C^z\\
&\left.\quad +g_{tx}\partial_y C^t+g_{xx}\partial_y C^x+g_{xy}\partial_y C^y+g_{xz}\partial_y C^z\right]\\
&+T^{xz}\left[C^t\partial_t g_{xz}+C^x\partial_x g_{xz}+C^y\partial_y g_{xz}+C^z\partial_z g_{xz}\right.\\
&\quad +g_{tz}\partial_x C^t+g_{xz}\partial_x C^x+g_{yz}\partial_x C^y+g_{zz}\partial_x C^z\\
&\left.\quad +g_{tx}\partial_z C^t+g_{xx}\partial_z C^x+g_{xy}\partial_z C^y+g_{xz}\partial_z C^z\right]\\
&+T^{yz}\left[C^t\partial_t g_{yz}+C^x\partial_x g_{yz}+C^y\partial_y g_{yz}+C^z\partial_z g_{yz}\right.\\
&\quad +g_{tz}\partial_y C^t+g_{xz}\partial_y C^x+g_{yz}\partial_y C^y+g_{zz}\partial_y C^z\\
&\left.\quad +g_{ty}\partial_z C^t+g_{xy}\partial_z C^x+g_{yy}\partial_z C^y+g_{yz}\partial_z C^z\right].
\end{aligned}
$$

Finally, we use the ADM decomposition: $g_{tt}=\beta^2-\alpha^2$, $g_{ti}=\beta_i$, $g_{ij}=\gamma_{ij}$, $\sqrt{-g}=\alpha\sqrt{\gamma}$. Eliminating metric elements in favor of the lapse, shift, and components of the induced metric, we obtain the following result.

$$
\begin{aligned}
\mathcal{S} \;=\;\; & T^{tt}\Big[\tfrac{1}{2}\Big(C^t\partial_t\left(\beta^2-\alpha^2\right)+C^x\partial_x\left(\beta^2-\alpha^2\right)+C^y\partial_y\left(\beta^2-\alpha^2\right)+C^z\partial_z\left(\beta^2-\alpha^2\right)\Big) \\
& \qquad +\;\left(\beta^2-\alpha^2\right)\partial_t C^t+\beta_x\partial_t C^x+\beta_y\partial_t C^y+\beta_z\partial_t C^z\Big] \\
& +T^{tx}\Big[C^t\partial_t\beta_x+C^x\partial_x\beta_x+C^y\partial_y\beta_x+C^z\partial_z\beta_x \\
& \qquad +\;\left(\beta^2-\alpha^2\right)\partial_x C^t+\beta_x\partial_x C^x+\beta_y\partial_x C^y+\beta_z\partial_x C^z \\
& \qquad +\beta_x\partial_t C^t+\gamma_{xx}\partial_t C^x+\gamma_{xy}\partial_t C^y+\gamma_{xz}\partial_t C^z\Big] \\
& +T^{ty}\Big[C^t\partial_t\beta_y+C^x\partial_x\beta_y+C^y\partial_y\beta_y+C^z\partial_z\beta_y \\
& \qquad +\;\left(\beta^2-\alpha^2\right)\partial_y C^t+\beta_x\partial_y C^x+\beta_y\partial_y C^y+\beta_z\partial_y C^z \\
& \qquad +\beta_y\partial_t C^t+\gamma_{xy}\partial_t C^x+\gamma_{yy}\partial_t C^y+\gamma_{yz}\partial_t C^z\Big] \\
& +T^{tz}\Big[C^t\partial_t\beta_z+C^x\partial_x\beta_z+C^y\partial_y\beta_z+C^z\partial_z\beta_z \\
& \qquad +\;\left(\beta^2-\alpha^2\right)\partial_z C^t+\beta_x\partial_z C^x+\beta_y\partial_z C^y+\beta_z\partial_z C^z \\
& \qquad +\beta_z\partial_t C^t+\gamma_{xz}\partial_t C^x+\gamma_{yz}\partial_t C^y+\gamma_{zz}\partial_t C^z\Big] \\
& +T^{xx}\Big[\tfrac{1}{2}\left(C^t\partial_t\gamma_{xx}+C^x\partial_x\gamma_{xx}+C^y\partial_y\gamma_{xx}+C^z\partial_z\gamma_{xx}\right) \\
& \qquad +\beta_x\partial_x C^t+\gamma_{xx}\partial_x C^x+\gamma_{xy}\partial_x C^y+\gamma_{xz}\partial_x C^z\Big] \\
& +T^{yy}\Big[\tfrac{1}{2}\left(C^t\partial_t\gamma_{yy}+C^x\partial_x\gamma_{yy}+C^y\partial_y\gamma_{yy}+C^z\partial_z\gamma_{yy}\right) \\
& \qquad +\beta_y\partial_y C^t+\gamma_{xy}\partial_y C^x+\gamma_{yy}\partial_y C^y+\gamma_{yz}\partial_y C^z\Big] \\
& +T^{zz}\Big[\tfrac{1}{2}\left(C^t\partial_t\gamma_{zz}+C^x\partial_x\gamma_{zz}+C^y\partial_y\gamma_{zz}+C^z\partial_z\gamma_{zz}\right) \\
& \qquad +\beta_z\partial_z C^t+\gamma_{xz}\partial_z C^x+\gamma_{yz}\partial_z C^y+\gamma_{zz}\partial_z C^z\Big] \\
& +T^{xy}\Big[C^t\partial_t\gamma_{xy}+C^x\partial_x\gamma_{xy}+C^y\partial_y\gamma_{xy}+C^z\partial_z\gamma_{xy} \\
& \qquad +\beta_y\partial_x C^t+\gamma_{xy}\partial_x C^x+\gamma_{yy}\partial_x C^y+\gamma_{yz}\partial_x C^z \\
& \qquad +\beta_x\partial_y C^t+\gamma_{xx}\partial_y C^x+\gamma_{xy}\partial_y C^y+\gamma_{xz}\partial_y C^z\Big] \\
& +T^{xz}\Big[C^t\partial_t\gamma_{xz}+C^x\partial_x\gamma_{xz}+C^y\partial_y\gamma_{xz}+C^z\partial_z\gamma_{xz} \\
& \qquad +\beta_z\partial_x C^t+\gamma_{xz}\partial_x C^x+\gamma_{yz}\partial_x C^y+\gamma_{zz}\partial_x C^z \\
& \qquad +\beta_x\partial_z C^t+\gamma_{xx}\partial_z C^x+\gamma_{xy}\partial_z C^y+\gamma_{xz}\partial_z C^z\Big] \\
& +T^{yz}\Big[C^t\partial_t\gamma_{yz}+C^x\partial_x\gamma_{yz}+C^y\partial_y\gamma_{yz}+C^z\partial_z\gamma_{yz} \\
& \qquad +\beta_z\partial_y C^t+\gamma_{xz}\partial_y C^x+\gamma_{yz}\partial_y C^y+\gamma_{zz}\partial_y C^z \\
& \qquad +\beta_y\partial_z C^t+\gamma_{xy}\partial_z C^x+\gamma_{yy}\partial_z C^y+\gamma_{yz}\partial_z C^z\Big]
\end{aligned}
$$

Vita

Jay Michael Call was born in January 1979 in Murray, Utah, but grew up on a potato farm in the Raft River, Idaho, area. He attended Ricks College (now Brigham Young University—Idaho) for a semester, and then served a two-year church mission in Bolivia, thereby becoming fluent in Spanish. After returning from Bolivia, he completed his Bachelor of Science degree in physics at Brigham Young University (BYU) in Provo, Utah, in August 2003. He married Amber Van Slyke in August 2006, and earned his Master of Science degree from Louisiana State University (LSU) in August 2008. He and Amber currently have twin toddlers, Susan and Benjamin, and reside in Zachary, Louisiana, where he teaches astronomy, physics and calculus at the local high school. Jay plans to graduate from LSU with a Doctor of Philosophy degree in August 2010, and shortly afterward (in September 2010) he and Amber are expecting their third child.